Hydrogen production from fluctuating small-scale hydropower

Kamilla Valla Hagen

Master's Thesis in Energy

Thesis for Master of Science Degree written as a part of the Integrated Master's program in Energy at the Geophysical Institute at the University of Bergen.

Department of Physics and Technology
University of Bergen

June 2024

Year: June 2024

Title: Hydrogen production from fluctuating small-scale hydropower

Author: Kamilla Valla Hagen

Email: kamilla.v.h@gmail.com

Acknowledgements

This project marks the end of five years as a student at the University of Bergen. I deeply appreciate this period of my life and the people who have made it memorable.

This thesis is a collaboration between the University of Bergen, Sunnhordland Kraftlag AS (SKL), Hydrogen Solutions AS (HYDS), and Western Norway University of Applied Sciences. I want to thank the people who made this project possible, including my supervisor from the University of Bergen, Professor Pawel Kosinski; the teams at HYDS and SKL; and Liina Sangolt, a PhD student from the Western Norway University of Applied Sciences. A special thanks to Astrid Gunnarshaug and Emmanuel Quayson at HYDS for their enthusiasm, valuable guidance, data, and insights into the hydrogen industry. I also want to thank Arthur Uno Rognmo, a former SKL employee, for his valuable guidance and insight into the hydropower industry. Additionally, I want to show my deepest appreciation to my supervisor, Velaug Myrseth Oltedal from Western Norway University of Applied Sciences. I am beyond thankful you were my supervisor during this project; your guidance, understanding nature, and endless support have been invaluable.

I would also like to give a heartfelt thanks to my fellow students from the Master's Program in Energy at the Geophysical Institute for their hard work and friendship over the last five years. Special thanks to Håkon, Simen, and Akilavan, my partners in crime. A special thanks to Mali, my designated thesis buddy from Sal 363. Your unconditional support, both emotional and academic, and all the laughter we shared in Sal 363 over the past year have made this process more than bearable. Additionally, my friend Agathe deserves special thanks for her involvement in my project. I hope you all know how important you have been during this process. I would also like to thank my friends outside of my studies; when life brings lemons, you guys always make the most tasty lemonade with me.

Lastly, I would like to thank my mom, dad, and sister. Without your endless support and belief in me, I would not have gotten through the last five years.

Bergen, June 2024

Kamilla Valla Hagen

Abstract

As the world seeks renewable alternatives to fossil fuels, hydrogen emerges as a valuable energy carrier to facilitate the green shift. When produced from renewable energy, hydrogen is considered a green fuel that can be stored over a longer period, unlike the electricity it was produced from. This enables hydrogen to utilize renewable energy that might otherwise be trapped due to infrastructure limitations. This thesis explores the feasibility of generating hydrogen from a potential small-scale hydropower plant located in an area with a limited grid connection.

This thesis examines the fluctuating power output of a potential small-scale hydropower plant, using a dataset containing electricity generation from the potential plant. Additionally, various electrolyzer capacities, 1 MW, 3 MW, and 5 MW, were examined through simulation to identify the most suitable option for the hydropower plant. This was done using a MATLAB model to investigate how fluctuating power input influences the hydrogen production rate and the operational conditions of the electrolyzer. Moreover, a cost analysis was conducted, considering the levelized cost of hydrogen (LCOH), which is the price per kilogram of hydrogen produced. The thesis also compares AEL and PEM electrolyzer technologies and explores potential end-users for the simulated hydrogen production.

The results showed that none of the electrolyzer capacities fit perfectly with the potential hydropower plant. However, based on the information available in this thesis, the 3 MW electrolyzer is a compromise between the other two capacities, which are shown to be two extremes. For this capacity, the yearly production of hydrogen would be 117 100 kg in a typical dry year, 146 700 kg in a median year, and 194 300 kg in a typical wet year. Additionally, the LCOH for this capacity is 70.90 NOK/kg in a year with median power production and middle grid prices. The results also indicate limited differences in response time between the PEM and pressurized AEL electrolyzer technologies. Lastly, there are many potential end-users in the area around the potential hydropower plant, primarily in the industrial and maritime sectors. Additionally, there is a highway nearby, making hydrogen for the transport sector an option. The results provide a knowledge foundation and valuable insights into hydrogen production from fluctuating power, aiding in investment decision-making.

Contents

Acronyms

AEL alkaline electrolysis

AFC alkaline fuel cell

CH_2 compressed hydrogen

CAPEX capital expenditures

HYDS Hydrogen Solutions AS

LH_2 liquefied hydrogen

LCOE levelized cost of energy

LCOH levelised cost of hydrogen

LOHC liquid organic hydrogen carrier

NVE The Norwegian Water Resource- and Energy Directorate

OPEX operational expenditures

PEM proton exchange membrane

PEMFC proton exchange membrane fuel cell

REGINE "Register over nedbørsfelt"

SKL Sunnhordland kraftlag AS

SOEL solid oxide electrolysis

Chapter 1

Introduction

1.1 Motivation

Over centuries of human existence on Earth, we have exploited its resources, forging ahead with little regard for sustainability. The pursuit of growth and development has led to a society heavily dependent on fossil fuels, resulting in human-made greenhouse gas emissions and global warming. Consequently, Earth is now exposed to an imminent climate crisis, with the average global surface temperature exceeding pre-industrial levels by approximately 1.2 °C [1]. The world is already experiencing heatwaves and other extreme weather events, signaling the overdue need for change.

Taking action to drive the green transition is essential. Politicians can influence society by fostering initiatives, as the Paris Agreement exemplifies. By signing the 2015 Paris Agreement, Norway and other UN parties have committed to fight climate change. The agreement aims to prevent the global temperature from rising more than 2 °C above pre-industrial levels.

In the midst of a severe climate crisis, the global energy demand is constantly growing. The energy sector is responsible for 75 % of global greenhouse gas emissions, with the distribution of energy emissions closely tied to economic status [2]. The top emitters worldwide are countries with advanced economies, contributing around 50 % of the total global energy emissions [3]. In contrast, the 10 % lowest emitting countries are from developing economies, contributing 0.2 %. There is an urgent need for change to meet ambitious climate targets. Transitioning from fossil fuels to a renewable energy mix is crucial, utilizing all available resources to their fullest potential.

However, the transition towards green energy leads to an increased demand for electricity and significant changes in our well-established infrastructure. This shift introduces new challenges, including managing the fluctuating behavior of renewable energy, integrating new electricity into the power grid, and the necessity for developing new technologies such as energy storage systems and alternative energy carriers. The distribution of energy emissions also underscores the responsibility of wealthier nations to lead by adopting energy-efficient and low-emission solutions. By pioneering these technologies, they can facilitate large-scale manufacturing and global adoption.

1.1.1 Introduction to small-scale hydropower

Hydropower is the foundation of the Norwegian electricity supply and was responsible for 89.2 % of the national power supply as of December 2023 [4] [5]. This accounts for 137.3 TWh per December 2023 [6]. Despite this significant contribution, numerous untapped concessions for hydropower present an unexplored potential for green energy. Of the total hydropower production, 12.1 TWh comes from small-scale hydropower plants [6], typically defined by an effect below 10 MW [7]. Small-scale hydropower plants are mainly built in connection with steep rivers or streams, making it possible to take advantage of the significant drop in elevation [8]. The concept of small-scale hydropower will be discussed further in Chapter 2.

In 2018, the Norwegian Oil and Energy Department published a report revealing 3 TWh worth of unutilized concessions for small-scale power plants in Norway [9]. The report highlighted the primary challenges associated with small-scale hydropower, including feasibility, environmental impact, connection to the power grid, and the competence of small power companies. Hydropower concessions in areas with poor or no connection to the grid contains potential power labeled as trapped power. The report suggests that generating hydrogen from small-scale hydropower plants could make them more feasible, particularly in areas with poor infrastructure. Thereby hydrogen provides a means to harness trapped green energy that would otherwise remain untapped.

1.1.2 Introduction to hydrogen

Hydrogen can be a valuable energy carrier to facilitate in the transition to clean energy and a low emission society. Producing hydrogen from surplus renewable energy offers a means of storing excess electricity for future electricity utilization, thereby helping to balance the power market. Alternatively, hydrogen can be used as fuel in industrial processes and vehicles or as a feedstock in chemical production [2].

In their 2023 report, the Norwegian Energy Commission gave the highest score of importance to the flexibility hydrogen brings to the market, particularly green hydrogen, produced from renewable energy sources [8]. Green hydrogen is produced through water electrolysis, which uses electricity to separate water molecules into hydrogen and oxygen gas. This process results in minimal greenhouse gas emissions. Currently, only 4 % of hydrogen is produced through electrolysis, while the remaining 96 % is derived from fossil fuels [10]. This form, known as grey hydrogen, is linked to substantial CO_2-emissions compared to green hydrogen.

While electrolyzers have a history dating back 230 years, their commercialization gained momentum in the 20th century, primarily for industrial hydrogen production in ammonia fertilizer manufacturing [11]. Consequently, electrolyzers were already an established technology when scientists began exploring hydrogen as an energy carrier for renewable energy in the 1990s. Traditionally, electrolyzers were operated at a constant load, requiring constant power. Given the increase in intermittent energy sources in today's energy market, utilizing the surplus electricity for green hydrogen production will require a fluctuating power supply as input. This results in a range of new challenges, requiring further understanding.

Small-scale hydropower plants have fluctuating power output, and by analyzing hydrogen production from such plants, it is possible to draw conclusions that may apply to all intermittent renewable sources, as they all experience fluctuations. Further, Section 1.2 details a specific case

study of a potential hydropower plant. The case builds the foundation of this thesis. In Section 1.3, the aims and objectives of the thesis are presented, including simulating hydrogen production and electrolyzer operation from said hydropower plant to analyze the feasibility of hydrogen production.

1.2 Case overview

This section is dedicated to presenting the case on which this thesis is based. The case is provided in collaboration with Sunnhordland kraftlag AS (SKL) and Hydrogen Solutions AS (HYDS). SKL is a hydroelectric power company dedicated to achieving a fully electrified society with minimal fossil fuel pollution [12]. In partnership with Liquiline, SKL established HYDS to produce scalable, locally produced green hydrogen and hydrogen derivatives.

In western Norway, SKL holds concessions for various hydropower plants in remote locations. These locations pose significant challenges for accessibility and grid connections, so SKL is exploring potential solutions to overcome these challenges and utilize the trapped power. On-site hydrogen production has been identified as a possible solution. In the case presented by SKL and HYDS, a potential hydropower plant is being considered at a confidential location referred to as location A due to ongoing negotiations with the landowners. SKL has a permit to build a hydropower plant at location A, which is situated on mountains by the sea. Based on the provided hydroelectric dataset, it is determined that location A has great potential for power generation.

Due to a weak grid connection, buying a small amount of power from the grid is possible, but selling power to the grid is not an option. It is in the interest of SKL to utilize the power potential available on this site. Given that the trapped power can be used for hydrogen production, producing hydrogen on-site in collaboration with HYDS is a possibility. HYDS has provided typical data for an electrolyzer that can produce hydrogen at location A. In essence, this case and the data provided are used in this thesis to explore the feasibility of producing hydrogen from a small-scale hydropower plant at location A. The aims and objectives of this thesis are described in detail below, outlining the overall goal, the aim, and how it is divided into smaller tasks or objectives that will help achieve the aim.

1.3 Aim and objectives of the study

1.3.1 Aim

This thesis aims to examine the necessary conditions for a profitable project with the purpose of establishing a hydropower plant for producing hydrogen from trapped power. This requires striking a balance between the interests of the power supplier, SKL, and the hydrogen producer, HYDS.

The power supplier's primary goal is to produce the maximum amount of power possible from the hydropower plant and sell it to the hydrogen producer. However, the hydrogen producer is focused on generating and selling a sustainable quantity of hydrogen. In order to achieve this, the electrolyzer must be dimensioned to fulfill several demands simultaneously. These include using a reasonable amount of power, promoting sustainable operating conditions for the

electrolyzer, and selling the hydrogen at the highest possible price while remaining competitive in the hydrogen market.

In addition, both parties are interested in determining whether the water source at location A is sufficient for hydrogen production. This depends on the amount of hydrogen produced and the operation of the electrolyzer from the fluctuating power source. Furthermore, for this to be a profitable project for HYDS, an end-user for the produced hydrogen is necessary.

1.3.2 Objectives

Production from hydropower plant

Small-scale hydropower plants can experience significant variations in power output on an hourly, daily, monthly, and seasonal basis. These variations can affect the use of the electrolyzer. To understand these variations and how they affect the electrolyzer, this study will:

- Analyze the provided hydroelectric dataset and determine the potential power production.
- Identify the median year, a typical dry year, and a typical wet year.
- Determine the amount of the electrolyzer capacity used in a year, including days the electrolyzer runs on full load and the number of zero production days.

Electrolyzer analysis

Maximizing the utilization of hydropower plant output and hydrogen production requires optimal electrolyzer capacity. Hence, this study will:

- Using a MATLAB model, investigate different electrolyzer capacities and determine the optimal electrolyzer capacity for the power plant conditions in the given case.
- Evaluate the impact of fluctuation power on the operation of the electrolyzers.
- Compare different electrolyzer technologies for fluctuating power input.
- Identify the most critical bottlenecks for a potential investment decision.
- Evaluate potential end-users.

1.4 Thesis outline

Chapter 1 serves as the introduction to the thesis, laying the groundwork for exploring hydrogen production using small-scale hydropower plants. Figure 1.1 illustrates the workflow of this thesis, representing the journey from hydropower generation to the end-user of the hydrogen. The primary focus of this thesis is on hydropower generation and hydrogen production. Hydrogen produced often requires compression before utilization, as well as a means to store the compressed hydrogen. Both compression and storage constitute significant expenses and are therefore included in the cost analyses. Additionally, transportation is illustrated, as an essential step in the hydrogen value chain before selling the hydrogen to an end-user. However, this thesis will not focus on this additional process step, as it is beyond the scope of this study.

Chapter 2 presents the relevant theoretical background about hydrogen and small-scale hydropower plants. This section includes a general outline of power generation from small-scale hydropower plants and the hydrogen value chain. Additionally, it consists of a literature study that examines related work. Chapter 3 explains the methodology of the thesis, including a description of the dataset provided by SKL, various assumptions made within the thesis, the calculations employed in the simulation of hydrogen production, and the method for cost analyses of electrolyzer capacities.

The results will be presented in Chapter 4, which will then be discussed in Chapter 5. In this discussion chapter, the key findings from the results are interpreted, and an evaluation of the technology and potential end-users is provided. Lastly, Chapter 6 concludes the thesis.

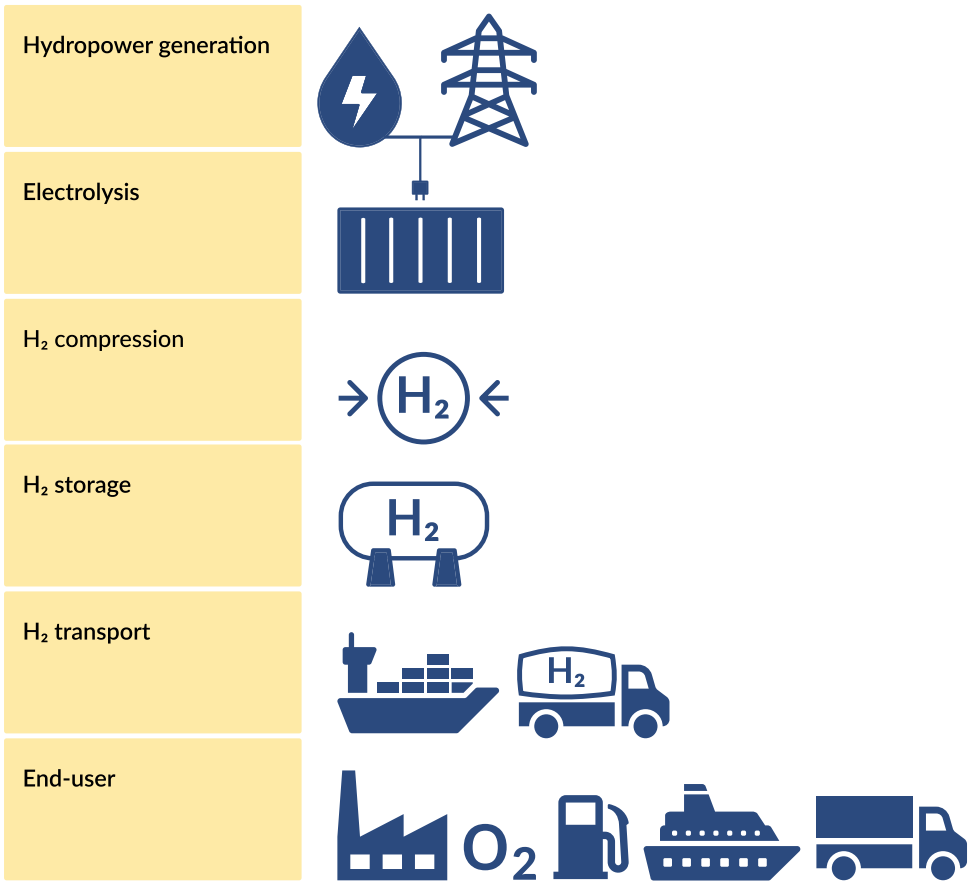

Figure 1.1: The workflow of this thesis starts with power generation, primarily from the potential hydropower plant but also from the grid, supplying the electrolyzer with electricity for hydrogen production. It then follows the hydrogen value chain, including hydrogen production, compression, storage, transportation, and utilization by the end-user. The transportation of hydrogen is not explored in this thesis but is included in the figure because it is an important part of the hydrogen value chain.

Chapter 2

Background

This chapter will introduce the theory that will be used to address the aims and objectives outlined in Section 1.3. The content will include a description of a small-scale hydropower plant. Furthermore, the chapter will provide an overview of how Norway is divided into hydrological areas, called precipitation fields, which can be utilized to identify regions suitable for hydropower generation. The text will also explain how to use precipitation fields to estimate the capacity of a turbine, and how energy production can be estimated based on the turbine's capacity at a specific location. Additionally, the chapter will present the hydrogen value chain excluding transportation, followed by a literature review to explore similar work.

2.1 Small-scale hydropower

The Norwegian landscape features areas with streams and steep rivers of varying size and flow rate, offering ideal conditions for hydropower plants to harness the kinetic energy of flowing water and convert it into electricity [8]. Norway has effectively harnessed these energy sources, with hydropower contributing to 89.2 % of the national power supply as of December 2023 [5]. Small-scale hydropower accounts for approximately 9 % of the country's hydropower-generated electricity [6]. Despite the great potential, there are currently 3 TWh of unused small-scale hydropower plant concessions in Norway [9].

Specifically designed for relatively concentrated small waterfalls, small-scale plants operate with a natural intake reservoir or pool, relying less on manufactured storage magazines for water retention, making them unregulated [7]. In contrast to the large-scale plants, the dependence on natural intake reservoirs exposes small-scale hydropower plants to annual, seasonal, and daily variations in energy production. This variability stems from the dynamic nature of water flow, emphasizing the importance of precise planning and forecasting. To aid in this complex task, The Norwegian Water Resource- and Energy Directorate (NVE) provides a comprehensive manual for guiding the planning, construction, and operation of small-scale hydropower plants [7].

When planning a new small-scale hydropower plant, the planning phase is crucial to estimate whether the specific water source is suitable for energy production. During this process, the manual describes methods for estimating the optimal installed capacity of a turbine at a potential hydropower plant by utilizing the water source of interest. Additionally, the power production

from the site can be approximated in terms of potential yearly power generation. In addition, it can be calculated based on historical data from the specific water source, for instance, on an hourly base over several years. The middle flow rate of a precipitation field is essential for calculating both turbine capacity and power production and can be determined using information from precipitation fields.

The following sections elaborate on the concept of precipitation fields, the method of dimensioning a plant's turbine, and assessing potential electricity production in a specific precipitation field. These methods provide an understanding of the process behind evaluating a new water source (specific precipitation field) for power production. Moreover, these estimations can be used to create a dataset to understand the nature of the water source better. However, these methods are not employed in this thesis. Instead, this thesis is based on an already calculated dataset provided by SKL, which is further explained in Section 3.2.

2.1.1 Precipitation field

A precipitation field refers to a specific hydrological area [7]. It is possible to visualize a precipitation field as a funnel. The wide opening at the top collects all the water, while the small opening at the bottom is where all the water is collected and measured as a single runoff. This makes measuring the amount of precipitation in that specific area possible. The runoff can be a river, sea, stream, or inlet of a hydropower plant. A precipitation field has several defining characteristics such as its area, the presence of mountains, swamps, vegetation, and water bodies. In addition to annual temperature variations, these characteristics affect water management in the field and the resulting quantity of outflow from the bottom of the funnel.

In mountainous areas, the border between fields is often marked by mountain tops or ridges, whereas in flat landscapes, they are less apparent. "Register over nedbørsfelt" (REGINE), in English "Record of precipitation fields", is the national hydrographic division of Norway that divides the country into precipitation fields [13]. According to the NVE website, Norway has over 20 000 precipitation fields. REGINE can be visualised in NVE Atlas, a website that contains a map database [14]. It is possible to display all the precipitation fields and weather measuring stations in Norway. It is important to emphasize that there is a substantial minority of fields that contain a measuring station. Furthermore, the Atlas provides additional details relating to the fields, including their area. Figure 2.1 illustrates a portion of the NVE Atlas web page. Another important value that can be obtained at NVE Atlas is the specific runoff.

Specific runoff

Each precipitation field in Norway is associated with a unique specific runoff (q), measured in units of [L/s km^2]. However, only a limited number of specific runoffs are grounded in empirical data from measuring stations. To theoretically determine specific runoff values in areas without measuring stations, NVE has developed a comprehensive runoff model. The model is a property of NVE and is not relevant to explain in this thesis. Moreover, the value of specific runoff for precipitation fields with or without a measuring station can be obtained at NVE Atlas.

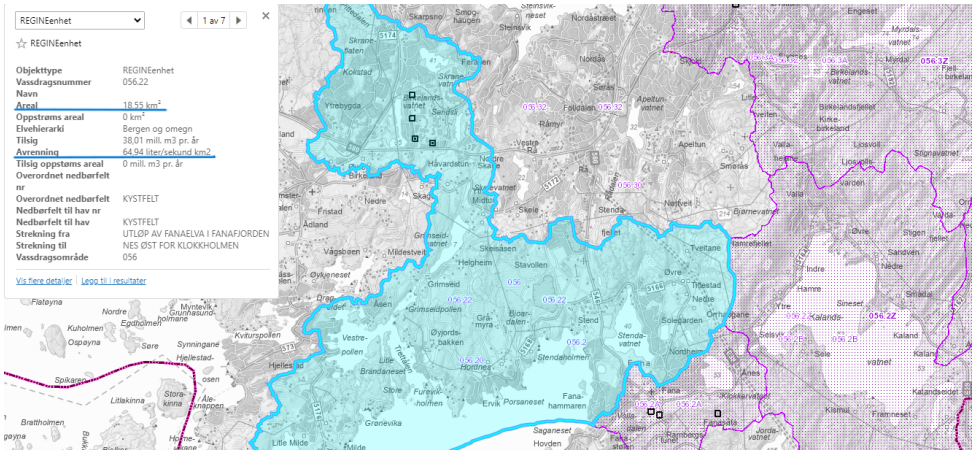

Figure 2.1: The NVE Atlas webpage displaying the precipitation field in Fana, Bergen (blue), including measuring stations (square). Outlined in the figure are the values of specific runoff and the area of the field. The adjacent precipitation field (056.2Z) does not have a measuring unit [14].

Middle water flow

From the specific runoff, it is possible to calculate the middle water flow (Q_{middle}) of a precipitation field [7]. Q_{middle} is the mean flow rate of a hydrological area and represents the amount of precipitation occurring 50 % of the time. To calculate Q_{middle}, the area A of the chosen precipitation field is multiplied by its corresponding q value and divided by 1000 to convert from liters to cubic meters, as illustrated in Equation 2.1 [7]. This value is crucial when determining the capacity of a hydropower plant and estimating energy production, as it describes the most likely water flow in the area and can be used to estimate the total yearly amount of water.

$$Q_{\text{middle}} = \frac{A \cdot q}{1000} \quad [\text{m}^3/\text{s}] \tag{2.1}$$

2.1.2 Installed capacity

A hydropower plant has a set capacity, often referred to as power. This is the rate at which the plant transforms water into electrical energy. The water above the plant has potential energy proportional to the vertical distance between the water and the turbine. As the water flows, it gains kinetic energy. In the power plant, the water loaded with both potential and kinetic energy powers the turbine, which in turn produces mechanical energy. The spinning turbine is then connected to a generator, which converts the mechanical energy into electrical energy. The power output is explained in Equation 2.2 [15].

$$P = \rho \cdot g \cdot Z \cdot \eta \cdot Q \quad [\text{MW}] \tag{2.2}$$

Where P is the power output in MW, ρ is the mass density of water equal to 1000 kg/m^3, g is the gravitational constant at 9.82 m/s^2, Z is the hydraulic head - the height difference between the top of the reservoir and the turbine center in m as shown in Figure 2.2, η is the efficiency of the turbine and Q is the water flow rate in m^3/s. The parameters ρ, g, and η remain constant.

Additionally, Z is specific to each location, and in small-scale hydropower the Z varies minimally (0.5-1 m of variation) [7]. Therefore, the most important variable affecting the power of a hydropower plant is the water flow, which depends on meteorological factors and seasonal variations.

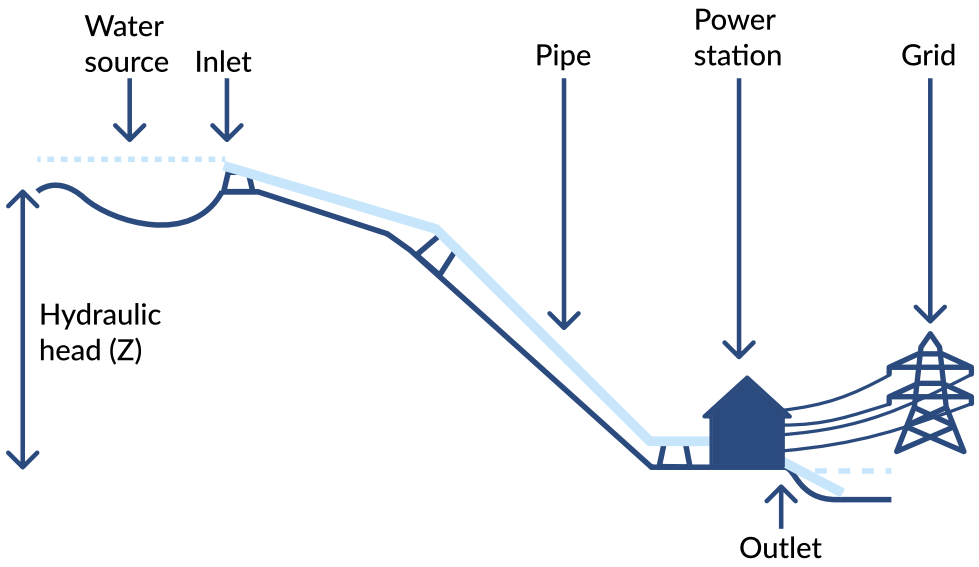

Figure 2.2: A general illustration of a small-scale hydroelectric plant

For an unregulated hydropower plant, the installed capacity is based on the turbine's maximum capacity [7]. Therefore, the maximum discharge, Q_{max}, is used in the power formula 2.2. The formula used to calculate an estimate of Q_{max} is shown in Equation 2.3 [7]. From project experience, NVE has found that a good initial estimate of Q_{max} is twice Q_{middle} [7]. This value is further optimized during the detailed power plant project phase.

$$Q_{max} = 2 \cdot Q_{middle} \quad [m^3/s] \tag{2.3}$$

A hydropower plant is considered small-scale when its installed capacity is under 10 MW. Table 2.1 lists the definitions of what is included in the definition of small-scale hydropower plant, according to NVE. The hydropower plant in this thesis falls within the range of 1 MW to 10 MW.

Table 2.1: The three classifications of small-scale hydropower plants, defined by NVE [7]

Classification	Production [MW]
Micro	> 0.1
Mini	0.1-1
Small-scale	1-10

2.1.3 Power production

The power produced over a certain period can be measured in GWh. NVE has developed a methodology for estimating potential annual power production from precipitation fields. This

approach is based on the percentage of water lost when the water flow exceeds the turbine's maximal discharge capacity Q_{max} and loss when it falls below the lowest discharge capacity Q_{min} [7]. As mentioned, Q_{max} represents the maximum water volume that a power plant can effectively utilize. In the event of a flood, water runoff exceeds the power plant's operational threshold, leading to a loss of water. Conversely, Q_{min} represents insufficient water runoff, preventing the turbine from functioning optimally and resulting in water loss. The calculations of Q_{max} and Q_{min} are based on Q_{middle}, as shown in Equation 2.3 and Equation 2.4 [7]. These formulas indicate an estimate of the values, and optimization will be required in a more detailed part of the project.

$$Q_{min} = 0.5 \cdot Q_{middle} \quad [m^3/s] \tag{2.4}$$

The amount of water lost in a precipitation area results from both flooding (Q_{max}) and low-flow (Q_{min}) losses due to the dimensioning of the turbine [7]. To calculate power production, it is necessary to determine the total loss percentage. This can be done by creating a duration curve, where daily water flow in a specific time series are sorted from highest to lowest values. Alongside the duration curve, two additional curves are plotted: one representing losses due to flooding (Q_{max}) and another representing losses due to insufficient runoff (Q_{min}). Using these three curves, it is possible to find the total percentage of water loss. However, these calculations are beyond the scope of this thesis and will not be explained in detail.

Inverting the loss percentage, the usable proportion of the total amount of water is obtained. Then, it is possible to calculate the amount of *available water* in a precipitation field for power production. Q_{middle} is multiplied by the number of seconds during a year ($3.2 \cdot 10^7$) and the percentage of *usable water*, as expressed in Equation 2.5 [7].

$$Available\ water\ = Q_{middle} \cdot 3.2 \cdot 10^7 \cdot usable\ water \quad [m^3] \tag{2.5}$$

Having determined the annual *available water*, a more in-depth analysis of the power potential in a field requires the use of energy equivalent. NVE defines the energy equivalent (e) as the energy obtained per cubic meter of water passing through the turbine [7]. Energy equivalent is obtained by multiplying the water density, gravitational constant, hydraulic head, and the efficiency of the turbine. This result is then divided by the seconds in an hour (3600) and scaled by a factor of 1000 to convert from Wh to kWh, as shown in Equation 2.6 [7].

$$e = \frac{\rho \cdot g \cdot Z \cdot \eta}{3600 \cdot 1000} \quad [kWh/m^3] \tag{2.6}$$

The *yearly power potential* obtained from the precipitation field is then calculated by multiplying the quantity of *available water* with the e of the area, as shown in Equation 2.7 [7].

$$Yearly\ power\ potential = e \cdot Available\ water \quad [GWh] \tag{2.7}$$

This calculation demonstrates how to estimate yearly potential power production, providing valuable insight into the feasibility of establishing a hydropower plant in the specific precipitation field. Moreover, historical data, such as available water on an hourly basis, can be accessed from the NVE Atlas [14]. By utilizing the hourly available water with Equation 2.7, a dataset can be

generated for the specific precipitation field. This dataset enables an examination of seasonal power generation at the location and allows for the study of fluctuations. This section describes a simplified and general process of how the turbine capacity is calculated and how a dataset with potential power production is created. These calculations are not done in this thesis.

2.2 Hydrogen

While hydrogen is the most abundant element on Earth, it is rarely found in its pure form. It typically exists as a component of other molecules, such as water or hydrocarbons [16]. Due to its high gravimetric density, hydrogen is an ideal secondary energy carrier and has become a frequently discussed topic in efforts to decarbonize the world's energy sector. For instance, one kg of hydrogen contains approximately three times the energy of an equivalent gasoline mass when comparing hydrogen to conventional gasoline [10].

Another valuable property of hydrogen is that it is considered an energy carrier with almost zero carbon emissions when utilized. However, the overall carbon footprint of hydrogen production depends significantly on the resources and production methods employed. As presented in Figure 2.3, grey hydrogen is produced by using fossil fuels, which can lead to carbon emissions and contribute to environmental pollution. In contrast, blue hydrogen is generated from fossil fuels with carbon capture and storage. Lastly, green hydrogen is created from renewable energy sources, making the production zero emission. In the following paragraphs, the hydrogen value chain will be presented, starting from production, followed by storage, and the utilization by an end-user.

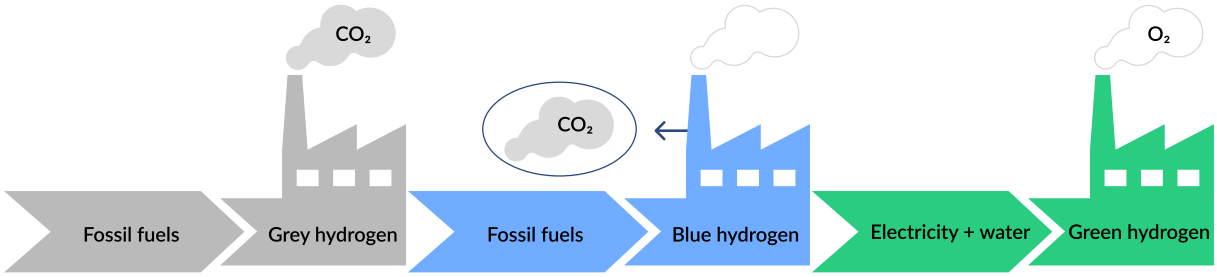

Figure 2.3: Illustration of gray, blue and green hydrogen

2.2.1 Hydrogen production

Today's global hydrogen production is 96 % fossil fuel-based and 4 % based on renewable energy [10]. The most common methods of producing hydrogen are steam methane reforming, partial oxidation, and autothermal reforming. The 4 % based on renewables is made from water electrolysis, a method using electricity and purified water [16]. Since this thesis focuses on hydrogen produced with electrolysis using hydropower as the electricity generation method, fossil fuel-based methods will not be discussed further. Electrolysis is the process of splitting water into hydrogen and oxygen using electrical energy. Although electrolysis generates twice as many hydrogen molecules as oxygen for each water molecule split, the mass of oxygen produced is higher than that of hydrogen. This is because oxygen has a higher molar mass than hydrogen.

The electrolysis reaction is described in Equation 2.8.

$$2H_2O \longleftrightarrow 2H_2 + O_2 \tag{2.8}$$

Different methods are available for producing hydrogen through electrolysis, which are categorized by high- or low-temperature electrolyzers. The most common high-temperature production method is solid oxide electrolysis (SOEL), with a temperature range of 700 to 900 °C [16]. The most common low-temperature electrolyzers are alkaline electrolysis (AEL) and proton exchange membrane (PEM), which have a temperature ranging from 60 to 80 °C. Additionally, these methods differ based on the electrolyte used, which determines the charge carriers or ions involved. The charge carriers are important because they can impact the environment in the electrolyzer cell, which in turn can affect the maintenance and cost of the electrolyzer. In the following paragraphs, a brief overview of the electrolysis technologies SOEL, AEL, and PEM will be given, followed by an introduction to the different modes of electrolyzer operation.

Solid oxide electrolysis cells

High-temperature electrolyzers are utilized to convert steam into hydrogen and oxygen [16], and are often integrated into industrial processes that utilize waste heat to generate the steam. Consequently, high-temperature electrolyzers require less electricity compared to their low-temperature counterparts. However, if water needs to be heated separately to produce steam for the process, it does not necessarily result in reduced electricity consumption. SOEL is a high-temperature electrolyzer that uses ceramic electrolytes to convert steam into hydrogen and oxygen. This method has proven to be useful for industrial processes, as well as for utilizing waste heat. However, despite the advantages of the high temperature, it also damages materials and seals within the stack. This is one of the reasons why SOEL is still in the research and development phase [16]. High-temperature electrolysis has yet to achieve the technological maturity required to be commercial and is therefore excluded from this thesis.

Alkaline electrolysis

The AEL technology has been used for large-scale hydrogen production in industrial settings since the 20th century [11]. The main component of the AEL is the stack, consisting of several electrolysis cells. Each AEL cell has two electrodes: the cathode, where H_2 is produced, and the anode, where O_2 is separated [16]. The electrodes are immersed in an electrolyte consisting of an alkaline solution, often KHO. Additionally, OH^- ions act as the charge carrier. The two electrodes are separated by a membrane that allows the OH^- ions to move between them but restricts the transportation of hydrogen and oxygen due to low gas permeability. This is beneficial as it prevents unwanted reactions that could harm the cell and improves the purity of the produced hydrogen. Additionally, mixing the gases is undesirable due to safety concerns, as it can lead to explosions. Figure 2.4 illustrates the basic structure and processes in the AEL cell.

In the cell, at the cathode side, water reacts with electrons from the electrical current to form hydrogen gas and OH^-. These OH^- ions then migrate to the anode side, where they are converted back into water and oxygen, while releasing their electrons. Equations 2.9, and 2.10 present the half-cell reactions in the cell. The total reaction for the cell is presented in Equation 2.11.

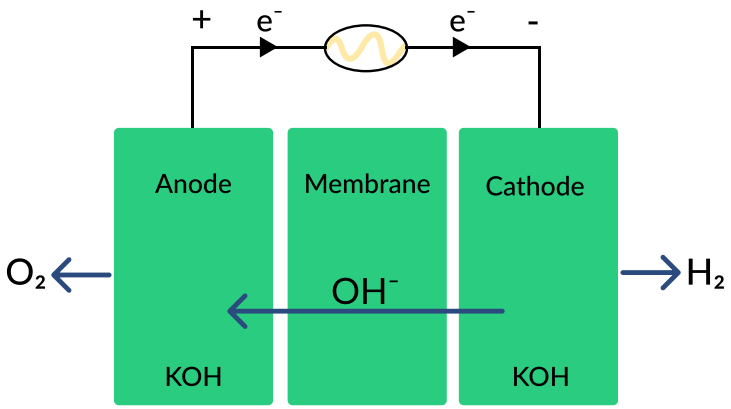

Figure 2.4: Illustration of AEL cell

$$\text{Anode} : 2\,OH^- \longrightarrow H_2O_{(g)} + \frac{1}{2}O_{2(g)} + 2\,e^- \tag{2.9}$$

$$\text{Cathode} : 2\,H_2O_{(g)} + 2\,e^- \longrightarrow H_{2(g)} + 2\,OH^- \tag{2.10}$$

$$\text{Total} : H_2O_{(l)} \longrightarrow H_{2(g)} + \frac{1}{2}O_{2(g)} \tag{2.11}$$

There are two main types of AEL: pressurized and atmospheric. Pressurized AEL has a quicker response time compared to atmospheric [17]. Since renewable energy often has fluctuating power input, it is desirable for the technology to respond quickly to changes in the load. This ensures that the power is used efficiently and not wasted due to delays in starting production by the electrolyzer. In this thesis, pressurized electrolyzers will be used. A pressurized AEL operates at a pressure of around 30 bar [18] and has an electrical efficiency between 63 and 70 % [10]. It operates at a temperature range of 60 to 80 °C. The environment in an AEL cell allows for the use of simple and cost-effective nickel or iron compounds for electrodes and catalysts [16].

Proton exchange membrane water electrolysis

A critical component of the PEM system is the electrolysis stack, which contains an electrolyzer cell, as illustrated in Figure 2.5. The H^+ ion acts as the charge carrier in the cell, and it is conducted by the membrane that divides the two electrode sides. The membrane is typically made of a proton-conducting polymer that acts as an electrolyte [16]. The most commonly used membrane is a perfluorinated sulfonic acid membrane, like Nafion, which has favorable characteristics such as low gas permeability and high proton conductivity.

Moreover, water reacts at the anode electrode, causing protons to move through the membrane to the cathode. Simultaneously, electrons move through an external current to the cathode. On the cathode side, protons and electrons recombine, producing hydrogen. Equations 2.12, and 2.13 present the half-cell reaction in the cell. Further Equation 2.14 presents the total reaction.

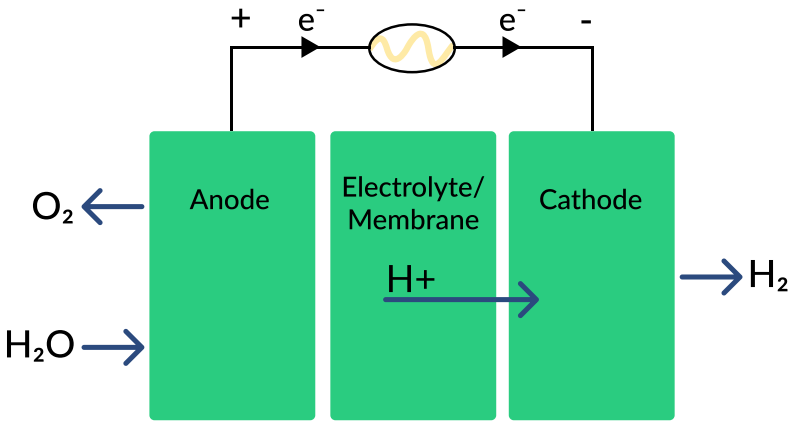

Figure 2.5: Illustration of a PEM cell

$$\text{Anode} : H_2O_{(l)} \longrightarrow 2H^+ + \frac{1}{2}O_{2(g)} + 2e^- \tag{2.12}$$

$$\text{Cathode} : 2H^+ + 2e^- \longrightarrow H_{2(g)} \tag{2.13}$$

$$\text{Total} : H_2O_{(l)} \longrightarrow H_{2(g)} + \frac{1}{2}O_{2(g)} \tag{2.14}$$

Proton conductive membranes possess highly acidic properties [16]. Because of the acidic environment created by the membrane and the high levels of electricity used during the electrolysis process, it is necessary to use expensive noble metals such as platinum and iridium as electrodes and catalyst materials. However, efforts are being made to reduce the amount of noble metals due to cost and limited availability, especially in the case of iridium [16]. This highlights the fact that although PEM is an established technology, there are still some challenges that need to be addressed. The PEM electrolyzer operates at a temperature range of 50 to 80 °C and a stack pressure between 30 to 80 bar [10]. Finally, the electrical efficiency of the stack falls between 56 and 60 %. This reflects the relationship between the electrical input and hydrogen output.

Comparing AEL and PEM

This section compares the AEL and PEM electrolyzer technologies, specifically pressurized AEL. The comparison will be continued later in this thesis. The comparison is conducted to evaluate whether one of the technologies is better suited for production with renewable energy. The technical specifications for AEL and PEM found in the literature are listed in Table 2.2 [10]. These two technologies have overlapping temperature ranges. However, the PEM system has a wider range of stack operating pressure, while the AEL system has a higher stack efficiency. Additionally, the AEL system has a longer predicted lifetime than the PEM system, which can be attributed to the harsh environment of the PEM stack. It is important to note that, for both AEL and PEM electrolyzers, the stack needs to be replaced to achieve the expected lifetime.

This thesis will extend the comparison of the two technologies, which will involve gathering information from electrolyzer suppliers. The comparison will focus on various technological

Table 2.2: Comparison of the electrolyzer technologies pressurized AEL and PEM [10]

Electrolyser	AEL	PEM
Status	Well established	Established
Electrolyte	KOH	Polymer
Charge carrier	OH^-	H^+
Cell temperature [°C]	60-80	50-80
Stack pressure [bar]	< 30	30-80
Stack efficiency [%]	63-70	56-60
System lifetime [years]	20-30	10-20

specifications such as stack efficiency, system efficiency, the lifetime of the stack, capital expenditures (CAPEX), and operational expenditures (OPEX). Additionally, operational parameters such as dynamic range and response time will be compared since response to fluctuating load is important. The gathered information will be presented in Chater 4, results.

Compression

The pressure of the hydrogen gas product varies but is around 30 bar, depending on the production method used. However, most applications require hydrogen at 350 to 700 bar, depending on the storage method and end use [16]. In such cases, hydrogen must be compressed before use, requiring a compressor as part of the electrolyzer system. The compression of hydrogen has a high electricity demand and is a significant expense in the electrolyzer system, both as an investment and operational cost. The storage and utilization of hydrogen will be discussed in Section 2.2.3 and Section 2.2.4, respectively.

2.2.2 Electrolyzer operation

While operating, the electrolyzer has three primary modes: production, standby, and off [19]. This is a general electrolyzer mode setup, which may vary between suppliers. Also, the terms of the different modes can vary between technologies. However, in this thesis, these terms are used for both AEL and PEM. An electrolyzer's installed capacity represents the maximum amount of electrical energy it can receive and utilize to produce hydrogen. Additionally, the electrolyzer is only in production mode within a specific operational window known as the dynamic range, measured as a percentage interval of the electrolyzer capacity. As long as the power input remains within this dynamic range, the electrolyzer produces hydrogen.

When the power input falls below the lower percentage of the dynamic range, the electrolyzer will switch to standby mode. Standby mode can be further divided into hot and cold standby. The stack is kept pressurized in both cases, shortening the startup time if production continues. However, when the stack is kept pressurized, although there is limited power supply to the stack, there may still be a marginal production of hydrogen. This hydrogen can build up inside the cell and cause unwanted reactions during production. In hot standby, the electrolyte is continuously circulated, effectively removing unwanted gas. Therefore, by increasing the power supply to the

stack, production can continue instantly. This is not the case for cold standby, where saturated gas may be released inside the cell. Therefore, the electrolyte must be circulated before the power supply to the stack is increased and hydrogen production can continue. Additionally, the electrolyzer consumes more power in hot than cold standby, making hot standby more expensive. The startup time from hot and cold standby to production depends on electrolyzer technology and the supplier.

The last primary mode of the electrolyzer stack is called off. The stack is completely powered down in this state, but some auxiliary systems still have an electricity supply, and detectors and sensors are turned on for safety purposes. This mode is primarily used for maintenance purposes but can also be utilized when the electrolyzer is not expected to be used for an extended period. However, it should be noted that the startup time from off to production is significantly longer than when it switches from standby to production.

2.2.3 Hydrogen storage

Storing hydrogen at atmospheric pressure using conventional methods poses significant challenges due to its unique characteristics. Firstly, hydrogen is the smallest element with a molecular weight of 2 g/mol, much lower than natural gas (CH_4), with a molecular weight of 16 g/mol [10]. This makes hydrogen a highly volatile substance that can penetrate materials and escape through the tiniest holes. In atmospheric conditions, hydrogen has a low volumetric density of 0.084 kg/m^3 compared to natural gas, which has 0.651 kg/m^3. Storing 1 kg of hydrogen at atmospheric pressure would require 12 m^3, a large impractical footprint. There are three primary methods of storing hydrogen: compressed hydrogen (CH_2), liquefied hydrogen (LH_2), and chemical storage [10]. Other methods for storing hydrogen have been excluded from this thesis because they are not relevant to the case on which this thesis is based.

Compressed hydrogen

The most common hydrogen storage method is CH_2 [10]. As previously mentioned, the electrolyzer produces low volumetric energy density hydrogen gas. To store the hydrogen as gas, it is pressurized, resulting in a smaller physical footprint. This allows for the storage of hydrogen in more practical volumes. There are several methods for hydrogen compression, such as mechanical pistons, non-mechanical compressors, and electrochemical hydrogen compressors [20].

CH_2 is typically stored at a pressure between 200 to 700 bars at room temperature, requiring robust pressure vessels [16]. These vessels are usually made of non-magnetic steel, aluminum alloys, and copper alloys, as these materials have good corrosion resistance and formability, making them suitable for high-pressure applications [10]. High-strength steel is not used because it is exposed to hydrogen embrittlement. This means that hydrogen molecules can penetrate the material and weaken it. Moreover, storage vessels crafted from composite materials emerge as a favorable alternative [21]. These vessels are often made of a blend of materials, for instance, metal hydrides and carbon nanotubes. They present numerous advantages over conventional storage vessel techniques, with increased capacity, reduced weight, and enhanced safety features.

Liquefied hydrogen

Another method for increasing the volumetric density of hydrogen is cooling it down to −253 °C, which results in its liquefaction [16]. However, LH_2 faces some challenges as 30 % of the energy stored in the hydrogen is lost in the liquefaction process. Additionally, −253 °C is the boiling point of hydrogen, which means that some liquid hydrogen will turn into gas. This process is known as boil-off, and it increases the pressure inside the tank. To prevent boil-off, hydrogen must be stored in an isolated tank, which can be costly [10]. Additionally, the container should have a relief valve to release the evaporated hydrogen and maintain a safe pressure level.

Chemical storage

Hydrogen can also be combined with other substances through chemical reactions to capture hydrogen in chemical storage. These methods result in higher volumetric density than CH_2 and LH_2 [10]. Additionally, chemically bound hydrogen is favorable for long-term storage and makes it easier to manage. However, separating hydrogen from the chemical substance can be an energy-demanding process, reducing overall energy efficiency. The following paragraphs present a selection of compounds and materials for storing hydrogen chemically: ammonia, methanol, and liquid organic hydrogen carrier (LOHC).

Hydrogen can be safely stored in traditional tanks by chemically binding it to ammonia or methanol [10]. These carriers can be stored in a liquid state at atmospheric pressure and room temperature for methanol and at -33 °C for ammonia, making them a stable storage alternative. CO_2 emissions may result from using methanol, while ammonia has no direct emission factors, making it more environmentally friendly. An advantage of methanol and ammonia is that they can be utilized whit existing liquid fuel infrastructure and be used directly, eliminating the energy loss involved in converting the carrier back to hydrogen.

When storing hydrogen in LOHC, hydrogen gets added to a hydrocarbon in a process called hydrogenation [16]. This results in a substance with similar properties to petrol or diesel, which makes it possible to store in large quantities and use in existing infrastructure [16]. However, precious metals are required as catalysts, increasing the cost of LOHC [10]. Additionally, the dehydrogenation process, where the LOHC is converted back to hydrogen, is energy-demanding.

Several parameters must be considered when choosing a hydrogen storage method. For example, the cost of the storage system significantly impacts the initial price of hydrogen. Additionally, the intended end use of the hydrogen influences key attributes such as the durability of the storage system, refueling times, and the phase of the hydrogen, whether it is stored as a gas or liquid. As explained in the following section, many hydrogen end-users require compressed hydrogen. There are exceptions, but for land transport and the maritime sector, hydrogen needs to be compressed. Consequently, compressed hydrogen is the storage method most relevant for this thesis. Therefore, the other methods will not be discussed further.

2.2.4 Hydrogen utilisation

Hydrogen is an energy carrier with a wide range of applications. As mentioned, hydrogen has been used in industrial sectors for decades. It is commonly used as a feedstock in producing ammonia for fertilizer manufacturing, in methanol synthesis, and in processing crude oil in

refineries [16]. Moreover, there is growing recognition of hydrogen's potential as a raw material in various industrial processes, offering an alternative to fossil fuels and serving as an energy carrier. In Norway, there are currently projects in the private industry sector exploring the application of hydrogen. For instance, INEOS, a smelter in Tyssedal, is working on a project to replace coal with green hydrogen in titanium dioxide production [22]. Similarly, Horisont Energi, in cooperation with Equinor and Vår Energi, has started The Barents Blue project, which aims to establish the first zero CO_2 emission ammonia plant using hydrogen.

In addition, hydrogen can be applied in the power- and transportation sectors, where fuel cells can extract electrical energy from the hydrogen. Fuel cells convert chemical energy into electrical and thermal energy with an electrical efficiency between 40 and 65 % [16]. Additionally, when hydrogen is used in a fuel cell, the only byproducts are typically water and heat, making it an emissions-free alternative. A fuel cell comprises two electrodes, an anode and a cathode, separated by a membrane. Figure 2.6 shows this basic setup of a fuel cell. The two main types of hydrogen fuel cells are the proton exchange membrane fuel cell (PEMFC) and the alkaline fuel cell (AFC).

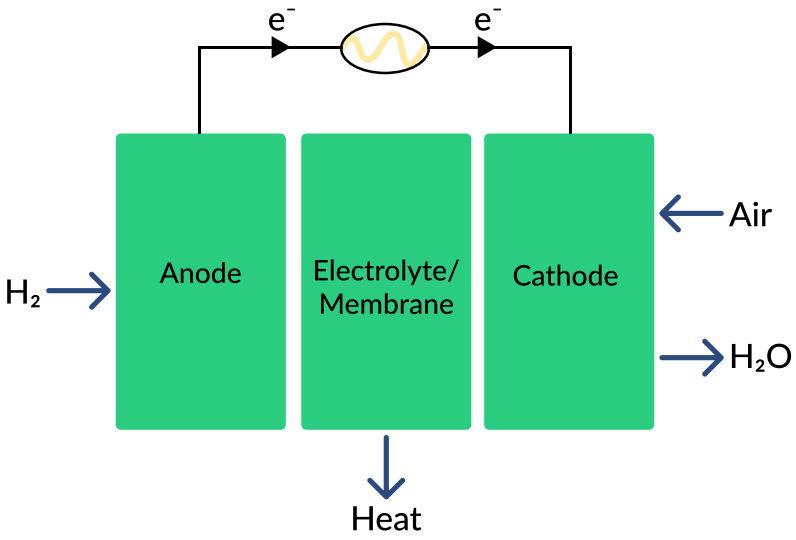

Figure 2.6: Basic concept of a fuel cell

Hydrogen can be an energy storage medium in the power sector [10]. One of the key benefits of hydrogen is its ability to store energy for an extended period, making it a valuable tool in addressing energy shifts and seasonal variations. Unlike batteries, which can only store electricity on an hourly or weekly basis, hydrogen can be stored for weeks, months, or years [10]. Excess electricity can be stored as hydrogen when production is higher than demand, and it can be utilized during high energy demand as grid stabilization or as a seasonal storage medium. An ongoing project demonstrating this is Technip FMC's Deep Purple Pilot [23]. The project aims to deliver stable, renewable energy in the ocean space by employing wind turbines and utilizing hydrogen to store electricity to even out fluctuations.

Additionally, hydrogen can be used to transport power from renewables without grid connections. This is a significant advantage, as it allows for the efficient use of renewable energy sources, even in areas without an existing electrical grid. Moreover, hydrogen can be used in micro-grid applications to electrify remote and rural locations where it is difficult to provide electricity

through grid connections [10]. This is achieved by producing electricity on-site from renewable sources, storing it in hydrogen through electrolysis, and producing electricity back with a fuel cell.

The most prominent areas of applying hydrogen and fuel cells in the transport sector include medium- and heavy-duty trucks, long-distance buses, large passenger cars, taxi fleets, regional trains, maritime vessels, and even forklifts [16]. While fuel-cell passenger cars typically operate at a standard pressure of 700 bar, other modes of transportation, such as buses, trains, ships, and trucks, rely on tanks with pressures ranging from 300 to 350 bar. In Norway, the growth of hydrogen-powered vehicles has been slower than that of electric vehicles. There are only five hydrogen-powered buses, 140 registered cars, and five filling stations nationwide [22]. However, among the notable advancements in hydrogen-powered transportation is the Norwegian ferry MF Hydra, which has gotten international attention as the world's first hydrogen-powered car ferry [24]. The Norwegian government released a roadmap and vision for green industry development [25]. According to the roadmap, hydrogen will play a pivotal role in the decarbonization of industrial and maritime sectors until 2030, with a projected expansion into land-based heavy-duty transport closer to 2050.

Lastly, oxygen and heat, which are byproducts of the electrolysis process, can also be utilized. Heat is needed for various industrial applications. Additionally, heat and oxygen are required for the fish farming industry which is a big industry in Norway.

2.3 Literature review

This subchapter reviews projects on hydrogen production from small-scale hydropower plants, along with relevant literature on modeling hydrogen production from energy sources with variable output. The literature study aims to provide an overview of similar work and identify knowledge gaps in the field, to further underscoring the importance of the aims and objectives presented in 1.3 and the work conducted in this thesis.

NVE has collaborated with Småkraftverkforeninga to conduct a three-year R&D project on hydrogen production from small-scale hydropower plants. The study aimed to determine if hydrogen production is a feasible way to utilize power from small-scale power plants and to investigate if the production can be carried out in areas with limited or no connection to the grid. In the project, PEM electrolyzer was chosen as the production technology. The study consists of three separate reports. The following three paragraphs summarize the study.

The article "Hydrogenproduksjon ved småkraftverk. Del 1: Casestudie Rotnes Bruk", NVE [26] discusses potential technological solutions for producing and distributing hydrogen from the Rotnes Bruk hydropower plant. Two cases are presented: in case 1, hydrogen is produced locally and distributed to an external filling station; in case 2, hydrogen is produced locally and distributed on-site. The article also explores the economics of both cases. After comparing the two scenarios, it was found that case 1 is more feasible, while case 2 poses challenges due to the need for transportation via ship. With 50 % investment support, the price of hydrogen sold in case 1 (86 NOK/kg) will be higher than the market price (72 NOK/kg) [26]. The article concludes that a small-scale hydropower plant, like the 200 kW facility in Rotnes, can be attractive in the early stages of hydrogen market development. However, it cannot compete with larger facilities

in the long run because of its high investment costs.

"Hydrogenproduksjon ved småkraftverk. Del 2: Flerbruk av hydrogen, oksygen og varme ved Smolten settefiskanlegg", NVE [27] presents the possibility of producing hydrogen at the Storvatne power plant. The power plant is located near a fish farm, and the report explores the potential for using byproducts from the electrolyzer, such as oxygen and heat, in the fish farm. The report suggests that hydrogen could potentially be used as a backup power source at Smolten or as fuel for ships at the facility. Hydrogen could also be used for transportation locally. The report indicates this as an economically viable solution, but further detailed study is recommended.

Part three of the R&D is the article "Hydrogenproduksjon ved småkraftverk. Del 3: Potensial for lønnsom utbygging av vassdrag i Rullestad", NVE/ SINTEF [28]. The article discusses how hydrogen production can potentially aid in constructing three power plants - Skromme, Kvernhuselva, and Bordalen. These power plants have yet to be built due to a lack of connection to the grid. However, the article argues that the region has promising end-users, a highway nearby, a dock near the sites for product shipping, and a fish farm that can use the byproducts generated from the production process. Based on the information presented in the report, investing in electrolysis and building the power plants could prove profitable.

In the article "Alkaline Water Electrolysis Powered by Renewable Energy: A Review", J. Brauns discusses the challenges conventional electrolyzers face when dealing with variable inputs from renewable sources [29]. The article highlights problems such as high levels of gas impurities that can lead to system shutdown and reduced annual operation time. Additionally, the electrodes are the components most affected by repetitive start-stop cycles. In conclusion, the article emphasizes that the main goal is to enhance the operation time through intelligent system design and operational concepts, enabling alkaline electrolyzers to handle dynamic input directly.

In the article "Modeling of advanced alkaline electrolyzers: a system simulation approach" by Ø. Ulleberg, a mathematical model for an advanced alkaline electrolyzer, is presented [30]. The model predicts the electrolyzer system's cell voltage, hydrogen production, efficiencies, and operating temperature. The predicted data is compared with reference data from a stand-alone photovoltaic-hydrogen energy plant in Jülich, and the results show that the model can successfully predict data. Additionally, the article explores how the model can be used for system design and optimization of control strategies, which is beyond the scope of this thesis.

In the article "New multi-physics approach for modeling and design of alkaline electrolyzers," M. Hammoudi presents a unique model that can characterize the electrolyzer based on its structural parameters such as geometry, materials, and behavior under different operating conditions [31]. This differs from conventional models like Ulleberg, which require a minimum of a few weeks of experimental data to characterize the electrolyzer. Hammoudi's advanced model also considers a wider range of operating parameters, including temperature, pressure, and concentration. In contrast, most other models in the literature only consider temperature. The model was created using Matlab Simulink and can be used to predict energy consumption, efficiency, and hydrogen production rate. The model was validated using two industrial electrolyzers, with an relative deviation of less than 0.9 %.

The article "Modelling and Simulation of an Alkaline Electrolyzer Cell" by Z. Abdin describes a one-dimensional model for hydrogen production using an alkaline electrolyzer cell [32]. The

model is created in Simulink and consists of several modules based on the physical properties of the anode, cathode, electrolyte, and separator. These modules are interconnected to examine how these specific parts of the electrolyzer interact with each other. The model parameters are based on real-world characteristics of the system whenever possible. The model is tested against experimental data and performed better than other models tested with the same data.

Through this literature review, various knowledge gaps have been identified in the field of hydrogen production from fluctuating power. It is commonly believed that electrolyzers respond poorly to fluctuating power, leading to degradation. However, after reviewing the literature and consulting with various companies, it is clear that there is no precise understanding of how fluctuating power affects the lifespan of electrolyzers. Consequently, there is currently no method for quantifying the degradation of the electrolyzer due to fluctuating power input. This implies that this thesis does not accurately quantify how the fluctuating power at location A will lead to degradation of the stack, but there will be a simplified overall assessment. Furthermore, there is limited literature on the expected variability from a small-scale power plant. The literature on sizing the electrolyzer for a small-scale hydropower plant is also limited. These knowledge gaps highlight the importance of the aims and objectives of this thesis.

Chapter 3

Methodology

The following chapter presents the methodology used to assess the aims and objectives posed in Section 1.3. It begins with a detailed depiction of the case, followed by an explanation of the hydroelectric dataset offered by SKL and the data provided by HYDS. Additionally, the model used to simulate hydrogen production is explained, followed by a description of the method behind the cost analysis of various electrolyzer capacities.

3.1 Case description

The case presented in this thesis is developed in collaboration with SKL and HYDS, who aim to assess the feasibility of building a hydropower plant to produce hydrogen from trapped power. This section provides a detailed description of the case.

Location A is situated in a remote area surrounded by mountains, vegetation, and water. This location faces challenges related to accessibility and grid connection. The grid connection is weak, allowing for the purchase of a small amount of power, but selling power to the grid is not feasible. For this thesis, it is assumed that a maximum of 0.5 MW can be purchased from the grid.

Hydrogen production is a potential solution to utilize the trapped power. When analyzing the feasibility of hydrogen production, it is crucial to conduct a detailed analysis of the input fluctuations from the hydropower plant. This analysis is vital for selecting the appropriate electrolyzer technology and determining the frequency of its use and the extent to which the hydropower plant's power is utilized.

For the project to be feasible, there must be end-users who need hydrogen. Location A has a nearby dock that can be utilized. The location experiences significant daily ship traffic, including fishing boats, ferries, cargo ships, and fjord cruises. Additionally, there is a heavily trafficked highway nearby used by heavy-duty trucks, as well as nearby industrial activity.

3.2 Data sets

A hydroelectric dataset and electrolyzer data have been shared as a result of collaboration with industry partners. The following sections explain the structure of the hydroelectric dataset and an explanation of the the years from the dataset investigated in this thesis. This is followed by a general explanation of how SKL calculated the installed capacity of the turbine at location A and calculated the hydroelectric dataset. In addition, a visual representation of the dataset is presented. Lastly, the electrolyzer data shared by HYDS is elaborated.

3.2.1 Hydropower plant

SKL made a significant contribution to this thesis by providing a dataset, which included the electricity generation of a potential hydropower plant at location A. The data was received in kWh, but it is plotted as GWh as it is a more common unit when discussing power production. The data was received in an Excel file with hourly production over 20 years. The dataset covers the period of 1st of January 2002 to 31st of December 2021; however, this thesis will mainly focus on 2010, 2007, and 2008. These years were chosen based on their total yearly production, as listed in Table 3.1.

To understand the variability in production from the hydropower plant at location A, the P10, P50, and P90 years are utilized. The year 2010 represents the P10 year, or the dry year, indicating that only 10 % of the years in the dataset have lower yearly production than 2010. The use of the typical dry year instead of the driest year avoids dimensioning for extreme values.

Moreover, 2008 represents the P50 year, or median year. Utilizing the median year instead of the average year offers a more accurate representation of typical production. Unlike the average, the median is not influenced by extreme values or outliers. For instance, if a 20-year period includes five years of extreme drought and only one year of extreme precipitation, using the average year would result in skewed dimensions. Therefore, the median year provides a more reliable measure to avoid such errors.

Lastly, 2007 is the P90 year, indicating that only 10 % of the years in the dataset have higher yearly power production than 2007. It is a typical wet year. Similar to the approach for the P10 year, using the P90 year instead of the wettest year avoids extreme values that could lead to a false interpretation of typical power production during a wet year. Utilizing a distribution of low, medium, and high-power production years to determine the optimal electrolyzer capacity ensures coverage of the variability in power production at location A. Using this method, the conclusion regarding the electrolyzer is expected to be sufficient for both dry, median, and wet years.

Table 3.1: The years investigated in this thesis

Years	Statistical parameters	Total yearly production [GWh]
2010	P10	11.63
2008	P50	15.41
2007	P90	19.48

Installed capacity

When SKL estimates the installed capacity for a potential hydropower plant, they aim to utilize as much water as possible. However, certain constraints make it challenging to use all the available water. For instance, the watergate leading to the turbine has economic limitations. NVE has formulated equations to estimate these costs, and SKL has used these formulas to create models that solve the optimization problem by maximizing energy production while considering economic constraints. These models also account for the principle of minimum water flow, a part of the "Vannressursloven," which governs the use of watercourses and groundwater. This principle mandates that a certain minimum amount of water must continue flowing in a regulated watercourse. The installed capacity at location A was calculated by SKL using these models, constraints, and Equation 2.2 explained in Section 2.1.2. The potential hydropower plant at location A has an installed capacity of 6.3 MW, indicating the turbine's size.

Energy production: estimating the dataset

SKL calculated the dataset with energy production from location A used in this thesis. This section provides a general description of the method behind the calculations of the dataset. Location A is in a precipitation field, now called field X, without a measuring station. In this case, the amount of precipitation in the area is estimated using nearby fields. SKL has a procedure where a competent person from the company screens nearby fields based on their characteristics and identifies 2-3 reference fields similar to the precipitation field of interest but with measuring stations.

Once the 2-3 reference fields are identified, the middle water flow is calculated for the chosen fields using Equation 2.1 explained in Section 2.1.1. Further, the average of the middle flow rate of the reference fields is calculated, denoted as $Q_{\text{refrence fields}}$. Then, the middle water flow for field X is calculated using the same equation, denoted as $Q_{\text{field X}}$. The values for specific runoff and areas of the fields needed in Equation 2.1 are found on the NVE Atlas webpage. From $Q_{\text{refrence fields}}$ and $Q_{\text{field X}}$, the scaling factor (f) can be calculated, as shown in Equation 3.1.

$$f = \frac{Q_{\text{field X}}}{Q_{\text{refrence fields}}} \tag{3.1}$$

The scaling factor is used to estimate water flow per hour or day in a time series that describes the quantity of available water in field X. Estimating the amount of available water in field X enables the calculation of potential energy generation at location A using comprehensive models, which are not detailed in this thesis.

Visual representation of the dataset

Figure 3.1 illustrates the monthly variation in power production throughout 2010, 2008, and 2007. It shows the total output in GWh per month per year, highlighting the seasonal variations in power production. Power production is relatively low from January to March. From March, it begins to increase and peaks in June. There is a significant drop in power production from June to August. During autumn and December, power production is inconsistent, with no clear pattern.

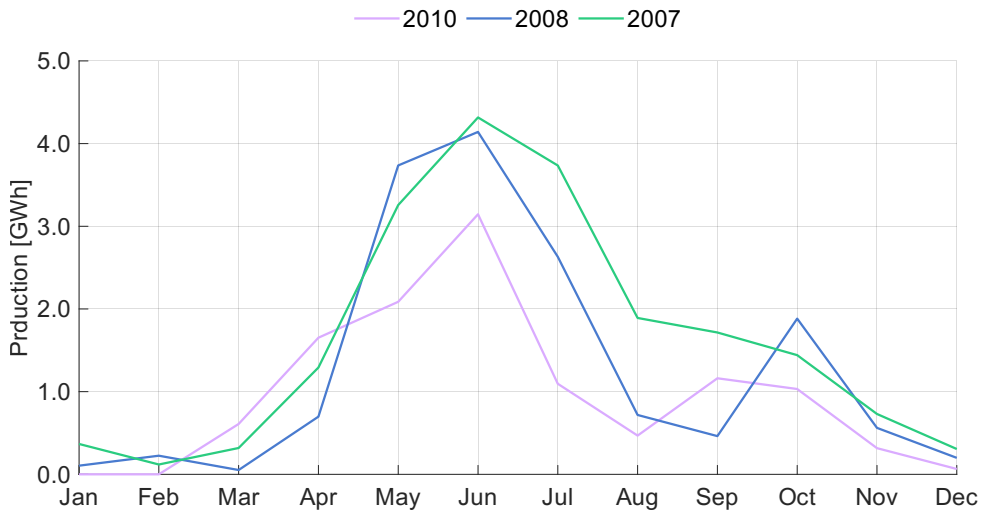

Figure 3.1: Seasonal variation in the production of energy in the dry year (2010), the median year (2008), and the wet year (2007)

Figure 3.2 depicts the hourly power production in GWh for the year 2008. It illustrates that aside from seasonal fluctuations, power generation can also exhibit hourly variability. Notably, the ceiling effect visible in the graph serves as a clear indicator of the 6.3 MW capacity of the hydropower plant.

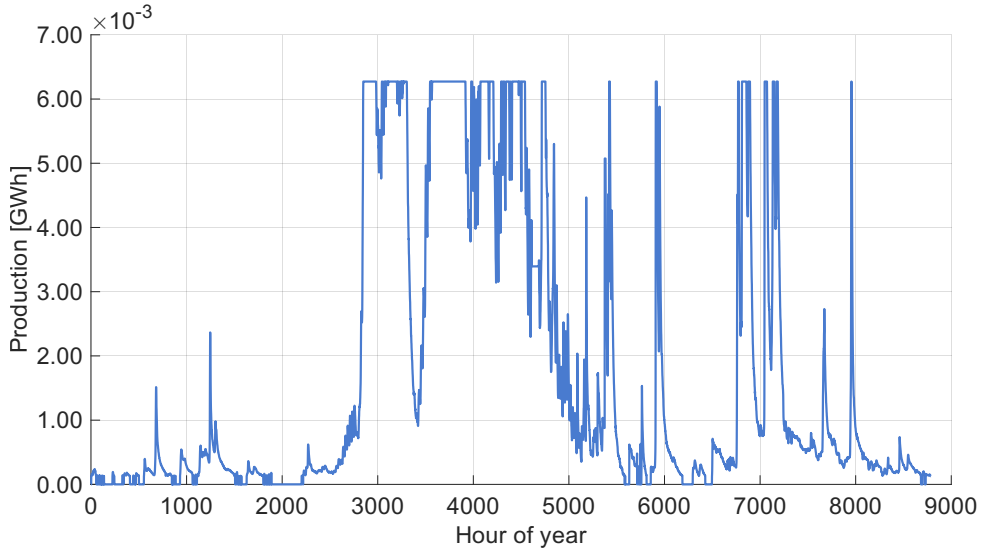

Figure 3.2: Hourly variations in the production of energy in the year the median year (2008)

3.2.2 Electrolyzer data

This thesis focuses on pressurized AEL, and technical details about a typical pressurized AEL electrolyzer are essential for the model's accuracy. The typical values used in this thesis, including the number of cells in series per stack, stack temperature, and electrode area, are obtained from a supplier and treated as confidential. An NDA was signed with the supplier company, and HVL collaborates closely with the company to ensure the accuracy and reliability of the data used in the model.

3.3 MATLAB modell

In this thesis, hydrogen production and electrolyzer operation were simulated using a MATLAB model. MATLAB is a programming platform designed for analyzing and designing systems or products, owned and developed by MathWorks [33]. The model of this thesis is based on a model created by Liina Sangolt, a Ph.D. student [34]. Further, Sangolt based her model on Ulleberg's article on modeling alkaline electrolyzers [30].

The initial model provided by Sangolt processed power production data for a specific year, filtering it to only include the power within the electrolyzer's dynamic range. Further, the model calculated the annual hydrogen production, which is detailed in Section 3.3.4. In this thesis, Sangolt's model was further developed. Firstly, Sangolt used a dataset with a different resolution than the dataset provided by SKL in this thesis, necessitating adjustments to the code filtering the power input from the hydropower plant. Additionally, the filtering of power production has been expanded to include the different modes of the electrolyzer. The modes and their impact on the power available for hydrogen production are detailed in Section 3.3.2.

In addition to filtering the power range produced by the potential hydropower plant for hydrogen production, the model has been enhanced to incorporate a standby mode. This provides a broader perspective on electrolyzer operation and enables the examination of periods when the electrolyzer is not producing hydrogen but is still consuming electricity from the hydropower plant or the grid. Additionally, the purchase of power during standby will impact the cost analyses, as the quantities of power needed during standby are required for the cost calculations. The following sections summarize the assumptions made in the model, the different electrolyzer modes and their incorporation into the model, the electrolyzer capacities utilized in this thesis, and the calculation of hydrogen production within the model.

3.3.1 Assumptions

Before simulating hydrogen production from location A, a few assumptions were made in this thesis. These assumptions are listed below:

- The location has a grid connection, and purchasing a maximum of 0.5 MW of electricity from the grid is possible.
- The electrolyzer operates at a constant temperature.
- A simplified electrolyzer model has been created with three modes: production, standby, and off.
- When the power input to the electrolyzer is less than 16 % of its capacity, it goes into standby. In standby, the electrolyzer uses 45 kW. The electrolyzer remains in standby until production resumes.
- The electrolyzer is turned off twice a year for maintenance, during week 10 and week 35.
- It is assumed that the electrolyzer takes less than an hour to start up from standby to production. Therefore, due to data resolution at one hour for the hydroelectric data, the start-up time of the electrolyzer from standby mode is neglected.

3.3.2 Electrolyzer modes

The power input from the dataset provided by SKL requires processing before calculating hydrogen production. In this thesis, filters have been incorporated based on different electrolyzer mode conditions. The following paragraphs explain the conditions of these modes.

Production

Filtering the power input based on the dynamic range of the electrolyzer capacity was included in the Sangolt model. During production mode, the electrolyzer utilizes power input ranging from its capacity limit to as low as 16 % of its capacity limit. The excess energy will be filtered out if the power input exceeds the capacity limit. However, if the power input is less than 16 % of the electrolyzer's capacity, it will automatically enter standby mode, which means it will stop producing hydrogen.

Standby

In this thesis, standby simulation has been incorporated into the model. The electrolyzer enters standby mode when production is below 16 % of its capacity and remains in this mode until an hour with power input exceeding 16 %, after which the electrolyzer resumes production. The standby mode can be used for as many consecutive hours as required. In order to keep the electrolyzer in standby mode, it requires some power input. There are two types of standby modes: hot standby, which requires 20 to 45 kW, and cold standby, which requires 10 to 30 kW. For the purpose of this thesis, 45 kW was chosen as the standby mode to model the most extreme situation. This power input is required for a 1 MW electrolyzer.

The model contains three different filters for electricity consumption in standby mode. The filters explained apply to a 1MW electrolyzer and will be scaled proportionally when higher capacities are used. Firstly, if the hydropower plant generates power between 16 % of electrolyzer capacity and 45 kW, all the required power is purchased from the hydropower plant. Secondly, if the hydropower plant only produces 10 to 45 kW, electricity is purchased from the grid to supplement the hydropower plant. Lastly, if the hydropower plant produces less than 10 kW, all the electricity needed to keep the electrolyzer at 45 kW is purchased from the grid.

Off

The electrolyzer requires maintenance twice a year, with each maintenance period assumed to last one week. The maintenance periods are scheduled to be exactly six months apart. During these periods, the electrolyzer is turned off, and no hydrogen is produced. Therefore, in this thesis, these periods are incorporated into the model, accounting for the stop in hydrogen production. A function was created in Matlab to determine the periods most suitable for maintenance. The function sums the weekly data from weeks 1 to 53 for 2010, 2008, and 2007. It then calculates the average for each week across the three years and sorts the weeks based on their production values, from the smallest to the highest. As a result, week number 10 had the lowest production, so weeks 10 and 35 are scheduled for maintenance. Table 3.2 displays the periods in each year where the production is set to zero due to maintenece.

Table 3.2: The maintenance period for the years 2010, 2008, 2007

	Maintenance period	
Years	**Week 10**	**Week 35**
2010	08.Mar - 15.Mar	30.Aug - 06.Sep
2008	03.Mar - 11.Mar	01.Sep - 08.Sep
2007	05.Mar - 13.Mar	27.Aug - 03.Sep

3.3.3 Electrolyzer capacities

After recommendations from HYDS, three electrolyzer capacities are used in the model: 1 MW, 3 MW, and 5 MW. For a 1 MW electrolyzer, values for the number of cells in series per stack, the area of the electrode, and the power required to maintain standby mode were provided. When modeling for 3 MW and 5 MW, these values are scaled proportionally with electrolyzer capacity.

3.3.4 Hydrogen production

The calculation of hydrogen production in this thesis is based on Sangolt's model [34], which is based on Ulleberg's model [30]. Using the assumptions from Section 3.3.1, confidential values from HYDS, and constants Sangolt has calculated from [30], the voltage and current required to run the electrolyzer at a given capacity can be estimated. This is achieved using equations 3.2 and 3.3 [30], which form a set of equations with two unknowns: Voltage (U) and current (I).

$$U = \frac{b_{\mathrm{M1}}}{n_{\mathrm{c}} \cdot I} \tag{3.2}$$

$$U = U_{\mathrm{rev}} + \frac{r_1 + r_2 T}{A} I + s \log\left(\frac{t_1 + t_2/T + t_3/T^2}{A} I + 1\right) \tag{3.3}$$

b_{M1} contains the power input for the electrolyzer after filtering the dataset, n_c represents the number of cells in series, U_{rev} is the ideal voltage of an electrolyzer at a given capacity, for a 1 MW electrolyzer at standard conditions U_{rev} is 1.295 V [30]. Further, A is the area of the electrode. Additionally, the constants r, s, and t were calculated by Sangolt following a curve fitting procedure from [30]. r are ohmic resistance of the electrolyte, while s, and t are related to overvoltage on the electrodes. Lastly, T is the operating temperature of the stack. The electrolyzer efficiency is calculated using Faraday efficiency (η_{F}), shown in equation 3.4 [30].

$$\eta_{\mathrm{F}} = \frac{(I/A)^2}{f_1 + (I/A)^2} f_2 \tag{3.4}$$

f_1 and f_2 are constants related to Faraday efficiency, and are obtained from [30] based on the operation temperature of the electrolyzer cell. Moreover, I is calculated from the set of equations

3.2 and 3.3. Further, the hydrogen production rate (m_{H_2}) is calculated using Equation 3.5 [30].

$$m_{H_2} = \eta_F \frac{n_c \cdot I}{2 \cdot F} M_{H_2} \cdot 3600 \quad [\text{kg } H_2/\text{h}] \tag{3.5}$$

The calculation of hydrogen production involves multiplying the electrolyzer efficiency by the number of cells in series per stack and then by the total electrical current in the external circuit. This result is divided by the number of electrons transferred per reaction and the Faraday constant. The number of electrons is two, obtained from [30]. Finally, the result is multiplied by M_{H_2}, the molar mass of hydrogen, which is equal to 0.002 kg/mol, and by 3600, representing the number of seconds in an hour. In this thesis, m_{H_2} is calculated for every hour in the dataset of the given year, the results are summed to calculate the annual production of hydrogen. Similarly, the oxygen production rate (m_{O_2}) is calculated as shown in Equation 3.6 [30].

$$m_{O_2} = \eta_F \frac{n_c \cdot I}{4 \cdot F} M_{O_2} \cdot 3600 \quad [\text{kg } O_2/\text{h}] \tag{3.6}$$

M_{O_2} denotes the molar mass of oxygen, which is 0.032 kg/mol. Moreover, the number of electrons transferred in this part of the reaction is four, a constant from [30]. In this thesis, the annual and monthly hydrogen production is calculated using power production data from the potential hydropower plant at location A for the years 2010, 2008, and 2007, as explained in Section 3.2.1. Moreover, the hydrogen production for each year is simulated for three capacities: 1 MW, 3 MW, and 5 MW, as detailed in Section 3.3.3. Additionally, oxygen production is simulated for the same scenarios.

3.4 Cost analysis of different electrolyzer capacities

In the comparison of the different electrolyzer capacities, it is essential to conduct a cost analysis in addition to assessing hydrogen production and electrolyzer operation. This thesis performs a simple cost analysis of various electrolyzer capacities. The calculations are done in MATLAB. In the following paragraphs, the electricity prices from both the hydropower plant and the grid, as well as the calculations utilized in the economic assessment, will be presented. These calculations include the variables of CAPEX, OPEX, the electricity consumption of the stack, and electricity used during compression, as illustrated in Figure 3.3. All the parameters are expressed in levelised cost of hydrogen (LCOH), a variable that shows the cost of producing 1 kg of hydrogen [35]. Calculating the LCOH is a way to assess the economic viability of a proposed plant. In this thesis, the LCOH represents the minimum price at which the hydrogen producer can sell the hydrogen to break even for the year being utilized in the calculations.

3.4.1 Prices

In 2023, NVE released a long-term power market analysis that predicted energy prices until 2040 [36]. According to the report, energy prices are expected to be 82 øre/kWh, 57 øre/kWh, and 49 øre/kWh for 2030, 2035, and 2040, respectively. To conduct a sensitivity analysis, the LCOH for electricity consumption is calculated for low, middle, and high grid prices.

Additionally, the cost of purchasing energy from the hydropower plant will be determined through negotiations between the power supplier and the hydrogen producer. However, for this

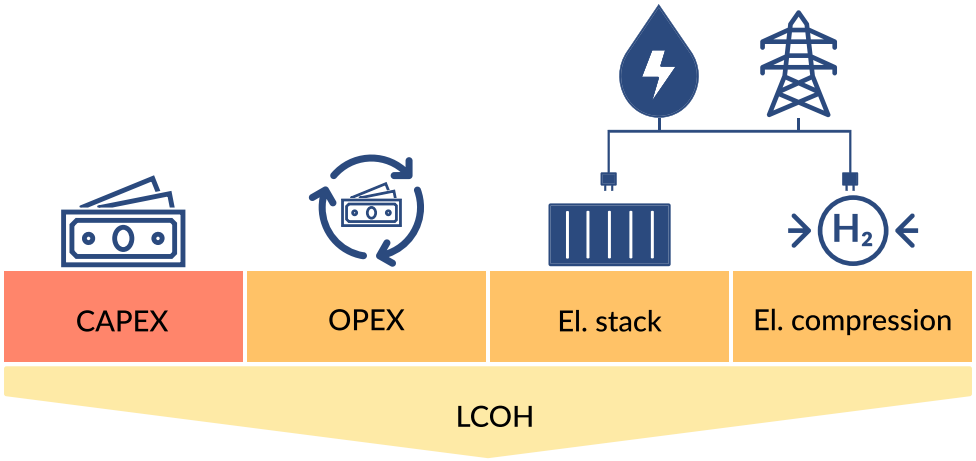

Figure 3.3: The variables in the simplified economic comparison between different electrolyzer capacities. The red color indicates investment cost (CAPEX), while the orange color indicates annual expenses (OPEX, electricity to stack, and electricity to compression).

thesis, the levelized cost of energy (LCOE) tool developed by NVE will be used to assume the energy price [37]. According to the tool, the LCOE for hydropower plants with a capacity of less than 10 MW is 40 øre/kWh. Therefore, in this thesis, the price of buying electricity from the small-scale hydropower plant will be 40 øre/kWh. The electricity prices used in the cost analysis are presented in Table 3.3.

Table 3.3: Cost of buying electricity from the hydropower plant, and the grid

	Cost of electricity [NOK/kWh]
Grid (low)	0.49
Grid (middle)	0.57
Grid (high)	0.82
Hydropower plant	0.40

3.4.2 Assumptions

Assumptions were made to simplify the cost analysis. These assumptions are listed below, and some of them are explained in more detail in the paragraphs that follow:

- The water electrolyzer stack has an estimated lifetime of 10 years [38].
- How the project is financed, cost of project planning, and civil works are excluded.
- The CAPEX of a 1 MW electrolyzer is provided in Table 3.4. To calculate the CAPEX of a 3 MW and 5 MW electrolyzer, the cost of 1 MW is scaled up. Additionally, as the capacity increases, the cost per kW decreases, resulting in a 10 % cost advantage from 1 MW to 3 MW, and an additional 10 % advantage to 5 MW.
- It assumed constant temperature from stack to compression.
- The extra cost of keeping the hydrogen pure in the compression process is not included.

3.4.3 LOCH CAPEX and OPEX

The CAPEX variable in this cost analysis includes the cost of the electrolyzer, balance of plant (BOP) components, high-pressure storage, and compressor. The BOP components include supporting and auxiliary components, electrical connections to the hydropower plant, and construction and assembly. The CAPEX of electrolyzer, balance of plant (BOP) components, and high-pressure storage are shown in Table 3.4 [39]. These are the cost of a 1MW atmospheric AEL, which this thesis uses despite its focus on pressurized AEL. The article was provided by a supplier of pressurized AEL, which states that it offers a good cost estimate applicable to both technologies. The CAPEX in the article was originally listed in euros and converted to NOK by multiplying by 10.

Table 3.4: CAPEX cost for a 1MW electrolyzer. Costs are presented in terms of NOK [39].

	1MW [NOK]
Electrolyzer	16 000 000
BOP components	3 000 000
High-pressure storage	2 000 000
Sum	21 000 000

Moreover, the investment cost of a compressor is influenced by its installed power, which depends on the mass flow of hydrogen and the source of electricity, whether it comes from a hydropower plant or the grid. This will further be explained in Section 3.4.5. Equation 3.7 provides the cost calculation for a specific compression unit (c), where P_{comp} represents the compressor's installed power in kW [35].

$$c = (43872 \cdot {P_{\text{comp}}}^{0.5861}) \cdot 10 \quad [\text{NOK}] \tag{3.7}$$

The compressor cost will be calculated across 36 scenarios, considering electricity from the grid and a hydropower plant and targeting end pressures of 350 and 700 bar. Additionally, the calculations will incorporate hydrogen flow rates from the three different years: 2010, 2007, and 2008, for all three electrolyzer capacities: 1 MW, 3 MW, and 5 MW. The installed power and investment costs for each compression scenario will be presented in the appendix. To simplify the cost analysis in this thesis, the compressor investment cost included in the CAPEX calculations will assume an end pressure of 350 bar and electricity sourced from the grid. The average of the compressor investment costs calculated over the three years will be included in $CAPEX_{1\text{MW}}$, $CAPEX_{3\text{MW}}$, and $CAPEX_{5\text{MW}}$, as $c_{1\text{MW}}$, $c_{3\text{MW}}$, and $c_{5\text{MW}}$.

According to Ulleberg's 2020 article, increasing the capacity of a small-scale hydrogen system would reduce capital expenses per kW [38]. Based on this, in this economic analysis it is assumes that investing in a 3 MW system would offer a 10 % advantage over a 1 MW system and an additional 10 % advantage between a 3 MW and a 5 MW system. Essentially, the cost per kW decreases as the size of the electrolyzer system grows. The calculations for CAPEX for a 3 MW electrolyzer are shown in Equation 3.8. Similarly, the Equation for CAPEX of a 5 MW is shown in 3.9.

$$CAPEX_{3MW} = (CAPEX_{1MW} \cdot 3 \cdot 0.9) + c_{3MW} \quad [\text{NOK}] \tag{3.8}$$

$$CAPEX_{5MW} = (CAPEX_{1MW} \cdot 5 \cdot 0.9^2) + c_{5MW} \quad [\text{NOK}] \tag{3.9}$$

In summary, the CAPEX for a 1 MW electrolyzer is obtained from [39], as presented in Table 3.4. The CAPEX for a 3 MW and 5 MW electrolyzer is calculated in this thesis based on the CAPEX of a 1 MW electrolyzer, with a reduction in CAPEX per kW of 10 % per increase in capacity. Also included in the CAPEX is the investment cost of a compressor, which will be calculated for each capacity with Equation 3.7. The LCOH of CAPEX is calculated by dividing the total CAPEX cost by the yearly hydrogen product and the lifetime of the stack. In this economic analysis, OPEX, representing the yearly operational cost, is set to be 3 % of CAPEX.

3.4.4 LOCH electricity to stack

This thesis categorizes the electricity consumption of the stack into two types: electricity consumption during production and electricity consumption during standby. As per Section 3.3.2, all electricity used during production is sourced from the hydropower plant, while electricity consumption during standby is shared between the hydropower plant and the grid.

When calculating LCOH for the stack in production, the annual power utilized by the electrolyzer in production mode for the given year is extracted from the electrolyzer model. The power is then multiplied by the cost of electricity from the hydropower plant and divided by the yearly hydrogen production.

On the other hand, when calculating LCOH for electricity consumption during standby mode, the electricity distribution between the grid and the hydropower plant is extracted from the electrolyzer model, and both values represent annual electricity consumption. Similar to LCOH in production, electricity consumption from the hydropower plant is multiplied by the cost of power from the hydropower plant and divided by annual hydrogen production. Further, the amount of power used from the grid during standby is multiplied by the grid cost and divided by annual hydrogen production.

3.4.5 LOCH electricity to compression

Compressing hydrogen is a significant expense that must be considered in an economic evaluation. Mechanical compressors, a standard in the industry for gas compression, operate by increasing the gas pressure through volume reduction [40]. This thesis assumes an electrically driven compressor, and the electricity required for compressing hydrogen produced at location A is calculated by first determining the specific work (w) of the compressor unit, as presented in Equation 3.10 [35].

$$w = \frac{\gamma}{\gamma - 1} \cdot R_{H_2} \cdot T_{in} \left[\left(\frac{P_{out}}{P_{in}} \right)^{\frac{\gamma-1}{\gamma}} - 1 \right] \quad [\text{kJ/kg}] \tag{3.10}$$

The adiabatic coefficient, denoted as γ, is 1.41 for hydrogen [35]. Additionally, the specific gas constant for hydrogen, R_{H_2}, has a value of 4.12 kJ/kg K [35]. The hydrogen inlet temperature,

T_{in}, is measured in K, and assumed to be the same as stack temperature. P_{in} and P_{out} are the initial and final pressures. The initial pressure is the pressure of the hydrogen when it leaves the stack, assumed to be 30 bar for a pressurized AEL [18]. The final pressure of hydrogen depends on its intended use. For this cost analysis, two scenarios will be considered. The first scenario involves a final pressure of 350 bar, at this pressure, the hydrogen can be utilized in heavy-duty transport and maritime transport [38]. Scenario two is a final pressure of 700 bar, which is required for an automobile. Both scenarios will be evaluated using power bought from the hydropower plant and the grid, with a sensitivity analysis of low, medium, and high grid prices. When the electricity needed for compression is bought from the hydropower plant, hydrogen production will decrease; this is not considered in the electrolyzer model.

After calculating the adiabatic compression work, it is used to estimate the installed power required to compress hydrogen at location A, denoted as P_{comp}, and shown in Equation 3.11 [35].

$$P_{comp} = \frac{w \cdot \dot{m}_{H_2}}{\eta_{is,c} \cdot \eta_m \cdot \eta_e} \quad [kW] \tag{3.11}$$

In this equation, the amount of electricity required in the compression is calculated by multiplying the specific work with the hydrogen mass flow of the specific year, which is then divided by the isotropic efficiency ($\eta_{is,c}$), mechanical efficiency (η_m), and electrical generator efficiency (η_e). The efficiency values are displayed in Table 3.5 [35]. However, the generator efficiency is ignored when buying electricity from the grid. In such cases, the exact amount of power required is bought from the grid, and any losses in the process are the power company's responsibility.

Table 3.5: The efficiencies used to calculate the amount of power needed in the compression of hydrogen [35]

	Symbol	**Efficiency**
Isotropic efficiency	$\eta_{is,c}$	80 %
Mechanical efficiency	η_m	98 %
Electrical generator efficiency	η_e	96 %

Furthermore, to calculate the cost of electricity consumption during compression, W_{comp} is multiplied by 8760 hours to get kWh used during one year. This value can then be multiplied by the cost of electricity from the hydropower plant and grid displayed in Table 3.3, which is measured in units of NOK/kWh. Finally, the LCOH of electricity consumption during compression is calculated by dividing the total annual cost of electricity used in compression by the total annual hydrogen production.

Chapter 4

Results

The following chapter presents the results of this thesis, using the methodology outlined in Chapter 3. The dataset from the potential hydropower plant at location A is utilized to generate a visual representation of power fluctuations. Additionally, the results of the Matlab model for hydrogen production in three different years and with three different electrolyzer capacities are presented. A cost analysis of the three different electrolyzer capacities based on the LCOH methodology is also included. This is followed by a comparison of hydrogen production technologies, namely AEL and PEM. Lastly, an assessment of potential end-users for the produced hydrogen at location A is presented. This chapter includes some comments and reflections about the results, but the overall discussion is presented in Chapter 5.

4.1 Hydropower plant: power output

The following section provides a quantitative description of the data set provided by SKL, focusing on fluctuations in power production. The dataset has an hourly resolution of power production from a potential small-scale hydropower plant. It covers the period from 1st of January 2002 to 31st of December 2021. The quantitative description includes a general overview of yearly total production and seasonal variation over the 20 years. A more detailed review is conducted for the typical dry year (2010), the median year (2008), and the typical wet year (2007). This review considers monthly, daily, hourly, and diurnal variations to better understand the fluctuations in power production over time.

4.1.1 Variation in yearly total production

The pink marker highlights the total production for the typical dry year 2010, a P10 year, indicating that 10 % of the years in the dataset have lower yearly production than 2010. In 2010, the annual output was 11.63 GWh. The blue marker represents the total production for the median year, 2008, with a yearly output of 15.41 GWh. Finally, the green marker represents the total production for the typical wet year 2007, classified as a P90 year, suggesting that 10 % of the years have a higher yearly production than 2007, which had a yearly production of 19.48 GWh. Additionally, pink, blue, and green dashed lines illustrate 2010, 2008, and 2007 compared to the rest of the dataset. This indicates that investigating these three years provides a

good representation of the variation within the dataset.

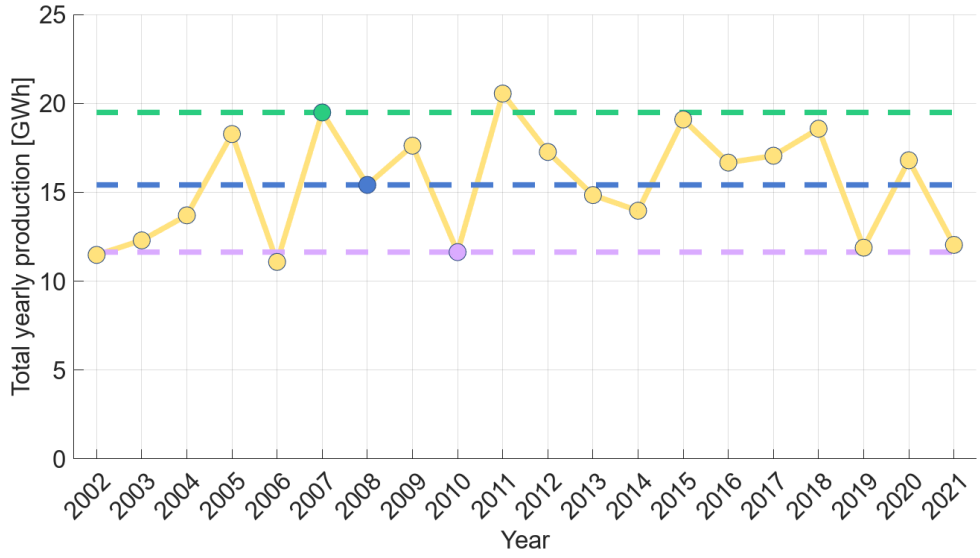

Figure 4.1: The graph displays the yearly total production from 2002 to 2021. It includes a pink marker representing 2010, the typical dry year. The blue marker represents the median year, 2008. Lastly, the green marker represents 2007, the typical wet year. These years are also plotted as pink, blue, and green dashed lines to make it easy to compare them with the other years in the dataset.

4.1.2 Seasonal variation

The monthly variation in power output over the 20-year period is illustrated in Figure 4.2, where the hourly power production is summed into monthly total production. The y-axis represents the total monthly production in GWh, while the x-axis displays the months. Notably, 2010, 2008, and 2007 are highlighted, with a pink, green, and blue line, respectively. This plot allows for the identification of any recurring seasonal trends.

Power production is relatively low from January to March, ranging from 0.00 to 0.75 GWh, suggesting limited water availability or lower hydrological flow during these months. Production begins to increase from March and reaches its peak in June with values between 2.75 and 4.45 GWh, likely due to snow melting. There is a significant drop in production from June to August, with production levels varying from 0.10 to 3.25 GWh, reflecting reduced snow melt. The pattern during autumn through December does not exhibit a clear trend, indicating yearly variations in hydrological conditions or other factors.

Figure 4.3 combines a seasonal variation plot with a display of monthly production for the year 2008, identified as the median year. The y-axis represents electricity production in GWh, while the x-axis spans from January to December, representing the months. Error bars are shown each month, where 2008 is the reference point, and the range of the error bar represents the monthly variation of the entire dataset spanning 20 years. This is plotted to illustrate the expected extent of variation in monthly power generation at location A, indicating a high probability of differing quantities of total monthly power produced from year to year.

The length of an error bar indicates the variation within that specific month over the 20 years, with longer bars indicating greater variability. July has the highest variability in power production,

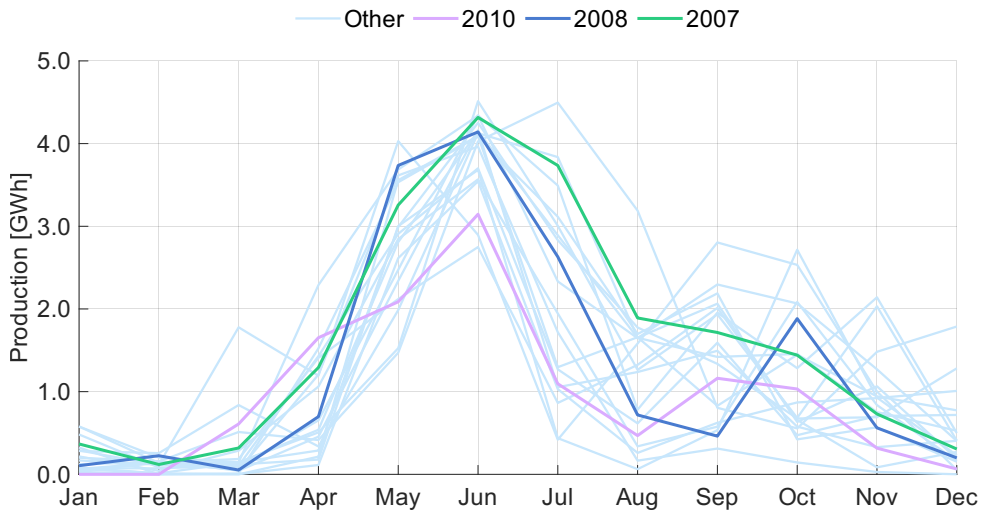

Figure 4.2: Variation in monthly power production from the year 2002 to 2021. Monthly power production over the 20-year period is displayed as overlapping line graphs, allowing examination of seasonal trends. The pink line represents the typical dry year 2010, the blue line represents the median year 2008, and the green line represents the typical wet year 2007. The remaining years are represented with a light blue line.

while February has the lowest. This visualization provides insights into the reliability and stability of monthly power production from the potential power plant.

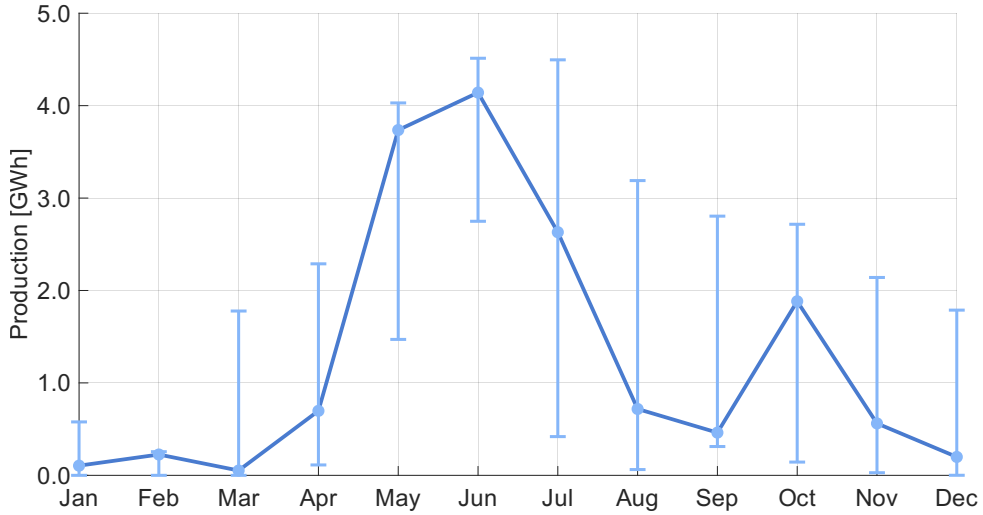

Figure 4.3: Monthly production of power during the median year (2008). The median year serves as a reference point for the light blue error bars, the length of the error bars representing the variation in monthly production for the entire dataset spanning 2002 to 2021.

4.1.3 Daily variation

The following sections will exclusively focus on the years 2010, 2008, and 2007. These years have been selected because they represent a typical dry year, the median year, and a typical wet year, respectively, as explained in section 3.2.1. In Figure 4.4, the hourly power production is summed to daily production for these three years. The y-axis represents the electricity production in GWh per day, and the x-axis shows the days of the year from 0 to 365 (366 for a leap year).

Specifically, Figure 4.4a represents the total daily production for 2010, Figure 4.4b for 2008, and Figure 4.4c for 2007. These plots display significant daily variations in total production, with an overall trend similar to the seasonal variations shown in Figure 4.2 but with a higher data resolution.

The plots show an upper boundary at 0.15 GWh, representing the production limit of the hydropower plant. This limit stems from the maximum hourly capacity of the plant, which is 6.3 MW. Consequently, the daily production ceiling is 0.15 GWh, as shown in Equation 4.1. In the typical wet year of 2007, the production ceiling was reached more frequently compared to the other two years. This suggests that in 2007, there was a surplus of water available for power production that exceeded the capacity of the hydropower plant. Consequently, the excess power in the water could not be fully utilized by the hydropower plant.

$$\text{Daily production ceiling} = 6.3\,\text{MW} \cdot 24\,\text{hours} \cdot 10^{-3} = 0.15\,\text{GWh} \tag{4.1}$$

4.1.4 Hourly variation

Further, October and November from the median year 2008 are used to analyze the hourly fluctuations in power production at location A. These months are selected as they exemplify months with high and low variation, respectively. Figure 4.5 displays the graphs that illustrate the months. The y-axis represents power production in GWh, while the x-axis indicates the hours within each month. Each tick on the x-axis represents a day of the month, but it is expressed in hours. The maximum effect of the turbine on an hourly basis is shown by the upper bound cut at $6.3 \cdot 10^{-}3$ GWh.

Figure 4.5a illustrates the data for the month of October. The graph reveals both periods of relatively stable hourly production and instances of significant increases or decreases in production. For example, from hours 0 to 72, the load remains relatively steady with a marginal decrease. However, from hour 168 to 192, hourly production steadily increases throughout the entire day, starting at $0.25 \cdot 10^{-3}$ GWh and reaching $6.3 \cdot 10^{-3}$ GWh by hour 192. Several peaks in the monthly production are observed; however, these peaks do not display as hourly spikes but rather as gradual increases in production over several hours.

In contrast, Figure 4.5b illustrates November's production, characterized by fewer peaks, suggesting a more steady production rate. There are two spikes, the first occurs from hour 336 to 360, representing a smaller spike, while the second, more significant spike, is observed from hour 624 to 648. At hour 624, production starts at $0.50 \cdot 10^{-3}$ GWh, peaks at $6.3 \cdot 10^{-3}$ GWh midday, and decreases to $2 \cdot 10^{-3}$ GWh by hour 648. Despite significant variation in production this day, the hourly production has an even flow, with no sudden spikes deviating from the rest. Figure 4.5 indicates that energy output from small-scale hydropower plants experiences fluctuations on an hourly basis, in the form of increasing or decreasing power production from hour to hour throughout each day. The production maintains a relatively even hourly flow every day of the two months, without sudden spikes that deviate significantly from the rest.

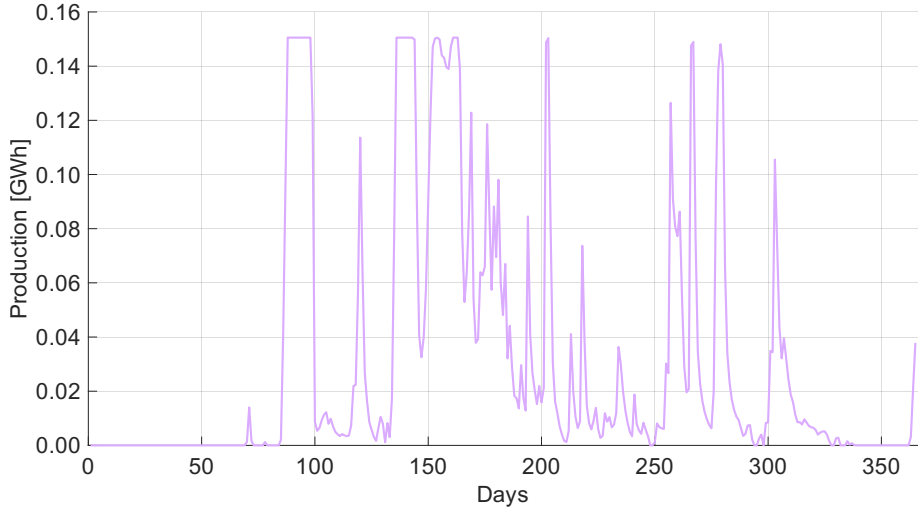

(a) The typical dry year (2010)

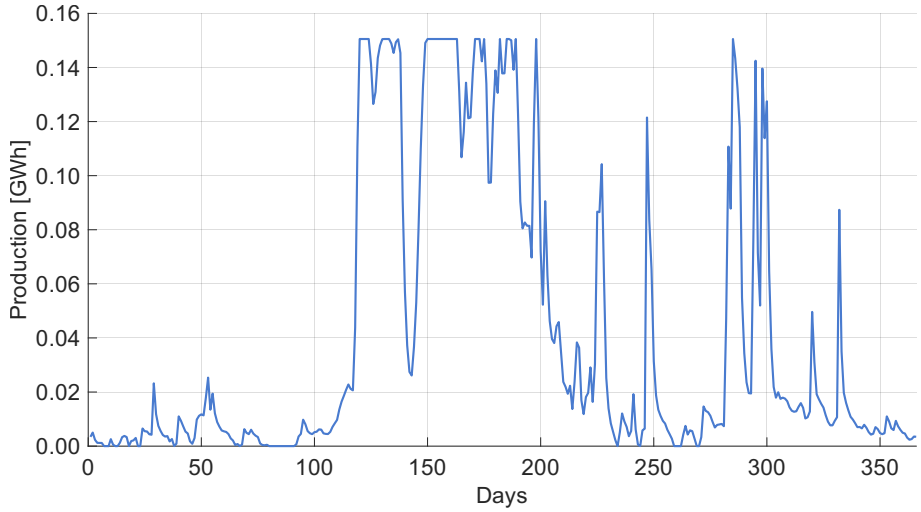

(b) The median year (2008)

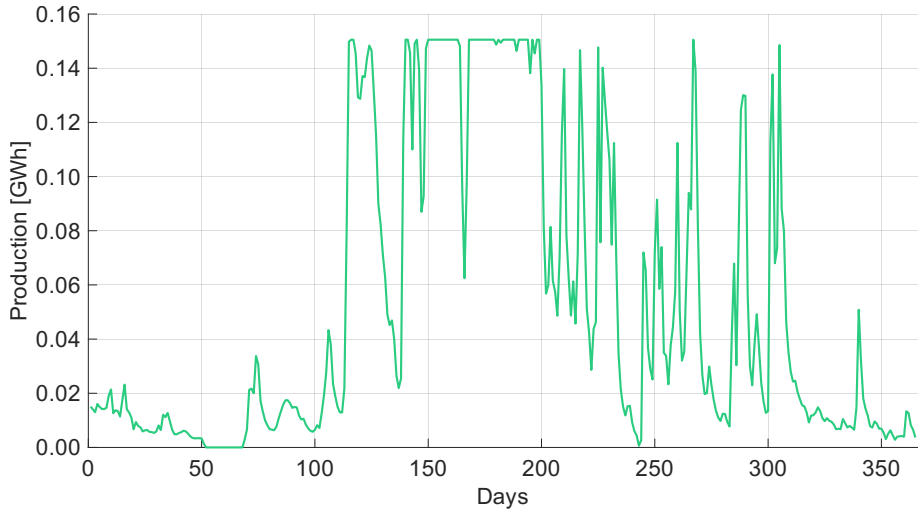

(c) The typical wet year (2007)

Figure 4.4: Daily variation in power production at the potential hydropower plant, for the different years: (a) the typical dry year (2010), (b) the median year (2008), and (c) the typical wet year (2007).

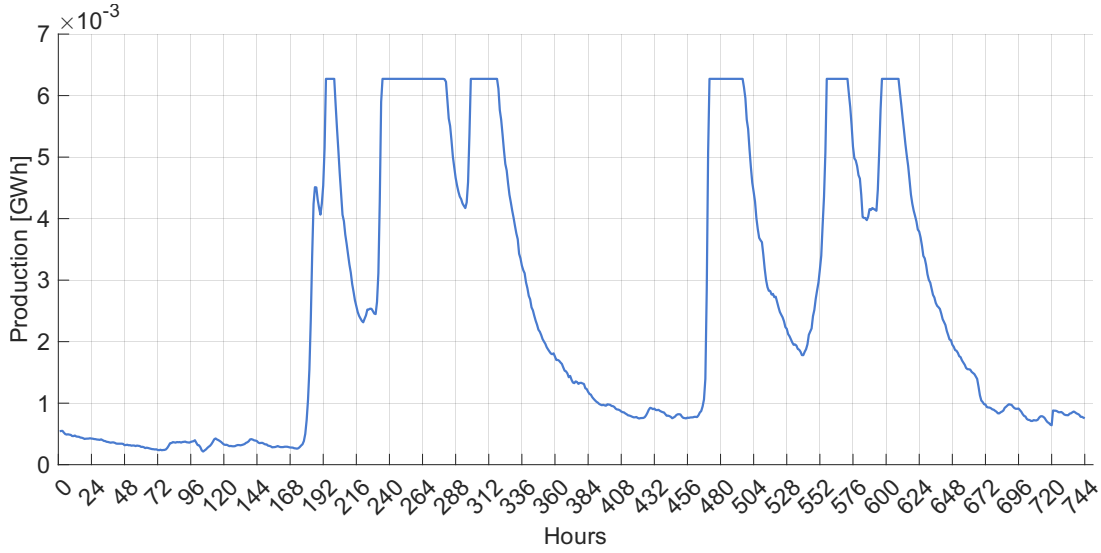

(a) October

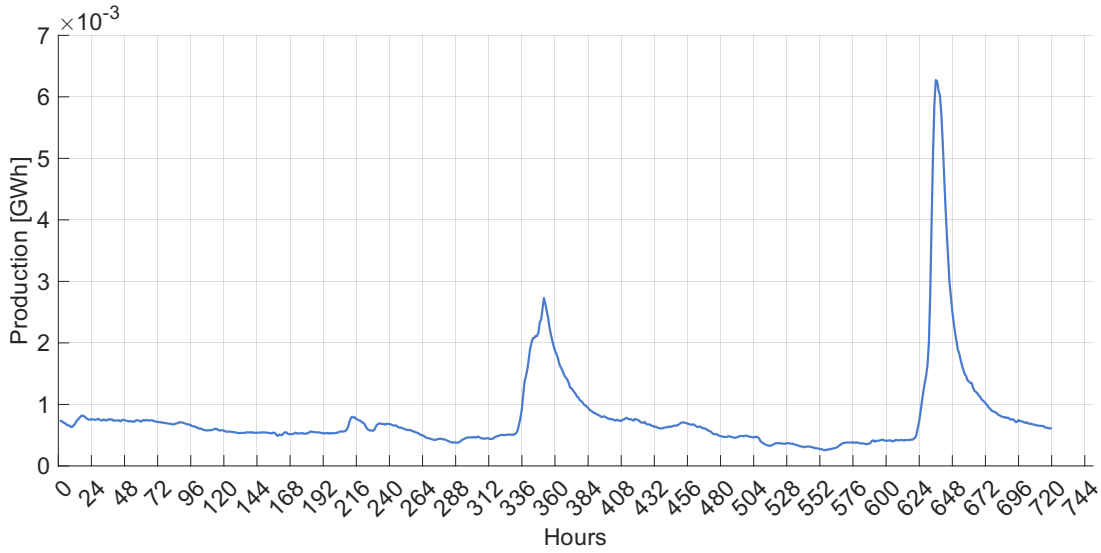

(b) November

Figure 4.5: Hourly fluctuations in energy production at the potential hydropower plant during November and October of the median year, 2008. (a) October, (b) November. The ticks on the x-axis denote the hour of the month, with each tick representing a day.

4.1.5 Diurnal variation

Figure 4.6 presents a plot that illustrates the average electricity production for each specific hour within a 24-hour day, averaged over the years 2010, 2008, and 2007. The x-axis displays the hours of the day from 00:00:00 to 23:00:00, and the y-axis shows mean production in GWh. The plot reveals a noticeable pattern in the diurnal cycle of power production. There is a gradual decline in production from the start of the day at 00:00:00 towards midday, showing the lowest average output. After midday, a slight uptrend in production continues until 23:00:00.

The production levels during the typical wet year 2007 were consistently highest throughout the day. The median year 2008 displays production levels between the other two, while the typical dry year 2010 shows the lowest hourly production.

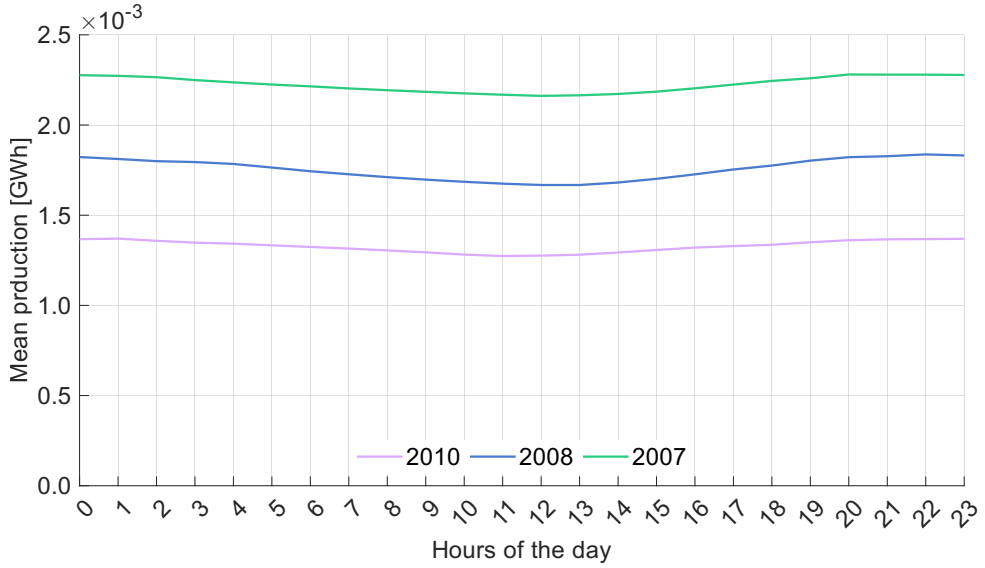

Figure 4.6: Average diurnal production of power for the typical dry year (2010), the median year (2008), and the typical wet year (2007)

4.2 Electrolyzer model

This section provides the results from the simulation of hydrogen production. The model was used to evaluate electrolyzer capacities of 1 MW, 3 MW, and 5 MW for hydrogen production at location A. The purpose of this comparison is to find the point at which investment in an electrolyzer intersects with the best utilization of power generated by the hydropower plant. As explained in Chapter 3, not all the power generated by the hydropower plant is used for hydrogen production. Hydrogen is produced only when the power input exceeds 16 % of the electrolyzer capacity. Also, any power exceeding the capacity limit is not utilized. When the power input is below 16 % of the electrolyzer capacity, the electrolyzer stops producing hydrogen and goes into standby mode. However, the electrolyzer still requires power to maintain standby mode, mainly supplied by the hydropower plant but also the grid when needed.

The first step in comparing the electrolyzer capacities is to visualize the extent to which each capacity can utilize power from the hydropower plant. Further, the quantity of hydrogen produced during the typical dry year (2010), the median year (2008), and the typical wet year (2007) for each capacity is determined. Also, the model was utilized to understand how the electrolyzer operates throughout the years. Therefore, the results are divided into three parts: utilization of electricity input, hydrogen production, and electrolyzer system utilization.

4.2.1 Utilization of electricity input

It is crucial to select an electrolyzer for the potential hydropower plant at location A that can effectively utilize the installed power. This is of interest both to the power supplier and to the hydrogen producer. The maximum capacity of the turbine at the hydropower plant is 6.3 MW. The electrolyzers have a dynamic range of 16 to 100 % of the capacity, meaning they utilize power within the following ranges:

- For 1 MW electrolyzer: 0.16 MW to 1 MW

- For 3 MW electrolyzer: 0.48 MW to 3 MW
- For 5 MW electrolyzer: 0.80 MW to 5 MW

Consequently, when the hydropower plant operates at full capacity, the 1 MW electrolyzer fails to use 5.3 MW of available power, the 3 MW electrolyzer fails to utilize 2.3 MW, and the 5 MW electrolyzer fails to utilize 1.3 MW. Thus, increasing electrolyzer capacity allows for more of the installed capacity at the hydropower plant to be utilized.

To analyze the effectiveness of different electrolyzers in harnessing power from the hydropower plant, Figure 4.4b illustrating daily production in the year 2008, is employed in combination with lines representing the dynamic range of the electrolyzers. This is illustrated in Figure 4.7. The y-axis represents the electricity production in GWh per day, and the x-axis shows the days of the year from 0 to 366.

Daily, the electrolyzer capacities have the potential to consume power within a range that spans 24 times the power utilization range. This is equivalent to:

- 1 MW electrolyzer: the area between 0.003 to 0.02 GWh
- 3 MW electrolyzer: the area between 0.011 to 0.07 GWh
- 5 MW electrolyzer: the area between 0.019 to 0.12 GWh

These ranges are plotted as lines in Figure 4.7. In Figure 4.7a it is evident that the 1 MW electrolyzer primarily utilizes power lows and fails to exploit power peaks effectively. Moreover, in Figure 4.7b the 3 MW electrolyzer demonstrates a more balanced approach, utilizing both power lows and tapping into the densest areas of power peaks. The 5 MW electrolyzer illustrated in Figure 4.7c, on the other hand, does not utilize power lows but covers a larger area of the power peaks. This is particularly noticeable during the summer months when the 5 MW electrolyzer can harness a significantly larger area of power peaks compared to the 3 MW electrolyzer. However, for the rest of the year, the power peaks that the 5 MW electrolyzer can utilize but the 3 MW cannot are less dense.

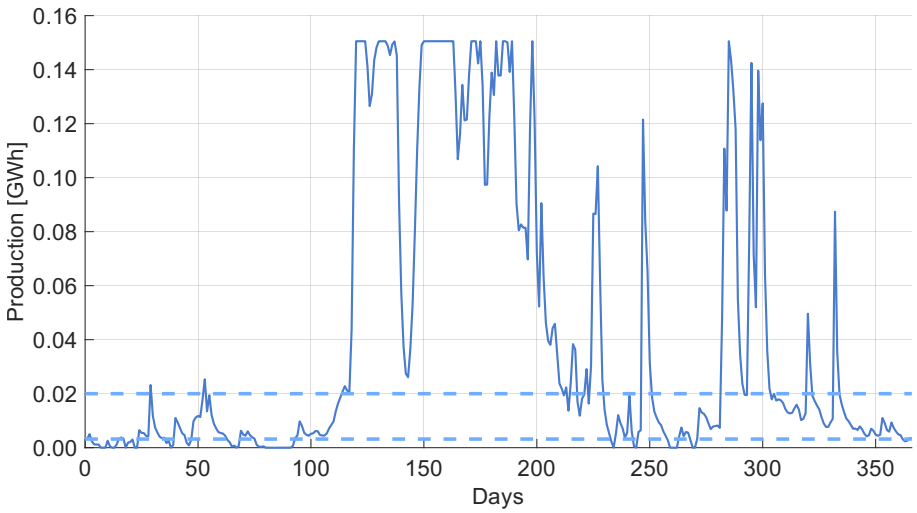

(a) 1 MW

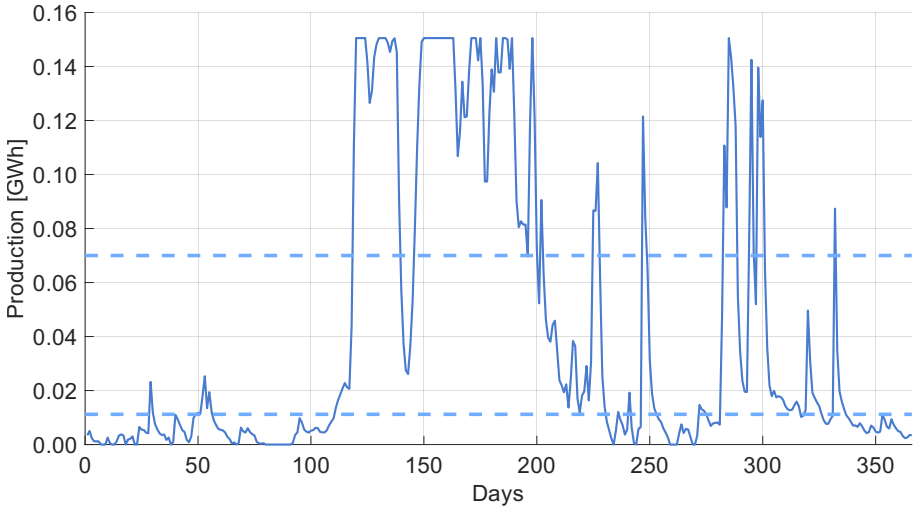

(b) 3 MW

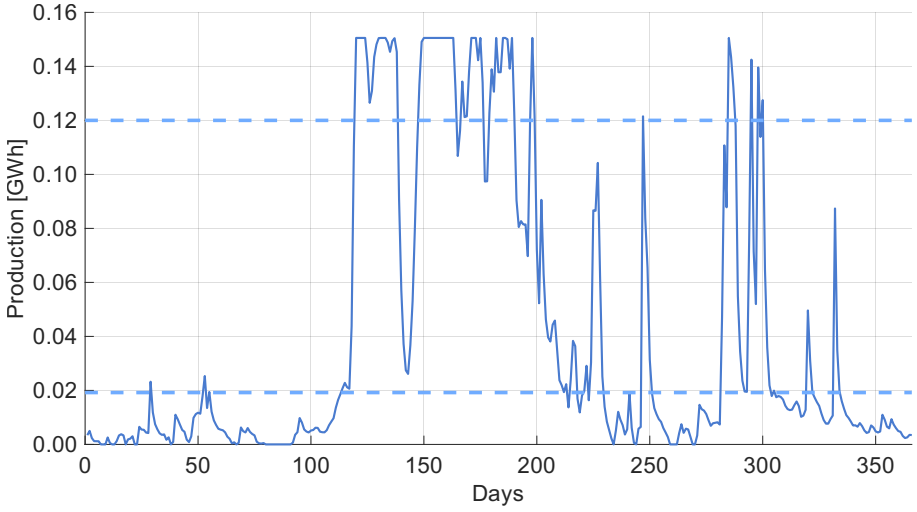

(c) 5 MW

Figure 4.7: A visual representation of the power produced at the potential hydropower plant and the corresponding utilization by three different electrolyzer capacities, 1 MW, 3 MW, and 5 MW, in the year 2008 (median year). The utilization interval is illustrated as two horizontal lines, indicating the area of power production that each specific capacity can utilize.

4.2.2 Production of hydrogen

The production of hydrogen is calculated hourly based on the power input received from the power plant. To present the results, the hourly production is first summed up to provide the total yearly hydrogen production. This is followed by an investigation of monthly production, where the hourly production is summed up per month.

Yearly total production

The following paragraphs will present the total yearly production of hydrogen for all three years and capacities. The production is calculated in a MATLAB model, the details of which are provided in Section 3.3. The results from the model are visualized in Figure 4.8. In Figure 4.8, the x-axis shows electrolyzer capacities, and the y-axis shows hydrogen production in kg per year. The typical wet year 2007, had the highest production for all capacities. In contrast, production was lowest in the typical dry year 2010. The production for the median year 2008 was in the middle range.

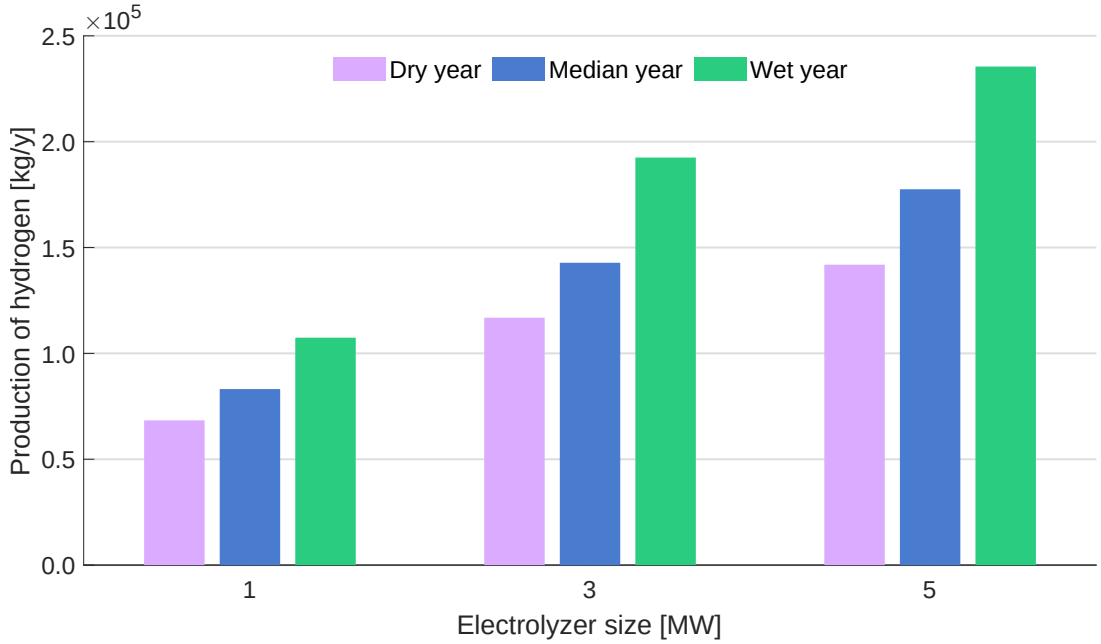

Figure 4.8: Total yearly production of hydrogen for the typical dry year (2010), the median year (2008), and the typical wet year (2007), per electrolyzer capacity

The annual production is summarized in Table 4.1. Considering the typical dry year, upgrading to a 3 MW electrolyzer resulted in a 40 % increase in production compared to a 1 MW electrolyzer. Further upgrading from a 3 MW to a 5 MW electrolyzer led to an additional 17 % increase in production. During the median year, utilizing a 3 MW electrolyzer resulted in a 41 % increase in hydrogen production compared to a 1 MW electrolyzer, with a further 19 % increase when upgrading from 3 MW to 5 MW. Similarly, in the typical wet year, upgrading to a 3 MW electrolyzer resulted in a 43 % increase in hydrogen production compared to a 1 MW electrolyzer, with an additional 18 % increase upon further upgrading to a 5 MW electrolyzer.

Consequently, upgrading from 1 MW to 3 MW doubles the production increase compared to upgrading from 3 MW to 5 MW. Thus, an upgrade in electrolyzer capacity does not necessarily

Table 4.1: Total production of hydrogen per year, for each of the capacities: 1 MW, 3 MW, and 5 MW. The production has been rounded to the nearest 100 kg. The percentage increase represents the increase in production between the capacities.

Years	1 MW [kg/y]	Increase	3 MW [kg/y]	Increase	5 MW [kg/y]
2010	69 300	40 %	117 100	17 %	142 000
2008	85 700	41 %	146 700	19 %	182 000
2007	109 100	43 %	194 300	18 %	236 800

result in a proportional increase in hydrogen production. Factors beyond electrolyzer capacity influence hydrogen production; one significant factor in this case is water availability for power production.

To assess the reliability of total yearly production estimates, the production rate of Green Hydrogen Systems' high-pressure alkaline electrolyzer "series-a" is utilized for comparison [18]. According to technical specifications, a 900 kW electrolyzer produces 16.2 kg/h when operating at 100 % load. Scaling this to represent the hourly production of 1 MW, 3 MW, and 5 MW electrolyzers, and multiplying it by the number of hours in a year, yields ideal yearly production figures for the three capacities. Consequently, a 1 MW, 3 MW, and 5 MW electrolyzer would ideally produce 145 200 kg/y, 435 500 kg/y, and 725 800 kg/y, respectively. The highest yearly hydrogen production calculated in this thesis was for the typical wet year, yielding 109 100 kg/y, 194 300 kg/y, and 236 800 kg/y for the 1 MW, 3 MW, and 5 MW electrolyzers, respectively. These values do not exceed the ideal annual hydrogen production, and therefore, the calculations in this thesis are considered valid.

Comparing the ideal production to the production at location A for the typical dry year reveals that a 1 MW, 3 MW, and 5 MW electrolyzer achieves 47 %, 27 %, and 20 % of its potential, respectively. For the median year, the figures are 59 %, 33 %, and 25 %, and for the typical wet year they are 75 %, 45 %, and 33 %. The analysis of hydrogen production at location A reveals that lower capacity electrolyzers tend to utilize a higher percentage of their ideal production than higher capacities. Furthermore, the significant influence of water availability for power production on hydrogen production is evident. Across the typical dry year, median year, and typical wet year, percentage utilization of the ideal hydrogen production increases with greater water availability, indicating that electrolyzers can better utilize their potential when more water is available.

Notably, both 3 MW and 5 MW electrolyzers consistently produce under 50 % of their ideal production across the three years. This suggests that these capacities may be excessive for the present case. The underutilization of electrolyzer potential raises questions about cost-effectiveness, a topic that will be further explored in Section 4.3.

Monthly variation in production

The graph in Figure 4.9 displays the monthly variation in hydrogen production. The y-axis indicates the production in kg of hydrogen monthly, while the x-axis displays the months. There are three bars for each month within each subfigure representing the years 2007, 2008, and

2010. Generally, the typical wet year 2007 shows the most hydrogen production; in contrast, the typical dry year 2010 shows the lowest monthly hydrogen production. The median typically falls between the two other years. This pattern is valid for all three electrolyzer capacities.

Figure 4.9a illustrates the monthly variation for a 1 MW electrolyzer, showing no significant variation in total monthly production between the three years. In addition, the 1 MW electrolyzer demonstrated marginal changes in production rates across all seasons despite the expectation of increased hydrogen production during the summer months, as indicated by the seasonal trend of hydropower production from Figure 4.2. This lack of differentiation between the median and wet years compared to the typical dry year suggests inefficiency in utilizing the power generated from the hydropower plant during periods of higher power input.

In contrast, the graph in Figure 4.9b, representing the 3 MW electrolyzer, exhibits a notable improvement in utilizing peak power periods for all three years. The increased capacity allows for better utilization of power generated at location A. Although upgrading to a 5 MW electrolyzer, as shown in Figure 4.9c, doesn't significantly benefit the typical dry year, it does enhance production during the median and wet years. However, the 5 MW unit proves less efficient than the 3 MW electrolyzer during off-peak hours, attributed to the dynamic range limitations of the 5 MW electrolyzer, as discussed in section 4.2.1. This is exemplified by the absence of production during September and December in the 5 MW electrolyzer for the median year. The production for these months decreases with an upgrade to 3 MW and is nonexistent at the 5 MW electrolyzer.

Analyzing the graphs in Figure 4.9, a clear seasonal trend in hydrogen output aligns with the pattern observed in Figure 4.2, seasonal variations in power production. Hydrogen production remains relatively low from January to March, steadily increasing from April and peaking in June. Production declines from June to August, with no distinct pattern observed during autumn. This seasonal trend becomes more significant with increasing electrolyzer capacity, leading to wider fluctuations in monthly production across the different years. Variation in monthly production over the three years is expected from an electrolyzer compatible with the plant, considering that these years represent a dry year, a median year, and a wet year.

After examining this seasonal production trend, it's apparent that the 1 MW electrolyzer can maintain a more consistent production rate throughout the year compared to the other two capacities. This makes production more predictable, which can be advantageous when planning hydrogen storage, transport and negotiating deals with end-users. However, the 3 MW and 5 MW electrolyzers have a less consistent production rate, which follows the seasonal trend of the hydropower plant. Further, this underscores how upgrading electrolyzer capacity facilitates better power utilization during periods of higher power production. However, this reduction also limits exploration of power lows, as production is cut off when the power input falls below 16 % of the electrolyzer's capacity.

4.2.3 Oxygen production

As detailed in Section 2.2.1, the electrolysis process yields two hydrogen molecules and one oxygen molecule. Figure 4.10 illustrates the annual volume of oxygen generated at location A. The x-axis represents different electrolyzer capacities, with one bar per year per capacity, while the y-axis denotes oxygen production in kg/y. The bar plot exhibits similar trends to the total

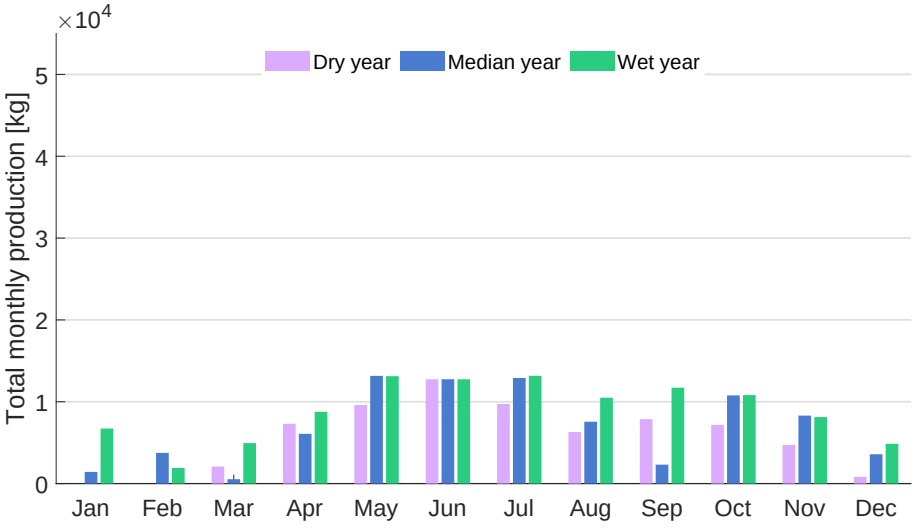

(a) 1 MW

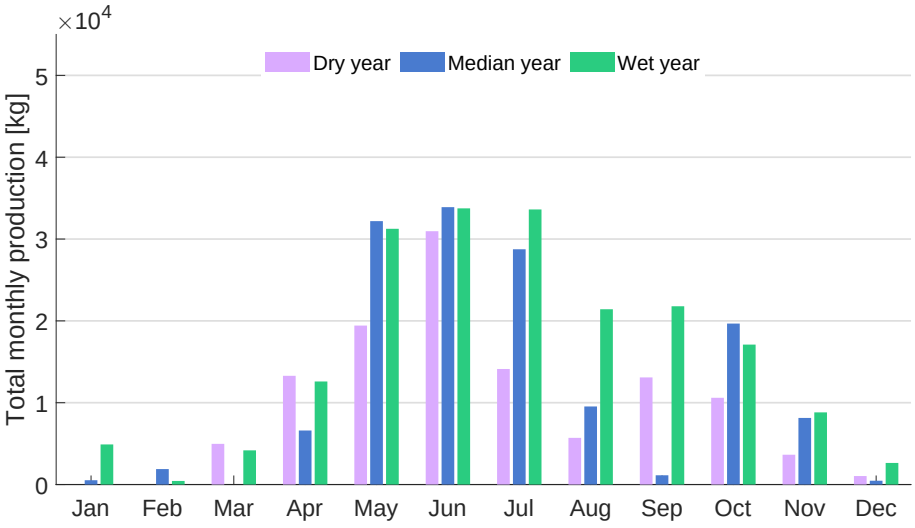

(b) 3 MW

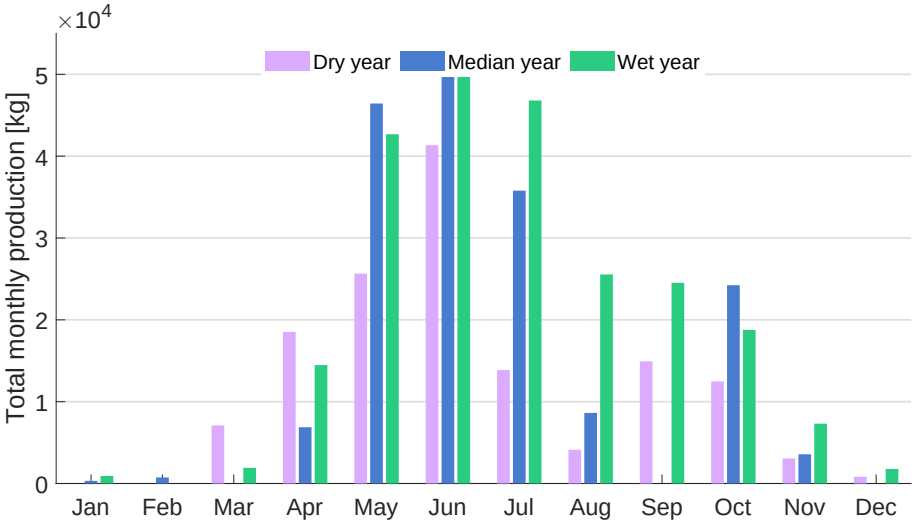

(c) 5 MW

Figure 4.9: Monthly total production of hydrogen for the typical dry year (2010), the median year (2008), and the typical wet year (2007) using different electrolyzer capacities: (a) 1 MW (b) 3 MW (c) 5 MW.

yearly hydrogen production in Figure 4.8, as expected due to their proportional relationship. Despite hydrogen molecules being produced in more significant quantities than oxygen molecules during electrolysis, the mass of oxygen generated exceeds that of hydrogen. This difference occurs because oxygen has a higher molar mass than hydrogen, as mentioned in Section 2.2.1.

The graph illustrates varying oxygen production levels across different years and capacities, with the typical dry year showing the lowest production, the median year demonstrating intermediate levels, and the typical wet year exhibiting the highest production across all three capacities. Specifically, in the median year, oxygen production amounted to 950, 1150, and 1550 tonnes annually for 1 MW, 3 MW, and 5 MW electrolyzers, respectively.

Oxygen is used in different industries, including fish farming, where it is essential for breeding fish in closed cages. For example, a facility with 10 closed cages requires an annual oxygen supply of 1500 tonnes [41]. This implies that the quantity of oxygen produced at location A is sufficient for utilization in fish farming. Therefore, the feasibility of the project can be enhanced by selling the oxygen produced in addition to the hydrogen.

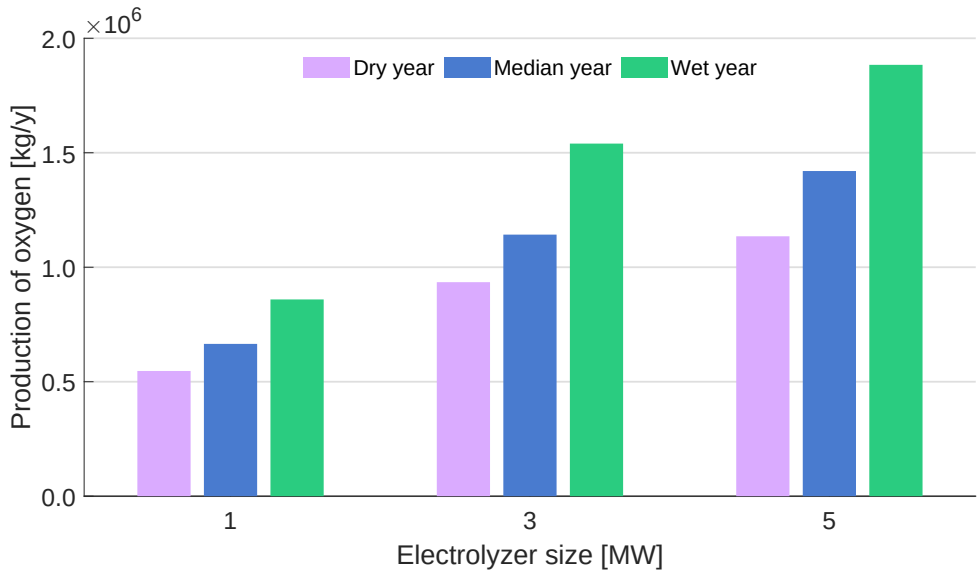

Figure 4.10: Total yearly production of oxygen for the typical dry year (2010), the median year (2008), and the typical wet year (2007), per electrolyzer capacity

4.2.4 Utilization of electrolyzer system

When deciding the most appropriate electrolyzer capacity, the amount of hydrogen produced is just one factor to consider; operational conditions also play a significant role. To better understand how the operating conditions differ between various electrolyzer capacities, the following paragraphs will examine the number of days in a year when the electrolyzer operates at full load, the number of days when it is not used at all (zero production days), instances of standby, and the distribution of power input during standby.

Full load

Days when the electrolyzer runs at maximum capacity at all hours during the day are called full load days. During these days, the electrolyzers can maximize hydrogen production without any

interruptions or efficiency losses. Figure 4.11 displays the days the electrolyzers operates on full load annually. The y-axis represents the number of days, and the x-axis shows the electrolyzer capacities with a bar for 2010, 2008, and 2007 for each capacity. A comparative look at the years shows that the typical wet year 2007, had the highest frequency of full production days. Conversely, the typical dry year 2010 had the least, with 2008 between the two extremes. This applies to all three electrolyzer capacities.

The graph indicates that as the electrolyzer capacity increases, the number of days it operates at full capacity decreases. This trend arises because the dynamic range of the electrolyzer increases with its capacity, requiring a higher power input to operate at full load. The median year exhibits a nearly linear decrease in full load days. On the other hand, the typical dry year and wet year display more noticeable changes in full load days from 1 MW to 3 MW, and less significant changes from 3 MW to 5 MW.

The 1 MW electrolyzer easily achieves a full load day, requiring only a power input of 1 MW, while the hydropower plant has an installed capacity of 6.3 MW. This situation is further highlighted by the fact that the 1 MW electrolyzer exhibits a wider internal variation between the three years than the variation in full load days observed for the typical dry year 2010 across different electrolyzer capacities, from 1 MW to 5 MW. This suggests that the capacity limit of the 1 MW electrolyzer is easily met, and the higher amount of power available during higher production years, such as 2008 and 2007, is not fully utilized due to the capacity limit of the 1 MW electrolyzer. For increasing capacity, the amount of full load days decreases for the median year and the typical wet year, indicating improved power utilization.

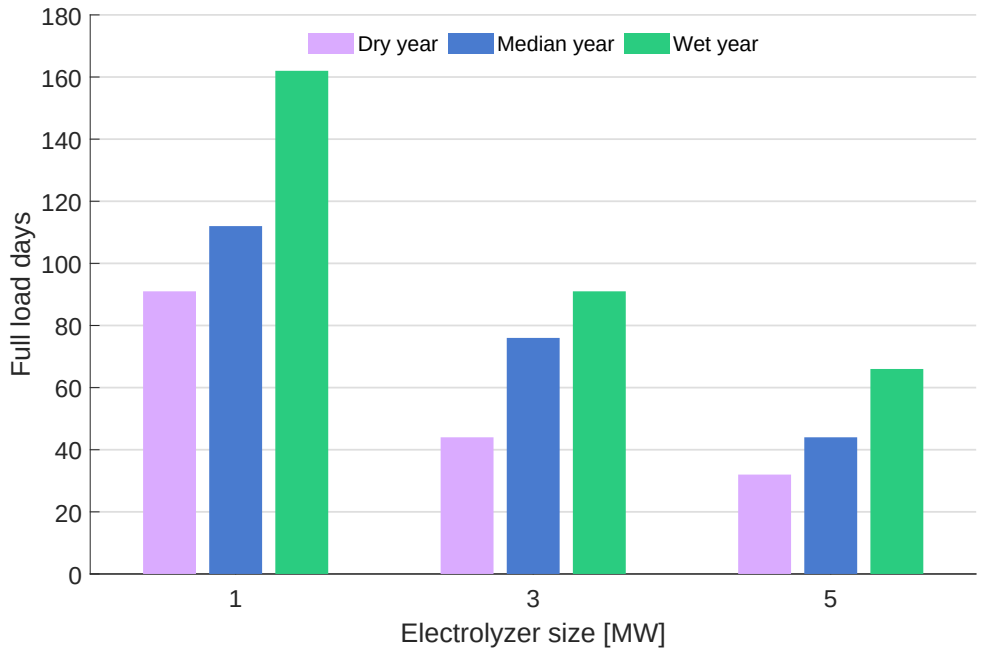

Figure 4.11: Number of days the electrolyzer is operating at full load for the typical dry year (2010), the median year (2008), and the typical wet year (2007), per electrolyzer capacity

Zero production days

The graph shown in Figure 4.12 represents the yearly instances of zero production days, which refers to the days when the electrolyzer is not in use. The typical dry year of 2010 experienced

the highest frequency of zero production days across all capacities, while the typical wet year of 2007 had the least. The median year is positioned between these two extreme years. Unlike the full load days in Figure 4.11, zero production days increase with increasing electrolyzer capacity. This trend also arises because the dynamic range of the electrolyzer increases with its capacity, requiring a higher power to reach minimum production limit. The most significant increase in zero production days occurs when upgrading from a 1 MW electrolyzer to a 3 MW electrolyzer. The increase is two to three times higher compared to the upgrade from 3 MW to 5 MW.

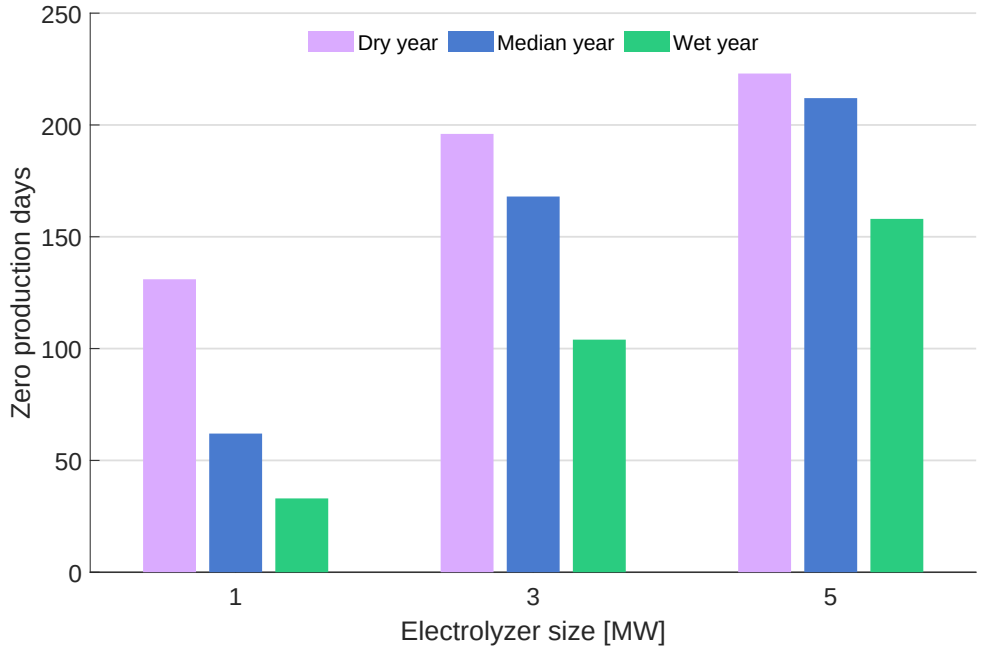

Figure 4.12: Number of zero production days for the typical dry year (2010), the median year (2008), and the typical wet year (2007), per electrolyzer capacity

Standby

When the power input from the hydropower plant is less than 16 % of the electrolyzer capacity, the electrolyzer goes into standby mode. However, in standby mode, the electrolyzer still requires power input. As explained in Section 3.3.2, this thesis defines three scenarios for electricity consumption during standby. The first scenario purchases all the required power from the hydropower plant. In the second scenario, when power from the hydropower plant is insufficient to keep the electrolyzer on standby, additional electricity is purchased from the grid. Lastly, in the third scenario, all electricity is purchased from the grid.

The process of switching the electrolyzer from production to standby has a degrading effect on the electrolyzer [42]. However, there is no good quantification of this degradation in the literature, as mentioned in the literature review in Chapter 2. Therefore, after discussions with different suppliers of electrolyzers, it is assumed in this thesis that turning the electrolyzer from production to standby more than five times a day significantly harms the electrolyzer. Based on this assumption, a MATLAB function was developed to identify the number of days during 2007, 2008, and 2010 when the electrolyzer switched from production to standby more than five times for all three electrolyzer capacities, 1 MW, 3 MW, and 5 MW. The results indicate that for all three years and three capacities, there were no instances of the electrolyzer switching modes

more than five times in a single day.

The monthly variation of instances of standby mode is illustrated in figure 4.13. It consists of three subfigures: 4.13a, 4.13b, and 4.13c, which shows the monthly variation for a 1 MW, 3 MW, and 5 MW electrolyzer, respectively. The figure excludes data on the electrolyzer's transition frequency between production and standby modes, focusing only on the total number of standby hours per month. The y-axis represents the number of standby hours within the month. While the x-axis displays the months. Three bars for each month within each subfigure represent the years 2010, 2008, and 2007.

There are generally more instances of standby hours when electrolyzer capacity is increased. This occurs because, as illustrated in Figure 4.7, power lows are utilized for hydrogen production with a 1 MW electrolyzer. However, increasing the electrolyzer capacity to 3 MW extends the lower production boundary, utilizing less power lows for hydrogen production, resulting in more standby hours. Similarly, with the increase to 5 MW, even fewer power lows are utilized.

The convex trend observed in all three subfigures reveals the fewest standby instances occurring in May, June, and July across all years. This pattern aligns with the seasonal variation of power production illustrated in Figure 4.2, where these months exhibit the highest power production from the hydropower plant. Consequently, the demand for 16 % of the electrolyzer capacity to produce hydrogen is more easily met during these months. However, in the typical dry year, there is an increase in standby hours in July from 1 MW to 5 MW. This suggests that there are periods in July 2010 with limited power available, regardless of July typically being a high-power production month.

From January to April and November to December, as the electrolyzer capacity increases, the variation between the three years within each month decreases. However, from August to October, there is significant variation in standby hours between the three years across all capacities. The typical dry year 2010 shows no significant change in standby hours with increasing electrolyzer capacity. This indicates that when power production is low during the typical dry year, it is generally under 16 % of the electrolyzer capacity for all three capacities. But when there is production from the plant this year, the power produced is primarily over 16 % of all three capacities. In contrast, the median year and the typical wet year exhibit an increase in standby hours with increasing electrolyzer capacity. The median year exhibits more standby hours than the typical wet year. This can be attributed to the generally lower occurrence of power lows during a typical wet year.

In summary, the results of Figure 4.13 suggest that standby hours are primarily linked to seasonal and yearly variations in water availability rather than sudden hourly fluctuations. Indicating that many of the standby hours occur consistently. This is supported by the fact that there are no instances of switching from production to standby more than five times in one day. Additionally, Figure 4.5 shows that there are no sudden changes in power production from hour to hour; instead, production remains stable or gradually changes throughout the day. This suggests that if standby occurs, production is unlikely to resume in the next hour. However, there will be a gradual increase in available power, eventually leading to the resumption of production. This assumption requires further examination to be confirmed with certainty.

The distribution between the power purchased from the hydropower plant and the grid when the electrolyzer is on standby mode is illustrated in Figure 4.14. The y-axis shows the power input in

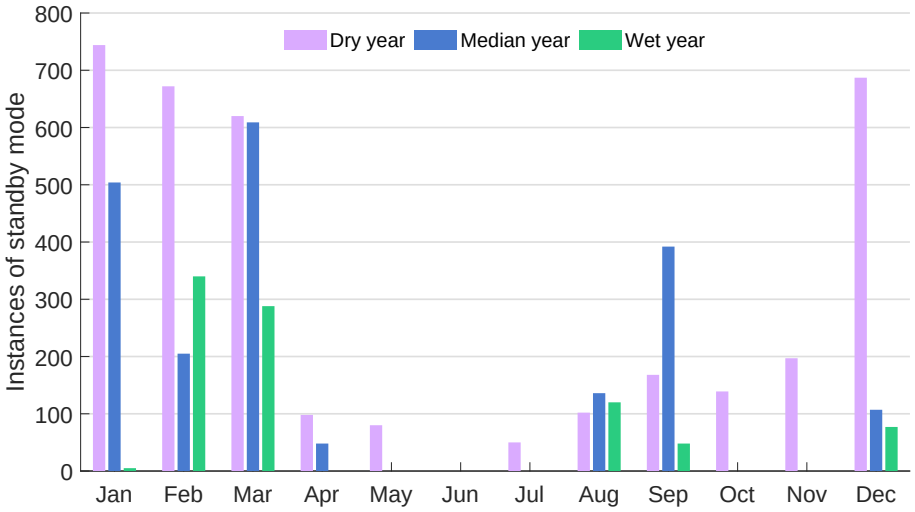

(a) 1 MW

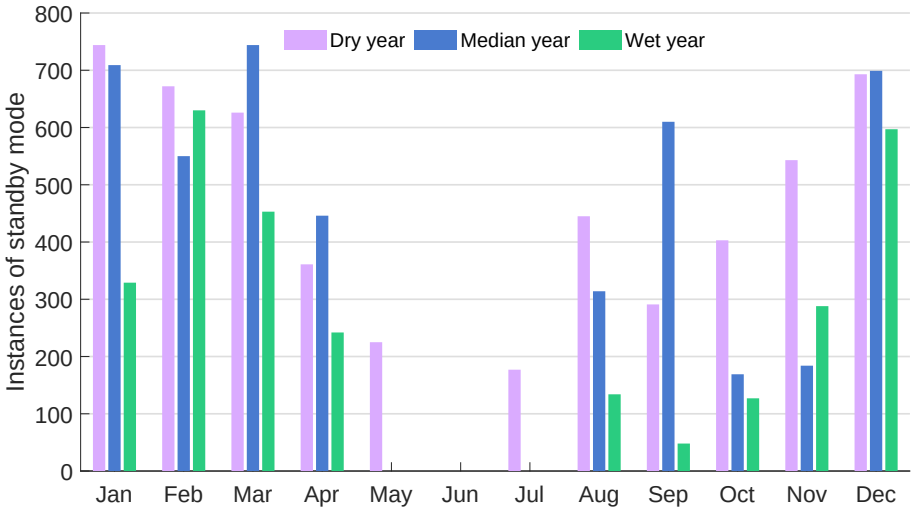

(b) 3 MW

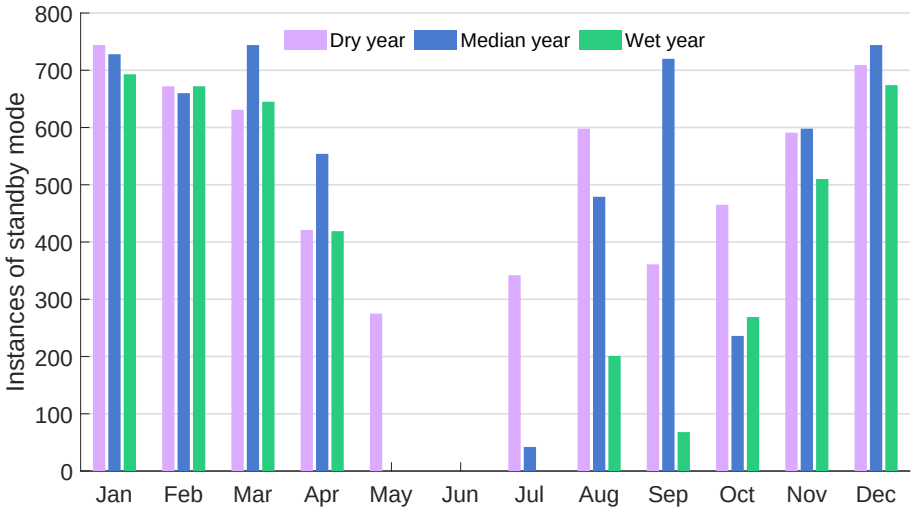

(c) 5 MW

Figure 4.13: Monthly instances of standby mode for the typical dry year (2010), the median year (2008), and the typical wet year (2007) using different electrolyzer capacities: (a) 1 MW (b) 3 MW (c) 5 MW.

kWh, while the x-axis displays the different capacities of the electrolyzer. Each capacity has two bars per year, representing the amount of power obtained from the hydropower plant and the grid, respectively. As the electrolyzer capacity increases, the energy required to maintain it on standby increases: 45 kW times the electrolyzer capacity.

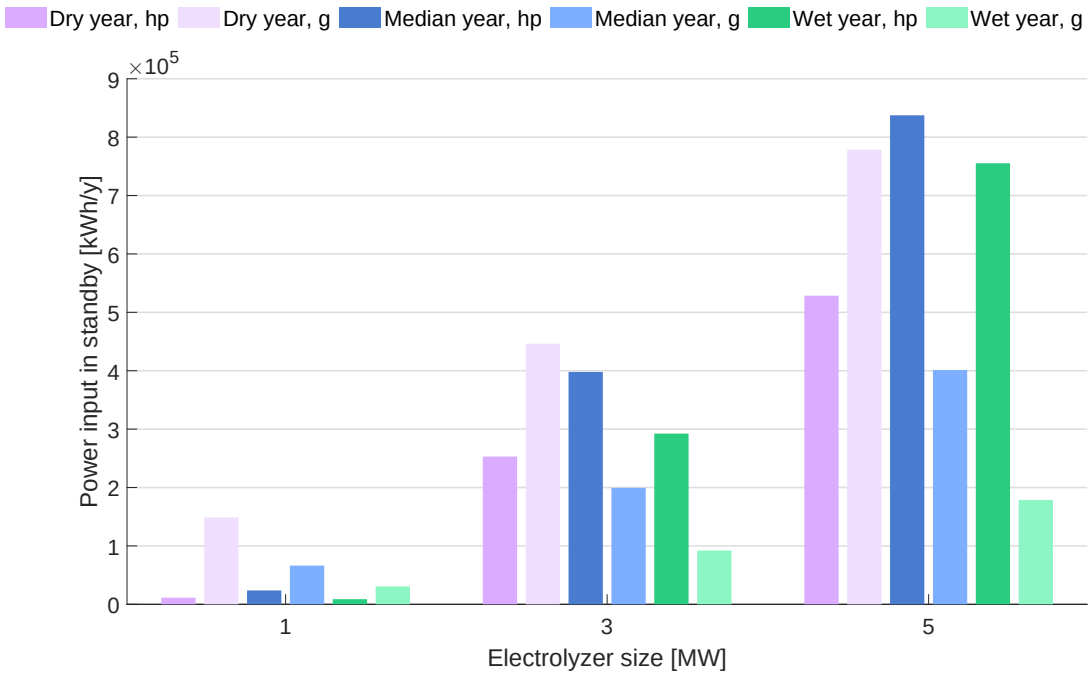

Figure 4.14: The distribution of power input in standby mode, between power from the hydropower plant and power bought from the grid, for the typical dry year (2010), the median year (2008), and the typical wet year (2007), per electrolyzer capacity. Hydropower is shortened to hp and grid to g in the legend.

Generally, there is a clear trend of increasing power purchased from the hydropower plant and grid in standby with increasing electrolyzer capacity for all years. The 1 MW electrolyzer mainly draws power from the grid during standby, a trend consistent across all three years. This can be attributed to the low power demand of the electrolyzer during standby, which stands at 45 kW. Given this minimal power requirement, when the electrolyzer transitions to standby mode, it's likely due to a significant reduction or near halt in production from the hydropower plant. In such scenarios, the available power solely from the hydropower plant may not suffice to sustain the electrolyzer in standby mode, necessitating additional grid power.

In the typical dry year, the grid supplies more power than the hydropower plant for both 3 MW and 5 MW electrolyzers. This is assumed to be a result of periods with low water availability, leading to insufficient power production from the hydropower plant to sustain the electrolyzer in standby without supplementary power from the grid.

However, for the median and wet years, the hydropower plant supplies most of the power. In the median year, the power from the hydropower plant is twice as much as the power from the grid both for the 3 MW electrolyzer and 5 MW. In the typical wet year, the hydropower plant supplies three times more power than the grid for the 3 MW electrolyzer and almost four times more power for the 5 MW electrolyzer. The fact that the hydropower plant provides the majority of the electricity during standby suggests that the electrolyzer may be oversized. This is because

the higher the electrolyzer's capacity, the higher the requirement for minimum power input for production before the electrolyzer switches to standby mode. This implies that power lows are used to keep the electrolyzer on standby during the median and typical wet years, instead of being utilized for production.

4.3 Cost analysis

In addition to assessing hydrogen production and electrolyzer operation, a cost analysis has been conducted to compare different electrolyzer capacities. This analysis included CAPEX, OPEX, and the costs associated with electricity for stack operation and compression. The calculation is done in units of LCOH, the cost of producing 1kg of hydrogen. The comparisons utilized data from the year 2008, identified as the median year. Additionally, a sensitivity analysis on grid costs was performed, evaluating scenarios with low, middle, and high electricity prices, as detailed in Section 3.4.1. The chosen end pressure for the hydrogen is 350 bar, which aligns with the requirements of maritime transport and heavy-duty trucks.

As detailed in Section 3.4.3, the investment cost of compressors has been calculated across 36 different scenarios. The calculations of these scenarios rely on the installed power required for compression in each scenario, utilizing Equation 3.11 [35]. Further, the installed compressor power is employed to calculate investment costs using Equation 3.7 [35]. These equations are also further detailed in Section 3.4.3. The results, including the required power installation and compressor investment costs across all 36 scenarios, are provided in Appendix A.

In the cost analysis, the scenarios considered for the investment cost of compressors are those with an end pressure of 350 bar and electricity sourced from the grid. Based on these assumptions, the average compressor investment costs across the years 2010, 2008, and 2007 were calculated to be 2 317 100 NOK for a 1 MW electrolyzer, 3 209 300 NOK for a 3 MW electrolyzer, and 3 618 400 NOK for a 5 MW electrolyzer. These figures were integrated into the respective CAPEX for each capacity before computing the LCOH.

Figure 4.15 presents the cost analysis of the hydrogen production at location A, where the production from the median year 2008 was utilized. The LCOH was calculated across varying electrolyzer capacities: 1 MW, 3 MW, and 5 MW. The x-axis categorizes these capacities, while the y-axis quantifies the cost of NOK/kg hydrogen. The total LCOH price is the minimum price at which the hydrogen needs to be sold for the hydrogen producers to break even the year 2008, refereed to as equilibrium price. Table 4.2 presents the total LCOH price in the cost analysis. To break even, the hydrogen supplier needs to sell the hydrogen between 53.70 to 54.50 NOK/kg, 70.70 to 71.70 NOK/kg, and 82.00 to 83.40 NOK/kg for 1 MW, 3 MW, and 5 MW, respectively.

The results underscore the significant role of plant size in influencing the LCOH for each electricity cost scenario. As the electrolyzer capacity increases from 1 MW to 5 MW, the total LCOH also rises. This increase is not linear but rather exponential, with the LCOH rising by approximately 30 % when capacity increases from 1 MW to 3 MW, followed by an additional 16 % increase from 3 MW to 5 MW. The primary drivers of the overall LCOH are CAPEX and the cost of electricity during stack production.

The CAPEX results for 1 MW, 3 MW, and 5 MW are 28.00 NOK/kg, 41.00 NOK/kg, and 49.90 NOK/kg, respectively. This accounts for 52 %, 59 %, and 60 % of the total LCOH cost in the

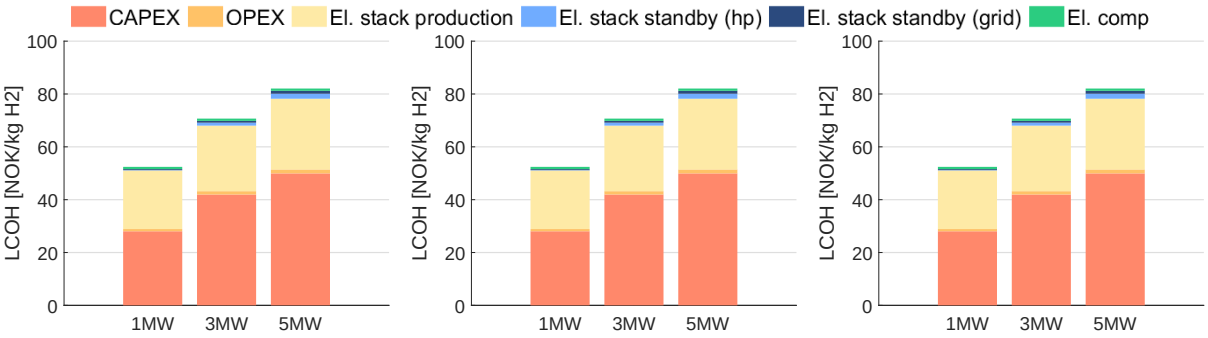

(a) Low electricity price (b) Middle electricity price (c) High electricity price

Figure 4.15: An economic comparison of 1 MW, 3 MW, and 5 MW electrolyzer capacities utilizing hydrogen production data from the median year 2008. The analysis focuses on the LCOH and considers CAPEX, OPEX, and electricity costs. A sensitivity analysis of grid prices, encompassing low, medium, and high scenarios, is included in the cost analyses.

Table 4.2: The equilibrium price of hydrogen in 2008, in units of NOK/kg

	Total LCOH [NOK/kg h2]		
	1 MW	**3 MW**	**5 MW**
Low grid price	53.70	70.70	82.00
Middle grid price	53.90	70.90	82.40
High grid price	54.50	71.70	83.40

middle grid price scenario. CAPEX accounts for a higher percentage of the total LCOH with increasing electrolyzer capacity. This indicates that the increased investment in higher capacity does not yield a proportional increase in the annual production of hydrogen. In other words, the increase in hydrogen production is not significant enough to neutralize the increased capital cost of installing a higher electrolyzer capacity. Moreover, the cost of electricity provided to the stack during production, a significant cost component, is 22.20 NOK/kg, 24.80 NOK/kg, and 26.80 NOK/kg, for 1 MW, 3 MW, and 5 MW, accounting for 41 %, 35 %, and 32 % of the total LCOH cost. As the electrolyzer capacity increases, electricity costs to the stack also increase. However, as electrolyzer capacity increases, the fraction of electricity costs for production in the total LCOH decreases.

Regarding LCOH, OPEX, electricity used in standby mode and for compression comprise a smaller portion of the total cost. When considering the middle scenario, OPEX accounts for 1.56 %, 1.76 %, and 1.81 % of the total cost for 1 MW, 3 MW, and 5 MW, respectively. This indicates that the operational cost increases as the electrolyzer capacity increases. Additionally, the cost of electricity during standby mode consists of 0.92 %, 2.52 %, and 3.61 % of total LCOH, when considering both electricity from the hydropower plant and the grid. As the electrolyzer capacity increases, the cost of standby has an increasing influence on the total LCOH. However, the compression price in the middle grid scenario is constant at 0.99 per kg of hydrogen across capacities. This results in the cost of compression accounting for 1.83 %, 1.39 %, and 1.20 % of the total LCOH for 1 MW, 3 MW, and 5 MW. This indicates that with higher electrolyzer

capacity, the compression cost per kg of hydrogen has a smaller impact on the overall cost.

In the sensitivity analysis examining grid prices, the costs are influenced during two specific phases: the electricity used for compression and the portion of standby mode where electricity is purchased from the grid. This is illustrated in Figure 4.16, as a segment of the total LCOH analysis. The LCOH for electricity purchased from the grid during standby varies by grid price scenario and electrolyzer capacity. For a 1 MW electrolyzer, the LCOH is 0.40 NOK/kg, 0.50 NOK/kg, and 0.70 NOK/kg for the low, middle, and high price scenarios, respectively. Similarly, for a 3 MW electrolyzer, the LCOH during standby is 0.70 NOK/kg, 0.80 NOK/kg, and 1.10 NOK/kg. Lastly, for a 5 MW electrolyzer, the LCOH is 1.10 NOK/kg, 1.30 NOK/kg, and 1.90 NOK/kg. As mentioned, the attribution of compression remains constant across different electrolyzer capacities. However, it increases with rising grid prices. Compression at a low grid price yields an LCOH of 0.90 NOK/kg, at a middle grid price 1.00 NOK/kg, and at a high grid price 1.40 NOK/kg.

The total influence on the sensitivity analysis per kg of hydrogen varies by approximately 0.80 NOK/kg from low to high grid prices for a 1 MW electrolyzer. For a 3 MW electrolyzer, the difference between low and high grid prices is approximately 1.00 NOK/kg, and for a 5 MW electrolyzer, it is approximately 1.30 NOK/kg. These results indicate that changes in grid prices will have a marginal impact on the overall LCOH.

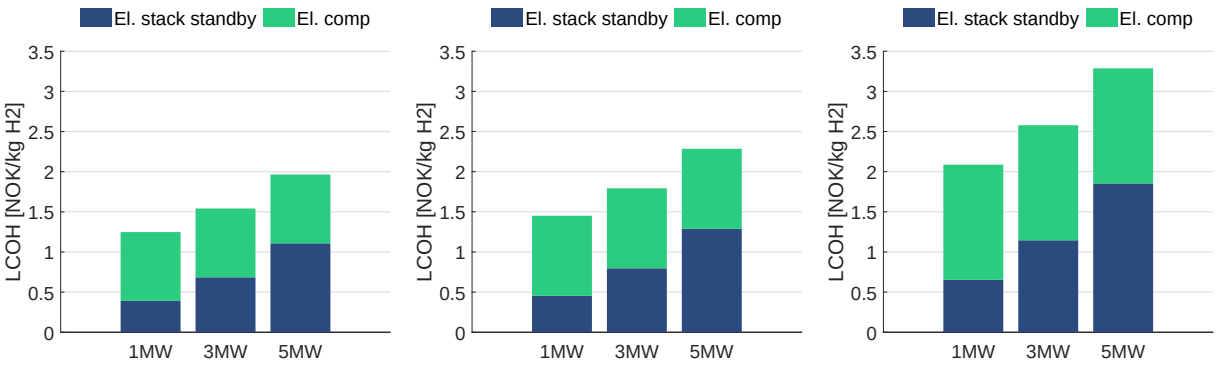

(a) Low electricity price (b) Middle electricity price (c) High electricity price

Figure 4.16: A segment of the cost analysis for the three electrolyzer capacities, based on hydrogen production from the median year 2008, highlights the impact of sensitivity analysis on grid prices. The grid price affects the LCOH of electricity consumption in standby and compression.

In addition to the cost analysis of 2008, similar calculations were made for 2007 and 2010. These additional calculations also include the LCOH of compression at 700 bar and purchasing electricity for compression from the hydropower plant at 350 bar and 700 bar. The results from the supplementary calculations are presented in Table 4.3. The CAPEX in the table still includes investment in a compressor where the product has 350 bar. Across all capacities, CAPEX and OPEX show linear decreases from the typical dry year 2010, through the median year 2008, to the typical wet year 2007.

As mentioned, the impact of the electricity cost during compression is constant per scenario across all electrolyzer capacities and even over the three years. When the end pressure is 700 bar, the most cost-effective option is to purchase electricity from the hydropower plant, similar to the

scenario where the end pressure is 350 bar. If the end pressure is increased from 350 bar to 700 bar, the cost of electricity from the hydropower plant varies by 0.30 NOK/kg. In addition, the difference in LCOH between 350 and 700 bar for the different grid prices, low, middle, and high grid prices makes up 0.40 NOK/kg, 0.40 NOK/kg, and 0.60 NOK/kg, respectively.

Table 4.3: Economic analysis of 1 MW, 3 MW, and 5 MW electrolyzer capacities for three different years (2010, 2008, and 2007) with a sensitivity analysis of low, medium, and high grid costs.

	1 MW			3 MW			5 MW		
LCOH [NOK/kg H2]	2010	2008	2007	2010	2008	2007	2010	2008	2007
CAPEX	34.10	28.00	21.70	51.30	42.00	31.00	62.50	50.00	37.70
OPEX	1.00	0.80	0.70	1.50	1.30	0.90	1.90	1.50	1.10
El. Stack production	22.30	22.20	22.30	24.70	24.80	24.80	26.40	26.80	26.60
El. stack standby (hp)	0.10	0.10	0.01	0.90	1.10	0.60	1.50	1.90	1.30
El. stack standby (grid, low)	1.10	0.40	0.10	1.90	0.70	0.20	2.70	1.10	0.40
El. stack standby (grid, middle)	1.20	0.50	0.20	2.20	0.80	0.30	3.10	1.30	0.40
El. stack standby (grid, high)	1.80	0.70	0.20	3.10	1.10	0.40	4.50	1.90	0.60
El. comp (350, hp)	0.70	0.70	0.70	0.70	0.70	0.70	0.70	0.70	0.70
El. comp (350, grid, low)	0.90	0.90	0.90	0.90	0.90	0.90	0.90	0.90	0.90
El. comp (350, grid, middle)	1.00	1.00	1.00	1.00	1.00	1.00	1.00	1.00	1.00
El. comp (350, grid, high)	1.40	1.40	1.40	1.40	1.40	1.40	1.40	1.40	1.40
El. comp (700, hp)	1.00	1.00	1.00	1.00	1.00	1.00	1.00	1.00	1.00
El. comp (700, grid, low)	1.20	1.20	1.20	1.20	1.20	1.20	1.20	1.20	1.20
El. comp (700, grid, middle)	1.40	1.40	1.40	1.40	1.40	1.40	1.40	1.40	1.40
El. comp (700, grid, high)	2.10	2.10	2.10	2.10	2.10	2.10	2.10	2.10	2.10

4.4 Comparison of technologies

The following section compares two electrolyzer technologies: pressurized AEL and PEM. Therefore, whenever AEL is mentioned in the following paragraphs, it refers specifically to pressurized AEL. The aim is to determine which technology is better suited for fluctuating power from a small-scale hydropower plant. Therefore, efficiency is compared, and also lifespan. Moreover, the CAPEX and OPEX associated with each technology will be compared. Operating conditions will also be compared. This includes evaluation of the dynamic range to understand the width of the operation. Also, the energy consumption on standby will be presented. Lastly, response time will be considered to assess how quickly each technology can adjust to changing power input. All the values in this section are for a 1 MW electrolyzer.

The values in Table 4.4 and Table 4.5 represent data collected from conversations and correspondences with various electrolyzer suppliers. All suppliers have requested to remain anonymous; hence, no source is attached to the values. In a rapidly growing market like the hydrogen market, it is crucial for suppliers of hydrogen technology to keep detailed information about their technology confidential to maintain a competitive edge. Despite the lack of sources, an assessment has been made to include the values because they significantly contribute to the value of this thesis.

Table 4.4 lists technical specifications for the two technologies. The stack efficiency measures the effectiveness of converting electrical energy and water to hydrogen fuel in units of energy consumed per kg of hydrogen. A higher value indicates lower efficiency. PEM electrolyzers exhibit a stack efficiency of 52 kWh/kg, marginally better than AEL electrolyzers, at 53 kWh/kg. In terms of system efficiency at the beginning of life, AEL shows a slightly lower performance at 59 kWh/kg compared to 57 kWh/kg for PEM systems. System efficiency refers to the effectiveness of the entire electrolysis setup. Different types of AEL and PEM electrolyzer technologies exist, and some may exhibit higher efficiency than those discussed in this thesis.

Table 4.4: Technical specifications for the electrolyzer technologies AEL and PEM. The values are provided by suppliers, and therefore, the source is confidential.

	AEL	**PEM**
Stack-efficiency [kWh/kg]	53	52
System-efficiency [kWh/kg]	59	57
Lifespan stack [h]	100 000	80 000
CAPEX [NOK/kW]	6 800 - 12 750	11 900 - 17 850
OPEX [% of CAPEX]	2-3	3-5

This thesis compares the lifespan of the stack rather than the system lifetime, as the former is often shorter. The lifespan of the AEL stack is noted to be 100 000 hours, which is longer than that of the PEM stack, which has a lifespan of 80 000 hours. This longer lifespan can impact the operational cost and frequency of maintenance. Considering the financial aspects, CAPEX for AEL technology ranges from 6 800 NOK to 12 750 NOK per kW, while PEM systems are notably higher, costing between 11 900 NOK and 17 850 NOK per kW. Moreover, OPEX as a percentage of CAPEX is 2 to 3 % for AEL and 3 to 5 % for PEM, suggesting that AEL may be

more cost-effective to maintain.

Moreover, the shorter lifespan of PEM electrolyzers can be attributed to the acidic conditions within the PEM stacks, which accelerate component degradation. The harsh environment in the PEM stack requires using materials that can endure it, such as noble metals. In contrast, the AEL stack operates without the need for noble metals. Additionally, PEM electrolyzers require more maintenance. Hence, the acidic stack environment can explain the higher CAPEX and OPEX costs for PEM electrolyzers. Additionally, when considering the choice between AEL and PEM, it's crucial to consider environmental and safety factors. While noble metals are necessary for PEM electrolyzers to function, their use raises significant environmental concerns due to the impacts associated with their extraction and processing.

Further, in Table 4.5, the operational dynamics of the technologies are listed. Dynamic range refers to the width of power inputs an electrolyzer can utilize to produce hydrogen. It is expressed in the percentage of the electrolyzer's capacity and can be calculated accordingly. PEM electrolyzers offer a dynamic range of 10 to 100 %, providing considerable flexibility in operation. On the other hand, AEL systems have a dynamic range of 16 to 100 %, which offers less flexibility but can operate efficiently over most of the capacity range.

Table 4.5: Operational dynamics of AEL and PEM electrolyzers. The values are provided by suppliers, and therefore, the source is confidential.

	AEL	**PEM**
Dynamic range [%]	16 – 100	10 - 100
Energy consumption in standby [kW]	45	28
From production to off [min]	$\leq$ 54	-
From off to production [min]	$\leq$ 45	-
From production to standby [sek]	$\leq$ 13	$<$ 4
From standby to production [min]	$\leq$ 6	$\leq$ 5
Response to load change [sek]	$\leq$ 3 - 9	$\leq$ 10 - 60

In standby energy consumption, PEM units are more economical. Response time is crucial for integration with renewable energy sources, PEM can quickly transition from standby to 100 % production within 5 minutes or less, and AEL requires 6 minutes or less. Both technologies perform similarly. However, AEL requires up to 54 minutes to turn off and up to 45 minutes to restart, whereas there is not enough available information about PEM. However, both technologies need to go through flushing when powering down and up. Therefore, the response time for powering down and up for both technologies will likely not differ significantly.

Switching from production to standby takes 13 seconds for AEL, while PEM is faster at less than 4 seconds. Regarding responding to load changes, AEL quickly adapts within 3 to 9 seconds. PEM electrolyzers also respond efficiently to load changes, adapting within 10 to 60 seconds. Load change is the time it takes for the electrolyzer to move from 25 to 75 % of its production capacity to 100 % of its production capacity.

4.5 End-user

It is important to understand the local demand for hydrogen and identify potential end-users to ensure the feasibility and success of the hydropower-to-hydrogen project. A report by EY entitled "Grønn region Sunnhordland" highlights the importance of HYDS's hydrogen production for local industry and as a zero-emission fuel for cars, heavy-duty trucks, and boats [43]. Additionally, the byproduct oxygen can be utilized.

4.5.1 Industry

Hydrogen can be an important input resource for decarbonizing the industrial sector. INEOS and Hydro Husnes, are located within 70 km from location A. As mentioned in Section 2.2.4, INEOS is a smelter aiming to transition from coal to hydrogen for titanium dioxide production, necessitating a hydrogen supplier. Similarly, Hydro Husnes, engaged in aluminum production, traditionally relies on natural gas in melting ovens. The large amount of heat energy from hydrogen combustion offers a promising alternative to natural gas in aluminum production, potentially reducing emissions. Hydro Havrand has conducted successful trials utilizing green hydrogen for aluminum production in Spain, indicating feasibility for similar initiatives in Norway [44]. Beyond aluminum, hydrogen combustion holds promise for other high-temperature processes, such as glass and cement production, where electrification may not suffice.

4.5.2 Transport

There is a European highway within a 10 km radius of location A. On the webpage of The Norwegian Public Roads Administration, there is statistical data on Norwegian roads. Data from a measuring point at the European highway near location A is presented in Table 4.6. The table displays the daily average number of vehicles per month for the year 2023. The website does not have a way of sorting the type of vehicle, but there is a distinction between vehicles under 5.6m and vehicles over 5.6 m. It is assumed that all the vehicles under 5.6m are passenger cars, and the ones over 5.6 m are heavy-duty transport.

The data in Table 4.6 underscores the need for fuel in the area, and as we move to a green society, these fuels need to be emission-free. The number of vehicles passing by per day on average slightly increased from January to May and peaked during June, July, and August. There was a minor decline in the number of vehicles from September to December. This pattern can also be observed in the daily average number of heavy-duty vehicles, where the number of vehicles increases from January to July and decreases from July to December.

As mentioned in Section 2.2.4, Norway has a well-established infrastructure for electric passenger vehicles, but the government aims to establish a hydrogen infrastructure for heavy-duty vehicles by 2050 [22]. In addition, hydrogen has some advantages over batteries as fuel, especially for vehicles with high energy demand, long-distance transport, and vehicles needing lighter energy systems [45]. Initiating this transition is Evig Grønn, leading the H2Truck project, which aims to import and deploy 100 hydrogen-powered trucks procured from MAN on the roads by 2025 [46]. Yet, the project's success depends on establishing hydrogen filling stations along Norwegian highways.

Table 4.6: The average number of vehicles passing the measurement point daily on a European highway within a 10 km radius of location A in the year 2023.

Month	Average daily traffic	Vehicle < 5.6 m	Vehicle > 5.6 m
January	1 361	1 052	306
February	1 595	1 252	341
March	1 873	1 461	409
April	2 151	1 732	412
May	1 987	1 402	568
Jun	2 399	1 665	695
July	3 333	2 497	806
August	2 751	1 989	728
September	1 859	1 335	515
October	1 768	1 274	490
November	1 331	953	374
December	1 257	947	306

In the maritime sector, there is great potential for finding a customer base. With nearness to a dock, location A serves as a strategic point for maritime activities, including fjord cruises, fast ships from Bergen, and ferries. Notably, fast ships are reported to have the highest emissions per passenger kilometer among all transportation segments in Norway [45]. Moreover, companies like Eidesvik, Wärtsilä, and Bremnes Seashore seek emission-free ship solutions [43]. Eidesvik specializes in ship management, Wärtsilä supplies technology to the maritime sector, and Bremnes Seashore is involved in fish farming. To underscore the maritime sector's importance as a key customer base, consider Enova's support program, "Hydrogen Production for Maritime Transport 2027" [47]. Enova provides up to 80 % support for hydrogen production facilities and vessels through this initiative.

4.5.3 Utilization of byproducts

The production of hydrogen yields oxygen and heat as byproducts. As discussed in Section 2.3, NVE has collaborated with Småkraftverkforeninga on an R&D project focusing on hydrogen production from small-scale hydropower plants. Part 2 of this project explores the potential for utilizing byproducts from the electrolyzer, like oxygen and heat, particularly in a nearby smolt facility [27]. The study found that selling the oxygen and heat from the electrolyzer could enhance the feasibility of the hydrogen facility. Smolt facilities are closed tanks onshore where fish are bred and raised until they are big enough to survive in the ocean [41]. These tanks require a continuous flow of water and a supply of oxygen for the fish to breathe. Additionally, during the winter months, they need a source of heat. In the area around location A, there are several fish farms with smolt facilities, within a 50 km radius.

Chapter 5

Discussion

The discussion chapter of this thesis examines key aspects of establishing profitable hydrogen production from a small-scale hydropower plant, focusing on striking a balance between the interests of the power supplier, SKL, and the hydrogen producer, HYDS. The following sections aim to provide an additional interpretation of the results presented in Chapter 4. The discussion will begin by addressing the optimal capacity of the plant's electrolyzer. Then, it will dive into the comparison of pressurized AEL and PEM in terms of their ability to manage fluctuating power. Finally, a summary of the key bottlenecks influencing investment decisions will be presented.

5.1 Electrolyzer capacity

First, the implications of different electrolyzer capacities on the project's feasibility are discussed. This includes the impact of power fluctuations on hydrogen production and electrolyzer operation, as well as the economic viability of the capacities in relation to the LCOH, which is dependent on the cost of the project and the amount of hydrogen produced. The electrolyzers are powered by the power production of the selected three years in Chapter 3.2.1: the typical wet year 2010, the median year 2008, and the typical dry year 2007.

Selecting an electrolyzer that can effectively utilize the installed power from the hydropower plant at location A is crucial. Illustrated in Figure 4.7, the comparison of power utilization intervals among 1 MW, 3 MW, and 5 MW electrolyzers, underscores the inability of the 1 MW electrolyzer to tap into potential power at location A. While both the 3 MW and 5 MW electrolyzers utilize power peaks, the former also utilizes power lows, unlike the latter. Hence, although none of the electrolyzers perfectly align with the power production from location A, the findings indicate that the 3 MW electrolyzer would be the best choice. This is also supported by the monthly production in Figure 4.9. The production of hydrogen during low and peak power periods ensures steadier production throughout the year and potentially benefits end-users.

Section 4.2.2 presents the key findings of hydrogen production over the three years. These findings underscore the direct impact of water availability for electricity generation on hydrogen production. Equally important is the role of the electrolyzer's capacity, with higher capacity directly correlating to higher production. The most significant increase in hydrogen production is observed when transitioning from a 1 MW to a 3 MW electrolyzer, which doubles the production

yield. However, upgrading from 3 MW to 5 MW does not result in a proportional increase in hydrogen production, suggesting that upgrading to a 5 MW electrolyzer may not provide significant benefits compared to upgrading from 1 MW to 3 MW electrolyzer. This observation aligns with the cost analysis, indicating that the marginal increase in hydrogen production from 3 MW to 5 MW fails to balance the increased capital cost of the installation.

Production of hydrogen utilizing a 3 MW and 5 MW electrolyzer follows a seasonal trend, as illustrated in Figure 4.9 monthly variation in production. Excess hydrogen with no market demand during the high hydrogen production season is not profitable. One solution to this issue could be to find end-users who only require hydrogen shipment during the summer, in addition to an end-user requiring hydrogen consistently throughout the year. Also, end-users who have the capability to store hydrogen over a longer period could be an alternative. Another suggestion is to have on-site hydrogen storage at location A, where surplus hydrogen can be stored and accessed when the production from the electrolyzer is insufficient for delivery to the end-user. However, this might be costly and will increase the LCOH.

As electrolyzer capacity increases, the number of full load days decreases, while zero production days increases. Figures 4.11 and 4.12 illustrate that the 3 MW electrolyzer balances the extremes represented by the 1 MW and 5 MW capacities. Additionally, standby instances illustrated in Figure 4.13 highlight underutilization of the 5 MW electrolyzer during low power seasons, reflecting a similar trend observed for the 3 MW but to a lower extent.

In Section 2.3, the absence of a standardized method for quantifying electrolyzer degradation is noted. However, based on the assumption that transitioning from production to standby over five times a day could negatively impact the electrolyzer cell, it's found that such instances are absent across all years and capacities studied. This suggests that fluctuating power does not significantly degrade the electrolyzer stack.

However, it's important to note that the data resolution utilized in this thesis is hourly. This indicates a lack of insight into how power production from the hydropower plant fluctuates within these hourly intervals. If the data were available at a higher resolution, such as every ten minutes, it's possible that the electrolyzer could switch modes up to five times a day. The degradation of the stack could mean a shorter lifetime, increased maintenance, a higher risk of damaging safety mechanisms within the stack, and consequently, a greater probability of accidents.

5.1.1 Economics

In this thesis, the validity of the LCOH values is assessed using Ulleberg's article from 2020 as a reference [38]. Ulleberg's calculations, which consider factors such as electrolyzer capacity, end pressure, the extent of electrolyzer capacity utilization, and on-sight hydrogen production at a filling station or not, provide a comprehensive range of hydrogen prices from 141 NOK/kg to 58 NOK/kg. These calculations also incorporate the storage and refueling of hydrogen. Importantly, Ulleberg's work highlights that for hydrogen to be competitive with diesel for vehicles, the price needs to be 52 NOK/kg.

Comparing these values to Table 4.2, the LCOH results from the high grid price scenario indicate turnover prices for hydrogen from the 1 MW, 3 MW, and 5 MW electrolyzers were 54.50 NOK/kg, 71.70 NOK/kg, and 83.40 NOK/kg, respectively. This suggests that the LCOH

calculated in this thesis is reliable when compared to Ulleberg's results, but the prices must be lower to compete with diesel.

In addition, the EU's Innovation Fund held its first hydrogen auction, attracting 132 bids from 17 European countries [48]. One purpose of the auction was to determine a market price for green hydrogen expressed in LCOH. Based on 14 bids from Norway, the average Norwegian marked price for green hydrogen was estimated by the EU to be 76 NOK/kg. This suggests that the LCOH calculated in this thesis for the 1 MW and 3 MW electrolyzers would be competitive in the Norwegian market. In comparison, the hydrogen produced from the 5 MW electrolyzer is too expensive.

Another goal of the hydrogen auction was to select seven hydrogen projects for subsidies [48]. The ceiling price of the auction was 45 NOK/kg, all bids above this were excluded. Also, there was a demand for the minimum capacity of the electrolyzer to be 5 MW. The bids in the auction ranged from 3.7 NOK/kg to 48 NOK/kg, with the winning bids for the seven selected projects falling between 3.7 NOK/kg and 4.8 NOK/kg. Notably, the Norwegian project SKIGA was among the winners, with a bid price of 4.8 NOK/kg. To achieve this price, the project requested 813 174 430 NOK in funding. To be competitive with this supplier, the hydrogen project at location A would need to be heavily subsidized.

Further, it's important to note that the economic analysis in this thesis is simplified. A more comprehensive cost analysis would include the cost of transporting the hydrogen, the entire electrolyzer setup (not only the cell), the facility, construction, personnel salaries, and other significant aspects, including the project funding strategy and financial cost. For instance, the cost of capital would need to be factored into the LCOH if loans are involved. Additionally, the LCOH calculated in this thesis represents the break-even price. If HYDS intends to generate profit from the hydrogen, this factor must be taken into account. All these factors would increase the LCOH cost, but to what extent is unknown.

As previously mentioned, the LCOH of produced hydrogen depends on various factors, including end-user, storage, and transportation. Notably, transportation is excluded from the cost analysis in this thesis. The price of hydrogen depends on the chosen storage method, whether it needs to be compressed, chemically bound, or liquefied. End-users may have preferences for specific storage methods, which can cause the cost of storage equipment to vary from what is used in this thesis. According to Ulleberg's article, the cost of transporting hydrogen from a production site to a filling station amounts to 25 NOK/kg, based on a weekly transport of 230 kg of hydrogen [38]. The cost of transportation includes the distance the hydrogen needs to be transported. In Ulleberg's article, he defines the transport cost based on the duration of transportation, estimating it at 1 200 NOK per hour. In his case, the transportation takes 5 hours. In this thesis, considering the median year, the average weekly production would be 1647 kg H_2 for 1 MW, 2821 kg H_2 for 3 MW, and 3500 kg H_2 for 5 MW, thus leading to higher transportation costs. Additionally, the duration of transportation depends on the end-user.

Moreover, the hydrogen auction highlighted the willingness to pay in the mobility and industrial sectors [48]. The willingness to pay is higher in the mobility sector at 83.4 NOK/kg, compared to 56.7 NOK/kg in the industry sector. These numbers are based on expected off-take prices in Europe and do not precisely reflect the willingness to pay in the Norwegian hydrogen market. However, they do provide an indication. Doing a more detailed cost analysis would increase the

LCOH, suggesting that the cost of the hydrogen produced at location A might fall outside the expected willingness to pay values.

5.2 AEL vs. PEM

In Section 4.4, a comparison was made between two types of electrolyzer technologies, pressurized AEL and PEM, to determine their suitability for managing fluctuating power inputs. The key findings revealed that while PEM exhibits slightly better system efficiency, AEL boasts a longer lifespan. It is worth noting that various types of AEL and PEM electrolyzer technologies are available, and some may be more efficient than the ones mentioned in this thesis. The comparison conducted in the research was done using commercial electrolyzers. Two examples of electrolyzer technologies with better efficiency than the one used in this thesis are Sunfire's AEL electrolyzer HyLink and Hystar's PEM electrolyzer. The Sunfire HyLink AEL electrolyzer has a stack efficiency of 46.5-50.5 kWh/kg and a system efficiency of 47.6-51.95 kWh/kg [49]. The system efficiency is significantly better than the 59 kWh/kg for the AEL used in the thesis. On the other hand, the Hystar PEM electrolyzer has a stack efficiency of 46.6 kWh/kg and a system efficiency of 51.0 kWh/kg [50]. In comparison, the values used for PEM in this thesis are 52 kWh/kg for stack efficiency and 57 kWh/kg for system efficiency.

PEM is often referred to as the technology best suited for fluctuating power input, while AEL is said to have a slower response time than PEM. However, after gathering operation specifications for both technologies, only minor differences in response time appear between the two.

In the comparative analysis of pressurized AEL and PEM electrolyzer technologies, technical data have been gathered from various electrolyzer suppliers. While references have not accompanied the values, they are assumed to be reliable since they are directly from the industry. However, the data quality can vary between different suppliers, influenced by their varying levels of experience and technology maturity. Some suppliers have technologies tested on a large scale and over a long period. In contrast, others may provide specifications based on laboratory-scale tests. Additionally, the electrolyzer market constantly evolves, with competition and innovation driving a wide range of technological offerings. This diversity makes it challenging to directly compare data between suppliers due to the significant variation in available technologies.

Therefore, a comprehensive comparison should not only consider efficiency, lifespan, economics, and operational parameters but also consider factors such as a deeper understanding of technology variations in the market, safety, materials used, system area, environmental footprint, product purity, and end-user application. However, after examining the data gathered in this thesis, it's clear that the differences between the two technologies are minimal.

5.3 Bottlenecks for an investment decision

The results in this thesis are not sufficient to provide a clear recommendation on whether to build a hydropower plant for hydrogen generation at location A, nor to determine the optimal capacity of the electrolyzer. However, this thesis provides a knowledge base that can be used in further decision-making to assess whether this is a good investment. When considering an investment in hydrogen production from fluctuating renewable power, these are the most critical bottlenecks

for investment decisions:

- Is there a consistent flow of hydrogen produced from the site throughout the year?
- Gain an understanding of the seasonal variations in fluctuating power, and consequently, the seasonal variations in hydrogen production.
- Assess the total yearly production. Is the production from the site sufficient for profitable operations?
- Do the increased electrolyzer capacity and higher hydrogen production balance out the higher investment cost?
- Is the LCOH of the hydrogen produced competitive in the Norwegian hydrogen market?
- Are there any nearby sectors in need of hydrogen?
- Are there any nearby sectors in need of oxygen or heat?
- Identifying the end-user is vital for accurately assessing the LCOH and feasibility of the project. This decision impacts factors like the end pressure of the hydrogen, storage methods, and the necessity of on-site filling or hydrogen transportation.
- If the hydrogen is intended for the transportation sector, is the production site near a highway or dock, or does the hydrogen need to be transported over a long distance?

Chapter 6

Conclusion

This thesis has studied the feasibility of producing hydrogen from a small-scale hydropower plant at location A with a turbine capacity of 6.3 MW. After investigating the suitability of 1 MW, 3 MW, and 5 MW electrolyzers for the plant, it is concluded that the 1 MW electrolyzer insufficiently utilizes the power available at location A. The 5 MW electrolyzer yields the highest annual production of hydrogen. However, the capacity fails to use power lows effectively, and the high investment is not balanced by a sufficient increase in hydrogen production. The 3 MW electrolyzer significantly increases hydrogen production compared to the 1 MW electrolyzer by better utilizing power peaks and some power lows. The LCOH of hydrogen produced from the 3 MW electrolyzer could be competitive in the Norwegian market, while subsidies might be needed when a more detailed LCOH is calculated. Although neither capacity is ideal, the 3 MW electrolyzer appears to be a reasonable compromise between the extremes.

The 3 MW electrolyzer can utilize power in the range from 0.48 MW to 3 MW. The yearly hydrogen production for the 3 MW electrolyzer is estimated to be 117 100 kg in a typical dry year, 146 700 kg in an median year, and 194 300 kg in a typical wet year, utilizing about 33 % of its ideal production potential. The calculated LCOH for this capacity is 70.70 NOK/kg with a low grid price, 70.90 NOK/kg with a middle grid price, and 71.70 NOK/kg with a high grid price. In the Norwegian hydrogen market, these prices could be competitive, but a more detailed cost analysis is required.

It is also found that although the PEM electrolyzer is widely recognized as the most suitable technology for fluctuating power due to its quick response time, a pressurized AEL responds to load changes almost as quickly, with the difference being in units of seconds. Lastly, the most prominent end-users of hydrogen in Norway are within the industrial, maritime, and transportation sectors. According to the EU, the transportation sector has the highest willingness to pay. Near location A, there is a European highway with average daily vehicle numbers varying from 1 267 to 3 333, depending on the month. Additionally, nearby industries currently using fossil fuels in their processes will need to switch to green fuels in the future. Furthermore, smolt facilities in the area around location A are prominent end-users of the byproducts of hydrogen production, such as oxygen and heat.

The findings of this thesis have the potential to aid in investment decision-making regarding hydrogen generation from fluctuating energy sources.

Chapter 7

Further work

This section discusses important aspects for further study regarding hydrogen production from a small-scale hydropower plant at location A that were not included in the thesis:

- To optimize the utilization of the available power from the hydropower plant, which has a turbine capacity of 6.3 MW, it is worth exploring the feasibility of installing two electrolyzers with different capacities. For example, integrating a 1 MW electrolyzer alongside a 3 MW electrolyzer would allow for a broader range of power utilization, from 0.16 MW to 4 MW. Simulating this setup could assess its potential for increased production and its impact on the LCOH.
- In the hydrogen auction the EU provided subsidies to hydrogen projects with capacities exceeding 5 MW. Exploring the integration of a 1 MW electrolyzer alongside a 5 MW capacity could be insightful. This configuration could efficiently utilize power lows while nearly maximizing the utilization of power peaks at location A. Furthermore, it would also be interesting to calculate the LCOH of the hydrogen produced from this setup, based on the assumption of EU subsidies being granted.
- Given the available 0.5 MW grid connection at location A, exploring the feasibility of utilizing base load from the grid for the electrolyzer is worthwhile. This could involve investigating whether a constant supply equivalent to 17 % of the electrolyzer capacity from the grid is feasible. Such an approach would maintain continuous production, preventing standby mode and potentially increasing the production rate. In this thesis, power from the hydropower plant and the grid is bought to keep the electrolyzer constant at 16 % of the installed capacity. This suggests that buying an additional 1 % of the installed capacity to produce hydrogen rather than just being on standby might be beneficial. However, a detailed analysis is required to determine whether this approach is more economical than putting the electrolyzer in standby mode.
- Integrating cost analysis into the production model would provide valuable insights. This analysis could help determine whether (1) purchasing electricity for compression from the hydropower plant and producing less hydrogen or (2) purchasing electricity from the grid for compression and producing more hydrogen is more economical.
- Simulating hydrogen production using data from a PEM electrolyzer would further enhance

the comparison of the two technologies. Alongside technical specifications and operational dynamics, a detailed comparison of production rates, visualization of electrolyzer operation, and LCOH would provide a comprehensive understanding of the differences between the two technologies.

- Conducting a literature review on real-life hydrogen projects would help understand if slight differences in response times to load changes between AEL and PEM technologies are significant. This will clarify whether the few seconds of response time are critical.

Bibliography

[1] IEA. World Energy Outlook 2023. Technical report, International Energy Agency, 2023. URL https://www.iea.org/reports/world-energy-outlook-2023.

[2] IEA. Global Hydrogen Review 2022. Technical report, International Energy Agency, 2022. URL https://www.iea.org/reports/global-hydrogen-review-2022.

[3] Laura Cozzi, Olivia Chen, and Kim Hyeji. The world's top 1% of emitters produce over 1000 times more CO2 than the bottom 1%. https://www.iea.org/commentaries/the-world-s-top-1-of-emitters-produce-over-1000-times-more-co2-than-the-bottom-1, 2023. Accessed: 2024.04.03.

[4] Energi21. Strategi 2022. Technical report, Energi21, 2022. URL https://www.forskningsradet.no/siteassets/publikasjoner/2022/energi21_2022_sammendragsrapport_no.pdf. Nasjonal strategi for forskning, utvikling, demonstrasjon og kommersialisering av ny klimavennlig energiteknologier.

[5] SSB. SSB - elektrisitet. https://www.ssb.no/energi-og-industri/energi/statistikk/elektrisitet, 2024.

[6] NVE. NVE - vannkraft. https://www.nve.no/energi/energisystem/vannkraft/, 2019. Accessed: 2024.03.11.

[7] NVE. Veileder i planlegging, bygging og drift av små kraftverk. Technical report, Norges vassdrags- og energidirektorat, 2010. URL https://publikasjoner.nve.no/veileder/2010/veileder2010_01.pdf.

[8] NOU. Mer av alt – raskere. Technical report, Energikommisjonen, 2023.

[9] Energi21. Strategi 2018. Technical report, Energi21, 2018. URL https://www.regjeringen.no/contentassets/23d2b1c0760d460092950426364d593e/energi21strategi2018lr.pdf. Nasjonal strategi for forskning, utvikling, demonstrasjon og kommersialisering av ny klimavennlig energiteknologi.

[10] Deepshikha Jaiswal-Nagar, Viney Dixit, and Sheila Devasahayam. *Towards Hydrogen Infrastructure : Advances and Challenges in Preparing for the Hydrogen Economy*. Elsevier, September 2023.

[11] Tom Smolinka, Henry Bergmann, Juergen Garche, and Mihails Kusnezoff. *Electrochemical Power Sources: Fundamentals, Systems, and Applications - Hydrogen Production by Water Electrolysis*. Elsevier, 2021.

[12] SKL. Berekraftsrapport. Technical report, Sunnhordland Kraftlag, 2021. URL https://skl.as/2022/03/10/skl-berekraftsrapport-2021/.

[13] NVE. Nedbørfelt (REGINE). https://www.nve.no/kart/kartdata/vassdragsdata/nedborfelt-regine/, 2021. Accessed: 2024.10.10.

[14] NVE. NVE Atlas. https://atlas.nve.no/Html5Viewer/index.html?viewer=nveatlas#. Accessed: 2024.01.31.

[15] R. L. Jaffe and T. Washington. *The Physics of Energy*. Cambridge University Press, 2018.

[16] Reimund Neugebauer, editor. *Hydrogen Technologies*. Springer International Publishing, 2023. ISBN 978-3-031-16296-1 978-3-031-22100-2. doi:10.1007/978-3-031-22100-2.

[17] Mahdi Kiaee, Andrew Cruden, Petr Chladek, and David Infield. Demonstration of the operation and performance of a pressurised alkaline electrolyser operating in the hydrogen fuelling station in Porsgrunn, Norway. *Energy Conversion and Management*, 94:40–50, April 2015. ISSN 01968904. doi:10.1016/j.enconman.2015.01.070.

[18] Green Hydrogen System. HYPROVIDE® A-SERIES. https://www.greenhydrogensystems.com/electrolysers/hyprovide-a-series-modular-plug-and-play-electrolysers. Accessed: 2024.04.19.

[19] Yi Zheng, Chunjun Huang, Jin Tan, Shi You, Yi Zong, and Chresten Træholt. Off-grid wind/hydrogen systems with multi-electrolyzers: Optimized operational strategies. *Energy Conversion and Management*, 295:117622, November 2023. ISSN 01968904. doi:10.1016/j.enconman.2023.117622.

[20] Aline Leon. *Hydrogen Technology: Mobile and Portable Applications*. Green Energy and Technology. Springer, Berlin, 2008. ISBN 978-3-540-79027-3.

[21] Mourad Nachtane, Mostapha Tarfaoui, Mohamed Amine Abichou, Alexandre Vetcher, Marwane Rouway, Abdeouhaed Aâmir, Habib Mouadili, Houda Laaouidi, and Hassan Naanani. An Overview of the Recent Advances in Composite Materials and Artificial Intelligence for Hydrogen Storage Vessels Design. *Journal of Composites Science*, 7(3): 119, March 2023. ISSN 2504-477X. doi:10.3390/jcs7030119.

[22] Jon Birger Skj, Tor Håkon Jackson Inderberg, and Mari Lie Larsen. Norway's internal and external hydrogen strategy. Technical report, Research Institute for Sustainability, June 2023. URL https://publications.rifs-potsdam.de/rest/items/item_6002936_1/component/file_6002937/content.

[23] TechnipFMC. Deep Purple Pilot. https://www.technipfmc.com/en/what-we-do/new-energy/hydrogen/deep-purple-pilot/. Accessed: 2024.05.21.

[24] Tore Stensvold. Første seilas med hydrogen for fergen Hydra. https://www.tu.no/artikler/forste-seilas-med-hydrogen-for-fergen-hydra/528872, March 2023. Accessed: 2024.04.29.

[25] Nærings og fiskeridepartementet. Veikart 2.0 – Grønt industriløft. Technical Report W-0051 B, Nærings og fiskeridepartementet, September 2023. URL https://www.regjeringen.no/no/dokumenter/veikart-2.0-gront-industriloft/id2996119/.

[26] NVE. Hydrogenproduksjon ved småkraftverk. Delprosjekt 1: Casestudie Rotnes Bruk. Technical report, Norges vassdrags- og energidirektorat, March 2017. URL https://publikasjoner.nve.no/rapport/2017/rapport2017_72.pdf.

[27] NVE. Hydrogenproduksjon ved småkraftverk. Delprosjekt 2: Flerbruk av hydrogen, oksygen og varme ved Smolten settefiskanlegg. Technical report, Norges vassdrags- og energidirektorat, August 2017. URL https://publikasjoner.nve.no/rapport/2017/rapport2017_73.pdf.

[28] SINTEF. Hydrogenproduksjon ved småkraftverk. Del 3: Potensial for lønnsom utbygging av vassdrag i Rullestad. Technical report, SINTEF, October 2019. URL https://publikasjoner.nve.no/eksternrapport/2019/eksternrapport2019_10.pdf.

[29] Jörn Brauns and Thomas Turek. Alkaline Water Electrolysis Powered by Renewable Energy: A Review. *Processes*, 8(2):248, February 2020. ISSN 2227-9717. doi:10.3390/pr8020248.

[30] O. Ulleberg. Modeling of advanced alkaline electrolyzers: A system simulation approach. *International Journal of Hydrogen Energy*, 28(1):21–33, January 2003. ISSN 03603199. doi:10.1016/S0360-3199(02)00033-2.

[31] M. Hammoudi, C. Henao, K. Agbossou, Y. Dubé, and M.L. Doumbia. New multi-physics approach for modelling and design of alkaline electrolyzers. *International Journal of Hydrogen Energy*, 37(19):13895–13913, October 2012. ISSN 03603199. doi:10.1016/j.ijhydene.2012.07.015.

[32] Z. Abdin, C.J. Webb, and E.MacA. Gray. Modelling and simulation of an alkaline electrolyser cell. *Energy*, 138:316–331, November 2017. ISSN 03605442. doi:10.1016/j.energy.2017.07.053.

[33] MathWorks. MATLAB. https://se.mathworks.com/?s_tid=gn_logo, 2024. Accessed: 2024.01.24.

[34] Liina Sangolt. Modeling hydrogen production from small-scale hydropower, a case study, March 2024.

[35] M. Minutillo, A. Perna, A. Forcina, S. Di Micco, and E. Jannelli. Analyzing the levelized cost of hydrogen in refueling stations with on-site hydrogen production via water electrolysis in the Italian scenario. *International Journal of Hydrogen Energy*, 46(26):13667–13677, April 2021. ISSN 03603199. doi:10.1016/j.ijhydene.2020.11.110.

[36] Jon Kirkerud, Magnus Buvik, Ingrid Holm, and Dag Spilde. NVE Rapport nr. 25/2023: Langsiktig kraftmarkedsanalyse 2023 : energiomstillingen – en balansegang. Technical report, Norges vassdrags- og energidirektorat, November 2023. URL https://publikasjoner.nve.no/rapport/2023/rapport2023_25.pdf.

[37] NVE. Kostnader for kraftproduksjon. https://www.nve.no/energi/analyser-og-statistikk/kostnader-for-kraftproduksjon/, October 2023. Accessed: 2024.10.04.

[38] Øystein Ulleberg and Ragnhild Hancke. Techno-economic calculations of small-scale hydrogen supply systems for zero emission transport in Norway. *International Journal of Hydrogen Energy*, 45(2):1201–1211, January 2020. ISSN 03603199. doi:10.1016/j.ijhydene.2019.05.170.

[39] D. J. Jovan, G. Dolanc, and B. Pregelj. Utilization of excess water accumulation for green hydrogen production in a run-of-river hydropower plant. *Renewable Energy*, 195:780–794, August 2022. ISSN 09601481. doi:10.1016/j.renene.2022.06.079.

[40] Maha Rhandi, Marine Trégaro, Florence Druart, Jonathan Deseure, and Marian Chatenet. Electrochemical hydrogen compression and purification versus competing technologies: Part I. Pros and cons. *Chinese Journal of Catalysis*, 41(5):756–769, May 2020. ISSN 18722067. doi:10.1016/S1872-2067(19)63404-2.

[41] Bio Marine. Bio Marine. https://www.biomarine.no/en/effective-addition-and-control-of-oxygen-in-closed-cages/. Accessed: 2024.05.11.

[42] Hirokazu Kojima, Kensaku Nagasawa, Naoto Todoroki, Yoshikazu Ito, Toshiaki Matsui, and Ryo Nakajima. Influence of renewable energy power fluctuations on water electrolysis for green hydrogen production. *International Journal of Hydrogen Energy*, 48(12):4572–4593, February 2023. ISSN 03603199. doi:10.1016/j.ijhydene.2022.11.018.

[43] Vegard Sjursen. Grønn region Sunnhordland. Technical report, EY, 2021. URL https://www.vestlandfylke.no/globalassets/innovasjon-og-naringsutvikling/gron-region-vestland/gron-region---regional-rapport-sunnhordland.pdf.

[44] Hydro. World's first batch of recycled aluminium using hydrogen fueled production. https://www.hydro.com/en/media/news/2023/worlds-first-batch-of-recycled-aluminium-using-hydrogen-fueled-production/, June 2023. Accessed: 2024.04.30.

[45] Klima- og miljødepartementet. Handlingsplan - Regjeringens handlingsplan for grønn skipsfart. Technical report, Klima- og miljødepartementet, June 2019. URL https://www.regjeringen.no/contentassets/2ccd2f4e14d44bc88c93ac4effe78b2f/handlingsplan-for-gronn-skipsfart.pdf.

[46] Norsk Hydrogenforum. 100 hydrogenlastebiler til Norge i 2025. https://www.hydrogen.no/aktuelt/nyheter/100-hydrogenlastebiler-til-norge-i-2025, April 2024. Accessed: 2024.05.14.

[47] Norsk Hydrogenforum. Enova satser stort på hydrogen til maritim sektor. https://www.hydrogen.no/aktuelt/nyheter/enova-satser-stort-pa-hydrogen-til-maritim-sektor, April 2024. Accessed: 2024.05.14.

[48] European Commission. European Hydrogen Bank pilot auction results. https://climate.ec.europa.eu/eu-action/eu-funding-climate-action/innovation-fund/competitive-bidding_en, February 2024. Accessed: 2024.05.09.

[49] Sunfire. SUNFIRE-HYLINK ALKALINE. https://www.sunfire.de/files/sunfire/images/content/Produkte_Technologie/factsheets/Sunfire-Factsheet-HyLink-Alkaline_202405.pdf, 2023. Accessed: 2024.04.15.

[50] Hystar. Hystar's PEM electrolyser technology. https://www.hannovermesse.de/apollo/hannover_messe_2024/obs/Binary/A1352055/1352055_04628705.pdf, 2022. Accessed: 2024.04.15.

Appendix A

Results from compression calculations

Table A.1: The specific investment cost of a compressor is calculated based on the power needed to compress hydrogen. This is explained in detail in section 3.4.3. The values in this table were calculated using hydrogen production from 2010 (a typical dry year).

	1 MW	3 MW	5 MW
End pressure of hydrogen 350 bar, electricity from the hydropower plant			
Compressor power [kW]	14.2	24.2	29.5
Investment cost compressor [NOK]	2 078 800	2 846 100	3 189 300
End pressure of hydrogen 350 bar, electricity from the grid			
Compressor power [kW]	13.6	23.3	28.3
Investment cost compressor [NOK]	2 029 700	2 778 800	3 113 900
End pressure of hydrogen 700 bar, electricity from the hydropower plant			
Compressor power [kW]	20.4	34.9	42.4
Investment cost compressor [NOK]	2 571 400	3 520 500	3 945 000
End pressure of hydrogen 700 bar, electricity from the grid			
Compressor power [kW]	19.6	28.3	40.7
Investment cost compressor [NOK]	2 778 800	3 113 900	3 851 700

Table A.2: The specific investment cost of a compressor is calculated based on the power needed to compress hydrogen. This is explained in detail in section 3.4.3. The values in this table were calculated using hydrogen production from 2008 (median year).

	1 MW	3 MW	5 MW
End pressure of hydrogen 350 bar, electricity from the hydropower plant			
Compressor power [kW]	17.2	29.6	36.9
Investment cost compressor [NOK]	2 331 600	3 201 300	3 636 800
End pressure of hydrogen 350 bar, electricity from the grid			
Compressor power [kW]	16.5	28.5	35.4
Investment cost compressor [NOK]	2 276 500	3 125 600	3 550 800
End pressure of hydrogen 700 bar, electricity from the hydropower plant			
Compressor power [kW]	24.8	42.6	53.0
Investment cost compressor [NOK]	2 884 100	3 636 800	4 498 600
End pressure of hydrogen 700 bar, electricity from the grid			
Compressor power [kW]	23.8	35.4	50.9
Investment cost compressor [NOK]	2 815 900	3 550 800	4 392 200

Table A.3: The specific investment cost of a compressor is calculated based on the power needed to compress hydrogen. This is explained in detail in section 3.4.3. The values in this table were calculated using hydrogen production from 2007 (a typical wet year).

	1 MW	3 MW	5 MW
End pressure of hydrogen 350 bar, electricity from the hydropower plant			
Compressor power [kW]	22.3	40.0	48.9
Investment cost compressor [NOK]	2 709 100	3 813 500	4 291 900
End pressure of hydrogen 350 bar, electricity from the grid			
Compressor power [kW]	21.4	38.4	47.0
Investment cost compressor [NOK]	2 645 100	3 723 400	4 190 400
End pressure of hydrogen 700 bar, electricity from the hydropower plant			
Compressor power [kW]	32.1	57.5	70.3
Investment cost compressor [NOK]	3 351 100	4 717 200	5 308 900
End pressure of hydrogen 700 bar, electricity from the grid			
Compressor power [kW]	30.8	55.2	67.5
Investment cost compressor [NOK]	3 271 900	4 605 700	5 183 400